

Izrada nelinearnog frekvencijski ovisnog modela dinamičke krutosti nosača motora

Kovarik, Borna

Master's thesis / Diplomski rad

2016

Degree Grantor / Ustanova koja je dodijelila akademski / stručni stupanj: **University of Zagreb, Faculty of Mechanical Engineering and Naval Architecture / Sveučilište u Zagrebu, Fakultet strojarstva i brodogradnje**

Permanent link / Trajna poveznica: <https://urn.nsk.hr/urn:nbn:hr:235:327651>

Rights / Prava: [In copyright](#)/[Zaštićeno autorskim pravom.](#)

Download date / Datum preuzimanja: **2024-09-13**

Repository / Repozitorij:

[Repository of Faculty of Mechanical Engineering and Naval Architecture University of Zagreb](#)



University of Zagreb

Faculty of Mechanical Engineering and Naval Architecture

MASTER'S THESIS

Borna Kovarik

Zagreb, May 2016

University of Zagreb

Faculty of Mechanical Engineering and Naval Architecture

**Modeling of the Nonlinear Frequency Dependent
Engine Mount Dynamic Stiffness**

Mentor:

doc.dr.sc. Darko Kozarac

Student:

Borna Kovarik

Zagreb, May 2016



SVEUČILIŠTE U ZAGREBU
FAKULTET STROJARSTVA I BRODOGRADNJE



Središnje povjerenstvo za završne i diplomske ispite
Povjerenstvo za diplomske ispite studija strojarstva za smjerove:
procesno-energetski, konstrukcijski, brodstrojarski i inženjersko modeliranje i računalne simulacije

| | |
|--|--------|
| Sveučilište u Zagrebu Fakultet strojarstva i brodogradnje | |
| Datum | Prilog |
| Klasa: | |
| Ur.broj: | |

DIPLOMSKI ZADATAK

Student: **Borna Kovarik** Mat. br.: 0035183206

Naslov rada na hrvatskom jeziku: **Izrada nelinearnog frekvencijski ovisnog modela dinamičke krutosti nosača motora**

Naslov rada na engleskom jeziku: **Modeling of the Nonlinear Frequency Dependent Engine Mount Dynamic Stiffness**

Opis zadatka:

In modern vehicle design increasing driver comfort and reducing sound emissions are among the key targets which can be achieved by appropriate NVH (Noise – Vibration – Harshness).

Internal combustion engines are one of the major NVH sources in vehicle. Decoupling the engine from vehicle structure is a common way to reduce the structure-borne vibration. This is done by using elastomeric or hydraulic engine mounts. The engine mounts dynamic stiffness is frequency and amplitude dependent.

Today, numerical simulations have become a standard part of the development process in automotive industry. Therefore, it is crucial to have models that can efficiently and accurately describe real mechanical systems. Main outcome of this thesis is to implement structural properties of engine mounts in multibody dynamics simulation model.

Based on everything said above in this study it is necessary to:

1. Study available literature and find different mathematical models to represent the frequency dependent behavior of engine mount for low and high frequencies in time domain.
2. Develop an optimization procedure of the mathematical model parameters and choose one mathematical model based on optimization results.
3. Verify the dynamic stiffness of chosen mathematical model analytically, in MSC Adams, MSC Nastran and AVL Excite
4. Apply chosen mathematical model to a real engine dynamic model in AVL Excite and compare the obtained results with available measurements.

During thesis preparation one must comply with the standard rules for preparation of Master thesis.

It is necessary to list all literature used and received assistance.

Zadatak zadan:

10. ožujka 2016.

Rok predaje rada:

12. svibnja 2016.

Predviđeni datumi obrane:

18., 19. i 20. svibnja 2016.

Zadatak zadao:


Doc. dr. sc. Darko Kozarac

Predsjednica Povjerenstva:


Prof. dr. sc. Tanja Jurčević Lulić

Izjavljujem da sam ovaj rad samostalno izradio koristeći stečena znanja tijekom studija i navedenu stručnu literaturu.

I declare that I have done this study using knowlegde and skills gained during my university studies and using specified scientific literature.

ZAHVALA

Zahvaljujem se tvrtkama AVL – AST d.o.o. iz Zagreba i AVL List GmbH iz Graza na pruženoj podršci tijekom istraživanja i izrade rada.

Posebno se zahvaljujem *mr.sc. Nikoli Naranči* iz tvrtke AVL – AST d.o.o. koji mi je pružio priliku i omogućio izradu rada u dinamičnom okruženju s kvalitetnom inženjerskom podrškom. Također, posebno se zahvaljujem *MSc. Mehdi Mehrgou-u* iz tvrtke AVL List GmbH na pruženoj podršci, predanosti i vodstvu tijekom izrade rada u Grazu.

Zahvaljujem se i svome mentoru *doc.dr.sc. Darku Kozarcu* na svim savjetima i komentarima tijekom izrade rada.

Simbolično zadnji u zahvali, ali uvijek na prvom mjestu,

veliko hvala *mojoj obitelji i djevojci Ines* na podršci tijekom svih ovih godina studija.

Hvala!

Borna Kovarik

ACKNOWLEDGMENTS

I would like to express gratitude to AVL-AST d.o.o. from Zagreb and AVL List GmbH from Graz for all technical support during this study.

Specially, I want to thanks to *mr.sc. Nikola Naranča* from AVL-AST d.o.o. for giving me opportunity and for providing me to do this study research in dynamic environment with good engineering support.

Also, I want to give special thanks to *MSc. Mehdi Mehrgou* from AVL List GmbH for giving me constant guidance and for his dedication throughout this thesis study during my time in Graz.

I would like to express gratitude to my mentor *doc.dr.sc. Darko Kozarac* for his support and advices during this thesis study.

Last but not least, I would like to express **special appreciation**

to my family and to my girlfriend Ines for all their support and understanding through all this years of my university studies.

Thank you!

Borna Kovarik

...

At this point they came in sight of thirty or forty windmills that there are on that plain, and as soon as Don Quixote saw them he said to his squire, "Fortune is arranging matters for us better than we could have shaped our desires ourselves, for look there, friend Sancho Panza, where thirty or more monstrous giants present themselves, all of whom I mean to engage in battle and slay, and with whose spoils we shall begin to make our fortunes; for this is righteous warfare, and it is God's good service to sweep so evil a breed from off the face of the earth."

"What giants?" said Sancho Panza.

"Those thou seest there," answered his master, "with the long arms, and some have them nearly two leagues long."

"Look, your worship," said Sancho; "what we see there are not giants but windmills, and what seem to be their arms are the sails that turned by the wind make the millstone go."

...

Miguel de Cervantes: Don Quixote, Part I



CONTENTS

| | |
|---|------|
| LIST OF FIGURES..... | IV |
| LIST OF TABLES | VII |
| LIST OF SYMBOLS AND UNITS | VIII |
| SAŽETAK..... | IX |
| SUMMARY | X |
| PROŠIRENI SAŽETAK | i |
| 1. Introduction..... | 1 |
| 1.1 Background..... | 1 |
| 1.2 Noise and vibration study in vehicles..... | 2 |
| 1.3 Engine vibration source | 3 |
| 1.4 Design demands of the engine mounts | 4 |
| 1.5 Engine mounting system implementation – example..... | 7 |
| 1.5.1 Elastomeric Engine Mounts | 8 |
| 1.5.2 Hydraulic engine mount | 9 |
| 1.6 Frequency response functions | 11 |
| 1.7 Dynamic stiffness | 12 |
| 1.8 Engine mount measurement procedure | 13 |
| 1.9 Idle speed vibration problem definition..... | 15 |
| 1.10 Thesis outcome | 16 |
| 2. Engine mounts mathematical model | 17 |
| 2.1 Modeling frequency dependency of the engine mount dynamic stiffness | 17 |
| 2.2 Parameter identification..... | 21 |
| 2.3 Results of the mathematical model parameter optimization | 22 |
| 2.3.1 Measurement data | 22 |
| 2.3.2 Elastomeric engine mount – Low frequency behavior optimization | 23 |

| | | |
|-------|---|----|
| 2.3.3 | Hydraulic engine mounts – Low frequency behavior optimization..... | 25 |
| 2.3.4 | Elastomeric engine mounts – High frequency behavior optimization | 28 |
| 2.3.5 | Hydraulic engine mount – High frequency behavior | 30 |
| 2.3.6 | Conclusion..... | 34 |
| 3. | Mathematical model verification | 35 |
| 3.1 | Triple mass oscillator mathematical model equations of motion (EOM) | 36 |
| 3.2 | Triple mass oscillator verification | 39 |
| 3.3 | Verification procedure results | 42 |
| 4. | Gasoline IC engine simulation | 43 |
| 4.1 | IC engine data..... | 43 |
| 4.2 | Mounting system dynamic stiffness optimization..... | 45 |
| 4.2.1 | Hydraulic engine mount dynamic stiffness..... | 45 |
| 4.2.2 | Elastomeric gearbox mount stiffness | 47 |
| 4.3 | Simulation model..... | 49 |
| 4.4 | Simulation results | 51 |
| 4.4.1 | Left engine mount – X direction..... | 51 |
| 4.4.2 | Left engine mount – Y direction..... | 53 |
| 4.4.3 | Left engine mount – Z direction..... | 54 |
| 4.4.4 | Right engine mount – X direction | 56 |
| 4.4.5 | Right engine mount – Y direction..... | 57 |
| 4.4.6 | Right engine mount – Z direction..... | 59 |
| 4.4.7 | Gearbox mount – X direction | 60 |
| 4.4.8 | Gearbox mount – Y direction | 62 |
| 4.4.9 | Gearbox mount – Z direction | 63 |
| 4.5 | Conclusion..... | 65 |
| 5. | Conclusions and Recommendations..... | 66 |
| 5.1 | Conclusions | 66 |

5.2 Recommendations and future work..... 67

6. Literature 68

APPENDIX A 69

APPENDIX B 71

LIST OF FIGURES

| | |
|--|----|
| Figure 1. Main vibration and noise sources in vehicle..... | 2 |
| Figure 2. Engine vibration caused by cyclic acceleration of reciprocating componets and gas pressure in each cycle [4] | 3 |
| Figure 3. Engine vibration modes [5]..... | 4 |
| Figure 4. Transmissibility function | 5 |
| Figure 5. Representation of ideal engine mount | 6 |
| Figure 6. Engine mounting system (courtesy of Rover Group Ltd) [1]..... | 7 |
| Figure 7. a) Kelvin – Voigt model and b) Maxwell model which are usually used for describing elastomeric engine mount behavior..... | 8 |
| Figure 8. Schematic representation of elastomeric engine mount [6]..... | 8 |
| Figure 9. a) Schematic representation of hydraulic engine mount b) Decoupler mechanism | 10 |
| Figure 10. a) Cross point and b) input point dynamic stiffness | 12 |
| Figure 11. Measurement procedure of dynamic stiffness [13]..... | 13 |
| Figure 12. Illustration of MTS 1000-Hz rate machine that can be used to measure cross point dynamic stiffness [13] | 13 |
| Figure 13. Measurement data shown in complex plane | 14 |
| Figure 14. Cross point dynamic stiffness measurement (frequency and amplitude dependency) a) real part and b) imaginary part | 15 |
| Figure 15. Single mass oscillator | 17 |
| Figure 16. Schematic representation of hydraulic and elastomeric engine mount and definition of engine mount coordinate system..... | 23 |
| Figure 17. Describing low frequency behavior of elastomeric engine mount dynamic stiffness by using SLS joint..... | 23 |
| Figure 18. Describing low frequency behavior of elastomeric engine mount dynamic stiffness by using single mass oscillator..... | 24 |
| Figure 19. Describing low frequency behavior of elastomeric engine mount dynamic stiffness by using dual mass oscillator | 24 |
| Figure 20. Describing low frequency behavior of hydraulic engine mount dynamic stiffness by using SLS joint..... | 25 |
| Figure 21. Describing low frequency behavior of hydraulic engine mount dynamic stiffness by using single mass oscillator..... | 26 |

| | |
|---|----|
| Figure 22. Describing low frequency behavior of hydraulic engine mount dynamic stiffness by using dual mass oscillator | 26 |
| Figure 23. Describing low frequency behavior of hydraulic engine mount dynamic stiffness by using triple mass oscillator | 27 |
| Figure 24. Describing high frequency behavior of elastomeric engine mount dynamic stiffness by using dual mass oscillator | 28 |
| Figure 25. Describing high frequency behavior of elastomeric engine mount dynamic stiffness by using triple mass oscillator | 29 |
| Figure 26. Describing high frequency behavior of hydraulic engine mount dynamic stiffness by using dual mass oscillator | 30 |
| Figure 27. Describing high frequency behavior of hydraulic engine mount dynamic stiffness up to 400 Hz by using triple mass oscillator | 31 |
| Figure 28. Describing high frequency behavior of hydraulic engine mount dynamic stiffness up to 700 Hz by using triple mass oscillator | 32 |
| Figure 29. Describing high frequency behavior of hydraulic engine mount dynamic stiffness by using penta mass oscillator | 33 |
| Figure 30. Mathematical model verification process | 35 |
| Figure 31. Triple mass oscillator with masses connected in parallel | 36 |
| Figure 32. Cross point dynamic stiffness used for verification process | 39 |
| Figure 33. Triple mass oscillator model in AVL Excite | 40 |
| Figure 34. Cross point dynamic stiffness verification results | 42 |
| Figure 35. Simulated longitudinal IC engine defined coordinate system and mounting brackets | 43 |
| Figure 36. Vehicle coordinate system as defined by ISO 8855 / DIN 70000 [14] | 44 |
| Figure 37. Engine mount dynamic stiffness – X direction | 45 |
| Figure 38. Engine mount dynamic stiffness – Y direction | 46 |
| Figure 39. Engine mount dynamic stiffness – Z direction | 46 |
| Figure 40. Gearbox mount dynamic stiffness – X direction | 47 |
| Figure 41. Gearbox mount dynamic stiffness – Y direction | 47 |
| Figure 42. Gearbox mount dynamic stiffness – Z direction | 48 |
| Figure 43. Simplified simulation model topology | 49 |
| Figure 44. Powertrain simulation model topology in <i>AVL Excite Power Unit</i> | 50 |
| Figure 45. Left engine mount - X direction - synthesis | 51 |
| Figure 46. Left engine mount - X direction – 2 nd order | 52 |

| | |
|---|----|
| Figure 47. Left engine mount - X direction - 4 th order | 52 |
| Figure 48. Left engine mount - Y direction – synthesis | 53 |
| Figure 49. Left engine mount - Y direction – 2 nd order | 53 |
| Figure 50. Left engine mount - Y direction – 4 th order..... | 54 |
| Figure 51. Left engine mount - Z direction – synthesis | 54 |
| Figure 52. Left engine mount - Z direction – 2 nd order | 55 |
| Figure 53. Left engine mount - Z direction – 4 th order..... | 55 |
| Figure 54. Right engine mount – X direction – synthesis | 56 |
| Figure 55. Right engine mount – X direction – 2 nd order | 56 |
| Figure 56. Right engine mount – X direction – 4 th order | 57 |
| Figure 57. Right engine mount – Y direction – synthesis..... | 57 |
| Figure 58. Right engine mount – Y direction – 2 nd order | 58 |
| Figure 59. Right engine mount – Y direction – 4 th order..... | 58 |
| Figure 60. Right engine mount – Z direction – synthesis..... | 59 |
| Figure 61. Right engine mount – Z direction – 2 nd order | 59 |
| Figure 62. Right engine mount – Z direction – 4 th order..... | 60 |
| Figure 63. Gearbox mount – X direction – synthesis | 60 |
| Figure 64. Gearbox mount – X direction – 2 nd order..... | 61 |
| Figure 65. Gearbox mount – X direction – 4 th order | 61 |
| Figure 66. Gearbox mount – Y direction – synthesis | 62 |
| Figure 67. Gearbox mount – Y direction – 2 nd order | 62 |
| Figure 68. Gearbox mount – Y direction – 4 th order | 63 |
| Figure 69. Gearbox mount – Z direction – synthesis | 63 |
| Figure 70. Gearbox mount – Z direction – 2 nd order..... | 64 |
| Figure 71. Gearbox mount – Z direction – 4 th order | 64 |

LIST OF TABLES

| | |
|---|----|
| Table 1. FRF commonly used in vibration and acoustic analysis..... | 11 |
| Table 2. Considered mathematical models during study | 18 |
| Table 3. Calculated engine mass displacement x_1 | 40 |
| Table 4. Calculated transmitted force F_T to ground (chassis) node..... | 41 |
| Table 5. Calculated cross point dynamic stiffness K_{CP} | 41 |

LIST OF SYMBOLS AND UNITS

| <i>Symbol</i> | <i>Unit</i> | <i>Description</i> |
|-------------------|-------------|---|
| A | N; mm | measurement force or displacement amplitude |
| F_I | N | input force |
| F_T | N | transmitted force |
| K_{imag} | N/mm | imaginary part of cross point dynamic stiffness |
| K_{real} | N/mm | real part of cross point dynamic stiffness |
| K^* | N/mm | cross point dynamic stiffness amplitude |
| X | mm | displacement amplitude |
| c | N/mm | stiffness coefficient |
| d | Ns/mm | damping coefficient |
| f | Hz | frequency |
| f_{obj} | N | optimization objective function |
| k_m | N/mm | measured cross point stiffness |
| k_t | N/mm | theoretical calculated cross point stiffness |
| r | / | frequency ratio |
| v | m/s | velocity |
| ϕ | degrees | measurement phase |
| ω | Hz | angular frequency |

SAŽETAK

Jedan je od glavnih izvora buke i vibracija u vozilima je motor s unutrašnjim izgaranjem koji je s karoserijom vozila povezan s nosačima motora. Dinamička krutost nosača motora, kao pokazatelj odziva na dinamičku uzbudu, ovisna je o frekvenciji i amplitudi uzbude te temperaturi okoline.

U okviru ovoga rada detaljno su opisani elastomerni i hidraulički nosači motora s unutrašnjim izgaranjem s posebnim naglaskom na izradu matematičkog modela kojim je moguće opisati nelinearnu ovisnost dinamičke krutosti nosača motora o frekvenciji uzbude. Proučeno je deset različitih matematičkih modela i za daljnje proučavanje odabran je model oscilatora s tri mase koji posjeduje četiri stupnja slobode gibanja. Dinamičku krutost odabranog modela moguće je opisati s 15 različitih linearnih koeficijenata. Proučavana dinamička krutost je dinamička krutost definirana silom prenesenom u oslonce (*engl. cross point dynamic stiffness*).

Za matematičke modele definiran je proces optimiranja njihovih parametara. Također, napravljena je verifikacija svojstva frekvencijske ovisnosti odabranog matematičkog modela u programskim paketima koji se često upotrebljavaju u svrhu simuliranja dinamike krutih ili fleksibilnih tijela koji su međusobno vezani u kinematičke lance (*engl. multibody dynamics*).

Nakon utvrđivanja da je s odabranim matematičkim modelom moguće opisati frekvencijsku nelinearnost dinamičke krutosti, matematički model implementiran je u cjeloviti simulacijski model motora s unutrašnjim izgaranjem u programskom paketu *AVL Excite Power Unit*. Za simulirani motor s unutrašnjim izgaranjem dostupna su mjerenja odziva nosača motora koja su uspoređena s dobivenim rezultatom simulacija. Rezultati i mjerenja odziva nosača motora prikazani su u obliku brzina.

Ključne riječi: *izolacija vibracija motora s unutrašnjim izgaranjem, nosači motora s unutrašnjim izgaranjem, frekvencijski ovisna dinamička krutost, matematički model dinamičke krutosti, optimiranje parametara*

SUMMARY

One of the main sources of noise and vibrations in the passenger car is internal combustion engine which is coupled with the car chassis by using elastomeric or hydraulic engine mounts. To describe dynamic response of the engine mounts, the dynamic stiffness is used. Engine mount dynamic stiffness behavior is frequency, amplitude and temperature dependent.

Emphasis of this study is on mathematical modeling of the dependency on frequency of the engine mount cross point dynamic stiffness. During this study 10 different mathematical models were considered and for further investigation triple mass oscillator was chosen based on optimization results. Triple mass oscillator is described with 15 different linear variables.

For all mathematical models the optimization procedure for finding the mathematical model parameter values is defined. Verification of chosen mathematical model is made in the commercial programs that are usually used for flexible multibody dynamics simulation.

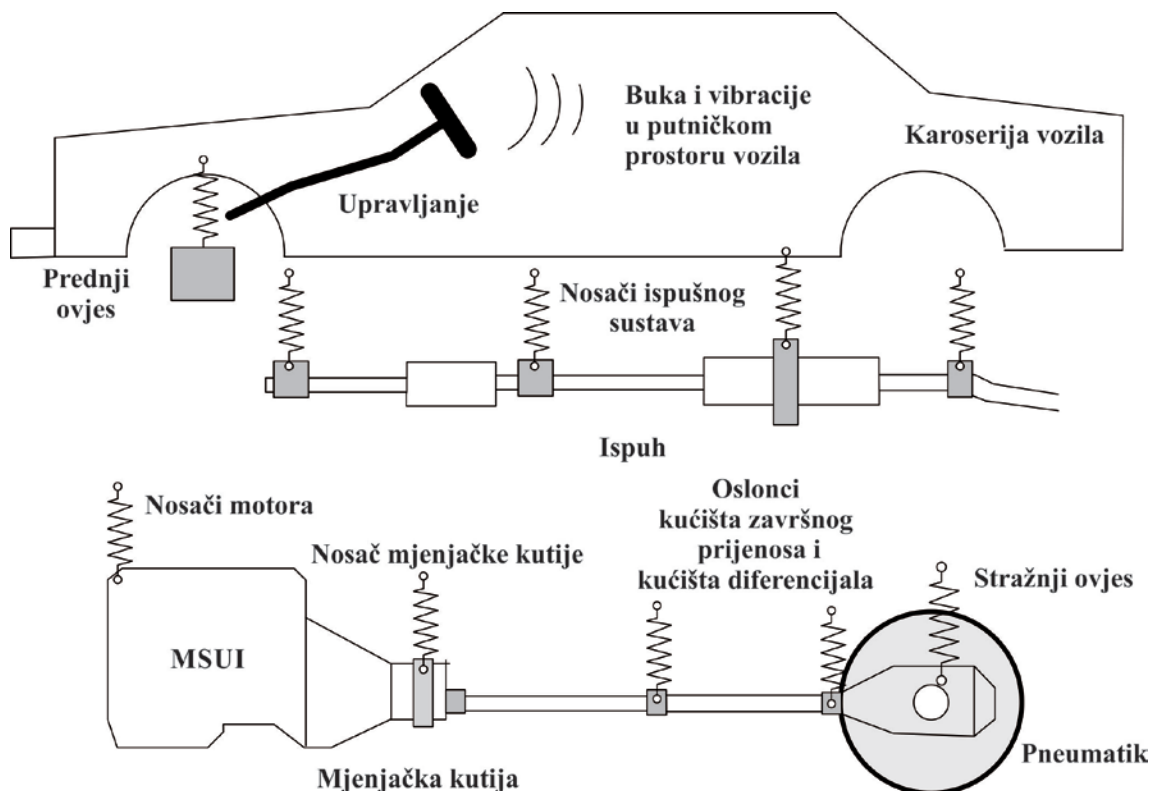
After mathematical model verification process, the chosen mathematical model was implemented in the internal combustion engine simulation model prepared in *AVL Excite Power Unit* environment. For simulated IC engine, measurements of engine mounts responses are available and simulation results are compared with the available measurements in form of engine mounts velocities.

Key words: *IC engine vibration isolation, engine mounts, dynamic stiffness frequency dependency, dynamic stiffness mathematical model, parameter optimization*

PROŠIRENI SAŽETAK

Ovaj diplomski rad izrađen je u suradnji s tvrtkama AVL - AST d.o.o. iz Zagreba i AVL List GmbH iz Graza. Cilj diplomskog rada je doprijeti razvoju matematičkog modela koji opisuje frekvencijski ovisnu dinamičku krutost nosača motora i implementirati odabrani matematički model u simulacijski model motora s unutrašnjim izgaranjem u programskom paketu *AVL Excite Power Unit* [1].

U proizvodnji modernih konvencionalnih automobila povećanje udobnosti i smanjenje emisija buke glavni su konstrukcijski ciljevi uz smanjenje potrošnje goriva za koju je izravno vezana emisija CO₂. Glavni izvori buke i vibracija u putničkom prostoru vozila, a prikazani su na slici 1.



Slika 1. Izvori buke i vibracija na putničkom vozilu.

Motor s unutrašnjim izgaranjem sa svojim pomoćnim sustavima (visokotlačna pumpa za gorivo, električni generator, itd.) jedni su od glavnih izvora buke i vibracija u vozilu. Za kontrolu razine prenesenih vibracija u putnički prostor vozila bitno je pravilno projektirati oslonce odnosno nosače motora s unutrašnjim izgaranjem. Nosači motora trebaju imati dovoljno veliku krutost da sprječavaju velike pomake motora u odnosu na karoseriju, a s druge

strane trebaju imati svojstvo unutarnjeg prigušenja kako bi prijenos vibracija i buke u putnički prostor bio sveden na minimum.

Bitniji konstrukcijski ciljevi za projektiranje nosača motora su [6]:

1. Sprječiti zamorni lom kućišta motora i mjenjača na mjestima prihvata na karoseriju automobila koji bi se dogodio kada bi motor i mjenjač bili kruto vezani na karoseriju.
2. Svojstvo unutarnjeg prigušenja kako bi se smanjila amplituda prenesenih vibracija i buke u putnički prostor vozila.
3. Smanjenje efekta pojačavanja buke koji se javlja u slučaju prijenosa buke preko karoserije (nosive konstrukcije) vozila (*engl. structure-borne noise*).
4. Sprječavanje prijenosa sile uslijed naglog (udarnog) opterećenja kotača sa karoserije vozila na motor.
5. Sprječavanje velikih relativnih pomaka između karoserije vozila i motora uslijed reakcije na izlazni moment motora na strani mjenjača.
6. Ograničavanje pomaka motora uslijed sila inercije u situacijama naglog ubrzavanja i naglog zaustavljanja vozila.

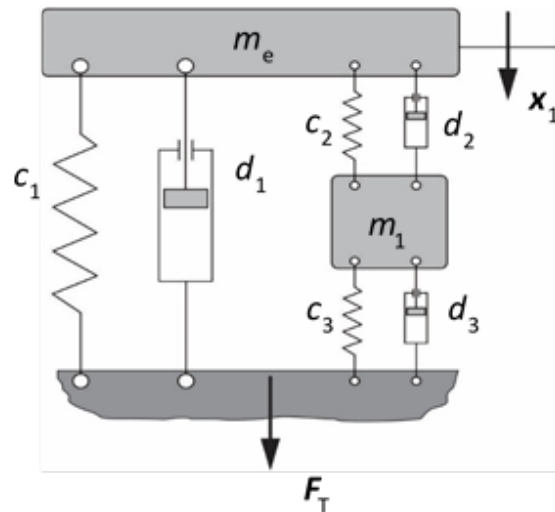
U motornim vozilima uglavnom se koriste hidraulički i elastomerni nosači motora. Hidraulički nosači motora su učinkovitiji u izolaciji vibracija motora, ali i složenije konstrukcije u odnosu na elastomerne nosače motora.

Na temelju iskustva i predznanja na području vibracija moguće je definirati idealizirani nosač motora koji ima veliki iznos krutosti i veliki iznos viskoznog prigušenja kada je frekvencija uzbude manja od 50 Hz, a amplituda pomaka motora veća od 0,3 mm. Za uspješno izoliranje visokih frekvencija uzbude (većih od 50 Hz) koji uzrokuju amplitude pomaka motora manje od 0,3 mm poželjno je svojstvo niže krutosti i nižeg iznosa viskoznog prigušenja.

Također, na temelju definiranih konstrukcijskih zahtjeva može se zaključiti da je nepohodno da dinamička krutost nosača motora bude ovisna o frekvenciji uzbude i amplitudi pomaka. U okviru ovoga rada promatrana je samo ovisnost dinamičke krutosti o frekvenciji uzbude.

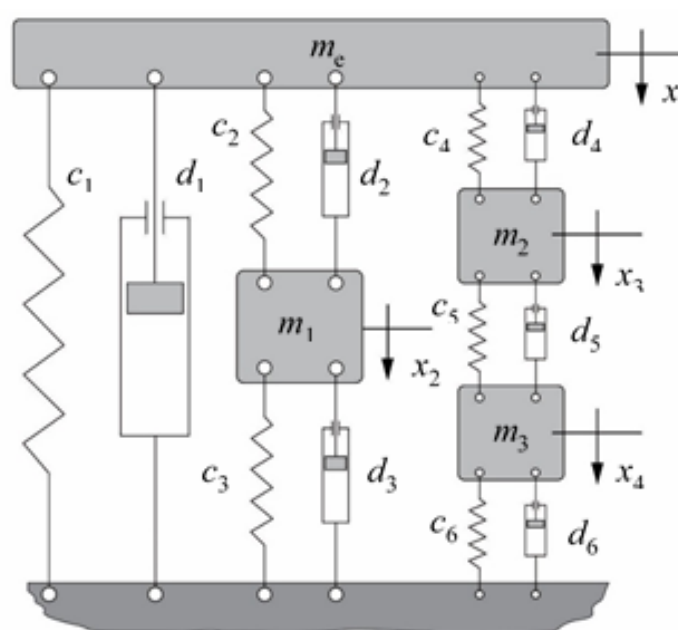
U numeričkim simulacijama koje su postale standardni dio procesa razvoja u automobilskoj industriji, potrebno je definirati matematičke modele za opisivanje ponašanja stvarnih sustava. Stoga, za implementaciju svojstva frekvencijske ovisnosti dinamičke krutosti nosača motora u numeričke simulacije potrebno je definirati matematički model kojim je moguće opisati frekvencijsku ovisnost.

Promatrana frekvencijski ovisna dinamička krutost je dinamička krutost definirana silom prenesenom u oslonce (*engl. cross point dynamic stiffness*), a prikazana na slici 2. Definirana je kao omjer sile prenesene u oslonce F_T i pomaka x_1 mase m_e koja u ovome slučaju predstavlja masu motora s unutrašnjim izgaranjem.



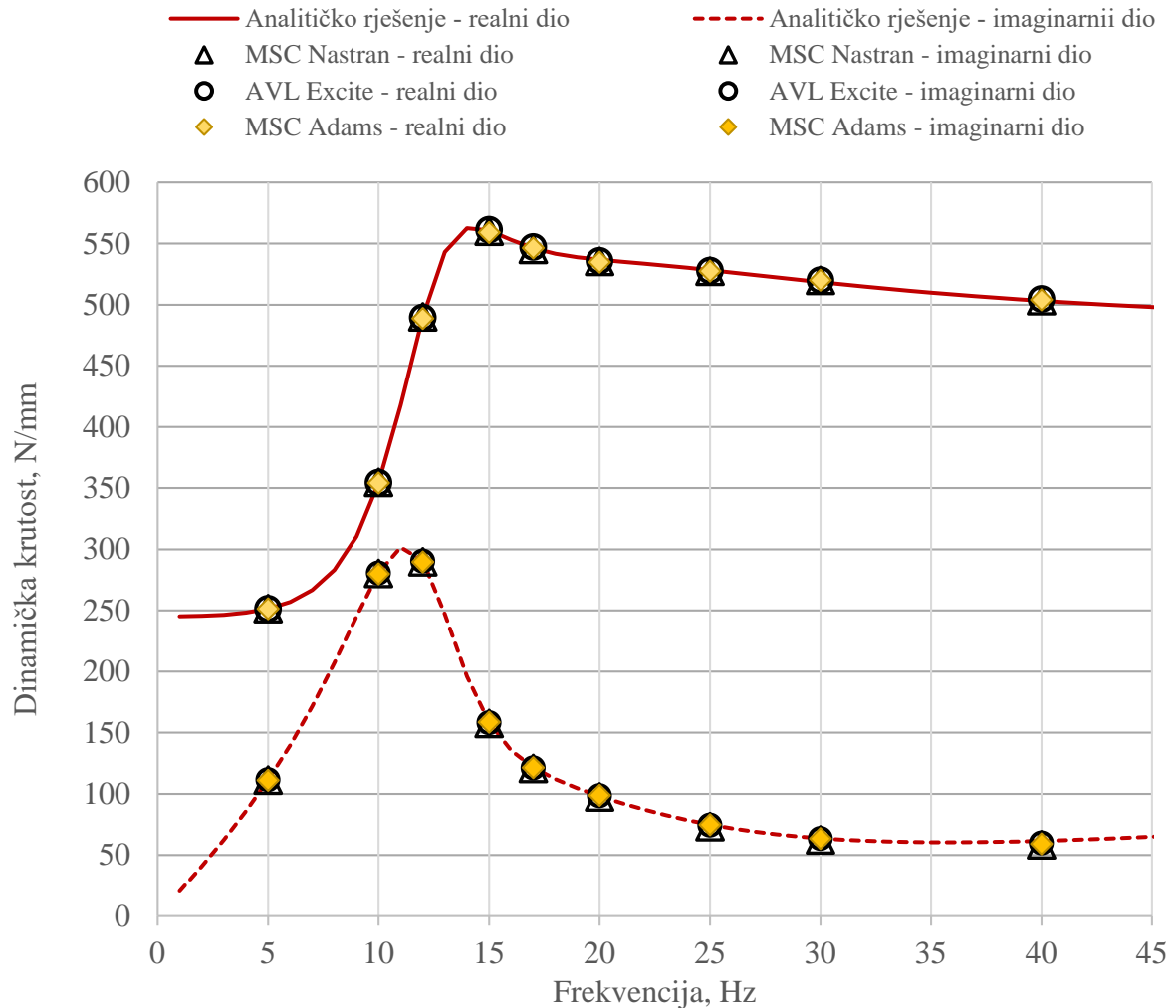
Slika 2. Dinamička krutost definirana sa silom prenesenom u oslonce (*engl. cross point dynamic stiffness*).

U okviru rada postavljeno je deset različitih matematičkih modela, a za daljnje proučavanje odabran je model oscilatora s tri mase koji posjeduje četiri stupnja slobode gibanja (4 SSG). Odabrani matematički model prikazan je na slici 3. Za definiranje matematičkog modela potrebno je optimirati 15 različitih varijabli ($c_1, d_1, c_2, d_2, m_1, c_3, d_3, c_4, d_4, m_2, c_5, d_5, m_3, c_6, d_6$).



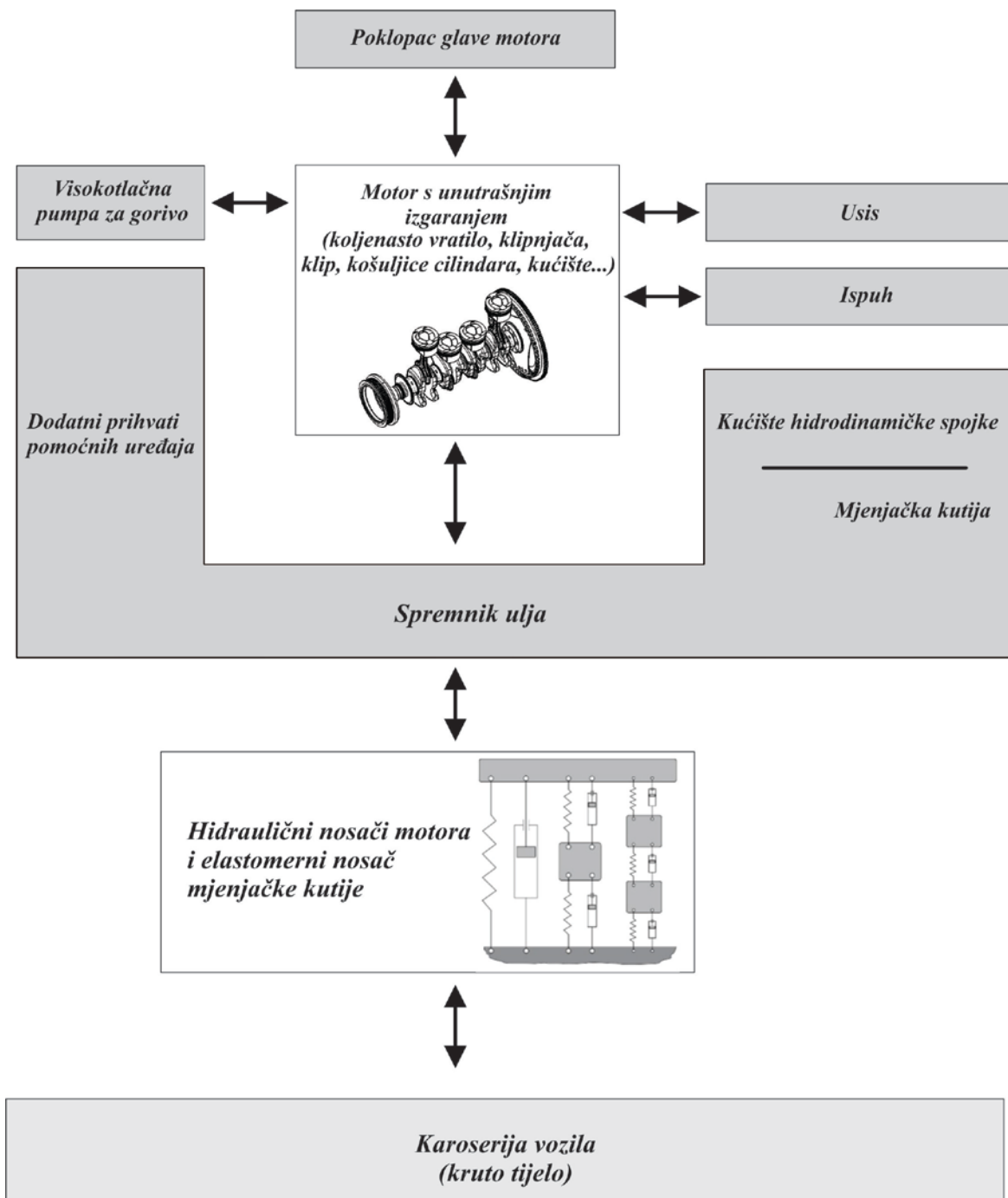
Slika 3. Matematički model oscilatora s tri mase (4 SSG).

Za odabrani matematički model napravljena je i verifikacija kako bi se vidjela mogućnost korištenja matematičkog modela u programskim paketima koji se često upotrebljavaju u svrhu simuliranja dinamike krutih ili fleksibilnih tijela koji su međusobno vezani u kinematičke lance (engl. multibody dynamics). Verifikacija je napravljena u programskim paketima *MSC Adams*, *MSC Nastran* i *AVL Excite Power Unit*. Rezultati verifikacije prikazani su na slici 5.



Slika 5. Rezultati verifikacije dinamičke krutosti oscilatora s tri mase.

Nakon uspješne verifikacije i zaključka da je odabrani matematički model moguće koristiti u svrhu opisivanja ovisnosti dinamičke krutosti o frekvenciji, matematički model implementiran je u programski paket *AVL Excite Power Unit* u cjeloviti simulacijski model Otto motora. Svrha simulacijskog modela je proučavanje utjecaja vibracija na pojedine komponente motora kao npr. koljenastog vratila ili glavne i leteće ležajeve. Također, svrha simulacijskog modela je vidjeti ukupni iznos prenesenih vibracija preko nosača motora na nosivu konstrukciju odnosno karoseriju vozila. Topologija simulacijskog modela prikazana je na slici 6.



Slika 6. Topologija simulacijskog modela.

Simulacijski model se sastoji od dva hidraulička nosača motora i jednog elastomernog nosača koji je postavljen na mjenjačkoj kutiji. Detalji simulacijskog modela nisu prikazani zbog ugovora o povjerljivosti korištenih informacija.

Nakon postavljanja simulacijskog modela i provedenih simulacija dobiveni rezultati simulacija uspoređeni su s rezultatima mjerenja, a usporedba rezultata prikazana je u poglavlju 4.4. U rezultatima se uspoređuju brzine na mjestima mjerenja odziva nosača motora.

Prikazane su usporedbe ukupne sume svih redova brzine odziva, 2. reda brzine odziva i 4. reda brzine odziva nosača motora.

Nakon usporedbe rezultata zaključak na kraju rada je da je moguće pomoću oscilatora s tri mase uspješno opisati frekvencijski ovisnu dinamičku krutost motora, te da su rezultati odziva simulacijskog modela u usporebi s mjerenjima prihvatljivi. Prema tome, koristeći oscilator s tri mase u simulacijskom modelu motora s unutrašnjim izgaranjem moguće je dobiti upotrebljive rezultate odziva nosača motora na uzbuđu u obliku tlaka plinova u svakome cilindru.

Na kraju rada izneseni su neki prijedlozi za daljnja istraživanja i unapređenja modela nosača motora. Implementacija drugog važnog svojstva nosača motora bila bi korisna za unapređenje matematičkog modela, a to je definiranje ovisnosti dinamičke krutosti o amplitudi pomaka mase koja predstavlja masu motora.

1. Introduction

This thesis is done in cooperation with AVL-AST d.o.o. from Zagreb and AVL List GmbH from Graz in purpose of understanding and applying frequency dependency of engine mounts in powertrain simulation procedure.

1.1 Background

In modern vehicle design it is necessary to achieve appropriate NVH (Noise – Vibration – Harshness) to fulfill noise level regulation restrictions. *Vibration* has always been an important issue closely related to reliability and quality, while *noise* is of increasing importance to vehicle users and environmentalists. *Harshness*, which is related to the quality and transient nature of vibration and noise, is also strongly linked to vehicle refinement. Controlling vibration and noise in vehicles presents a severe challenge to designers because unlike on many other machine systems, motor vehicles have several sources of vibration and noise which are interrelated and speed dependent [1].

Using traditional physical prototyping and testing is time consumable and expensive so it is gradually being replaced by virtual prototyping and simulations. The main advantage of virtual prototyping and simulation is the possibility to develop couple of different design models and to compare their behavior without producing physical prototype. Also, once the virtual prototype is developed the additional cost of further analysis is usually very low compared to building a new physical prototype.

Internal combustion engine is usually coupled with the chassis by using hydraulic or elastomeric engine mounts. Vibration response of engine mounts is frequency, amplitude and temperature dependent. To make a simulation of the NVH behavior of the internal combustion engine it is necessary to know engine mount dynamic stiffness. For more detailed analysis, chassis compliance should be involved in simulation model. Involving chassis compliance is not in the scope of this thesis.

Engine mounting systems have been successfully used to isolate the driver and passenger from both noise and vibration generated by the engine. However, there is still need for further improvements of the performance of engine mounting stiffness following two reasons. One reason is the requirement of vibration and noise level isolation in passenger cars. Second reason is that the modern car designs have a trend for lighter car bodies and more power-intensive engines [3].

1.2 Noise and vibration study in vehicles

Energy that influences on driver comfort in passenger car is transmitted through two different types of paths: structure-borne and noise-borne paths. Energy due to vibration is transmitted through structural paths and can be transformed to noise. One of the major source of structural-borne path in passenger car is internal combustion engine. Studying structure-borne and noise-borne paths is beyond the scope of this thesis, but it is important to emphasize that engine and transmission mounts on which engine is supported have a big influence on transmitted engine originating vibration into the vehicle interior.

In figure 1 major vehicle components and structure-borne paths that influence on vehicle comfort are shown.

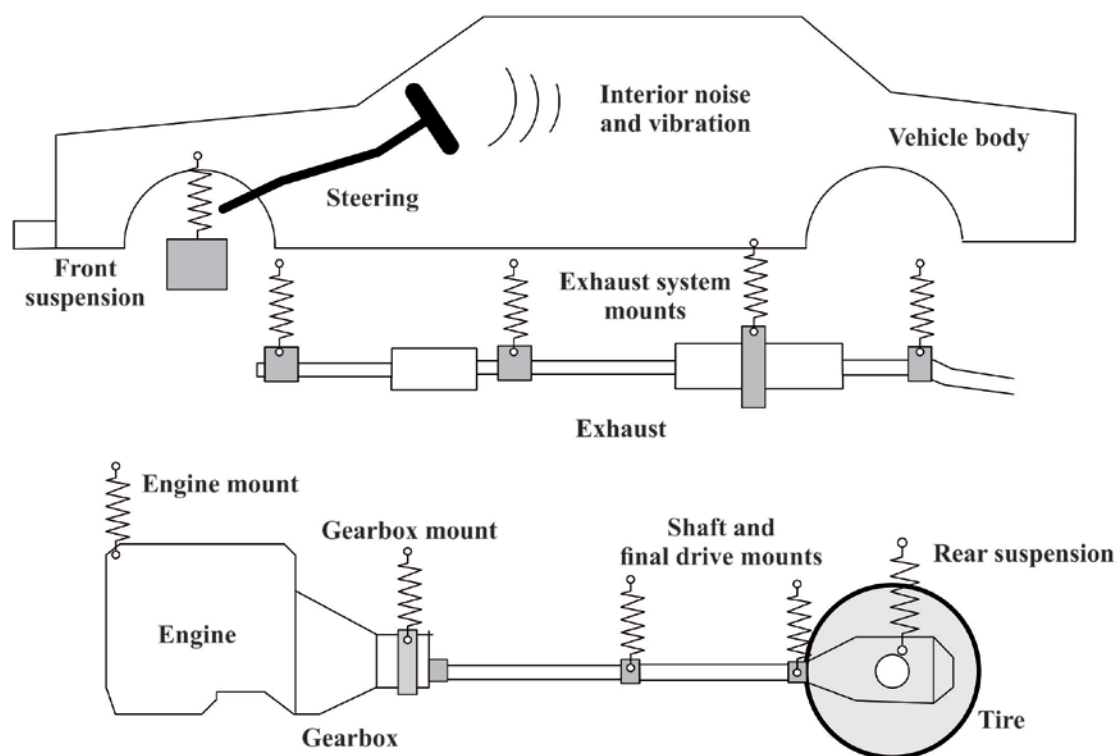


Figure 1. Main vibration and noise sources in vehicle

Vibration sources are characterized by their *time and frequency domain characteristics*. In automotive engineering, most vibration sources produce continuous disturbances as distinct from shocks and short duration transients encountered in some machine systems. They can therefore be categorized principally as either periodic or random disturbances. The former are the easiest to define and originate from the engine or transmission, while random disturbances arise from terrain inputs to wheels.

1.3 Engine vibration source

Vibrations of internal combustion engine is caused by cyclic acceleration of reciprocating components and the rapidly changing gas pressure which occurs throughout each cycle of operation. Both sources of vibrations in internal combustion engine generate three kinds of vibrations which are transferred to the engine mounting:

1. Vertical and/or horizontal shaking
2. Fluctuating torque reaction
3. Torsional oscillation (vibration) of crankshaft

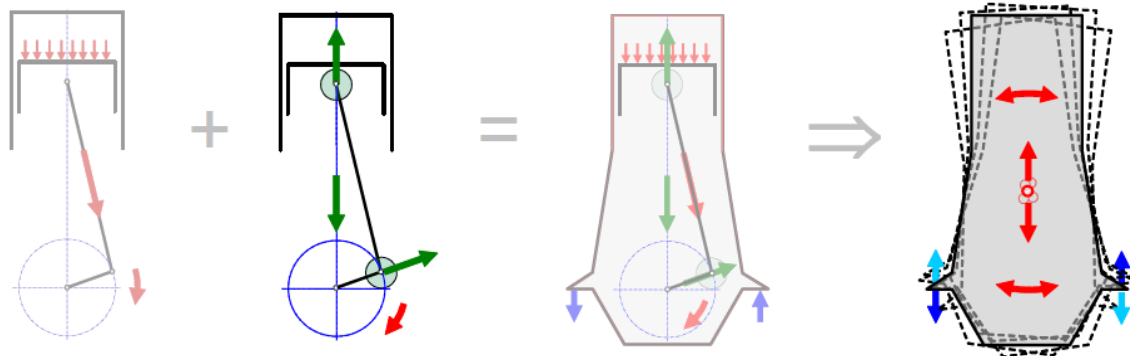


Figure 2. Engine vibration caused by cyclic acceleration of reciprocating components and gas pressure in each cycle [4]

Most of vibrations are transmitted to the engine mounts whose main task is to damp vibrations to prevent transmitting latter to chassis and to prevent engine large displacements, which means the mounts should be stiff enough.

For the multi-cylinder engine, the components of the engine unbalanced forces depend on the number and arrangement of the engine cylinders.

It is possible to consider internal combustion engine as a body with six DOF (degrees of freedom). Disturbances originating from internal combustion engine will excite the engine in various modes as shown in figure 3. For example, the torque caused by the firing pulse will cause engine pitch vibration. The frequency of the unbalanced disturbances are correlated to engine speed and depends on the number of cylinders in the engine, cycle stroke number and the engine speed. In inline four cylinder, four stroke engine, the frequencies of the fundamental disturbances are of the second order of the engine speed. This means that for speed range from 900 – 6000 rpm corresponded frequency range is 30 - 200 Hz.

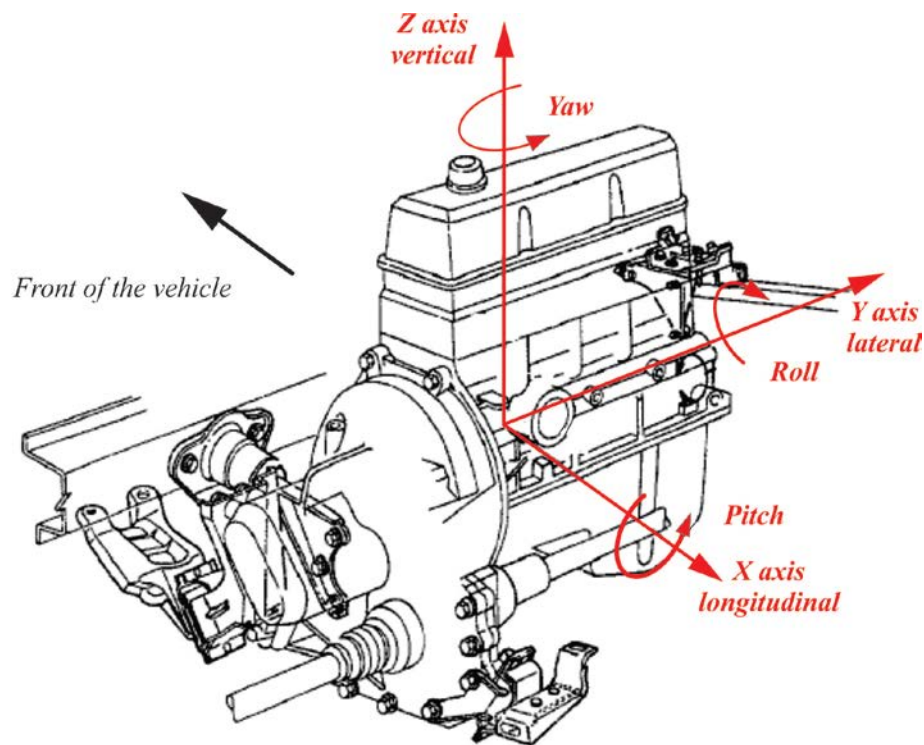


Figure 3. Engine vibration modes [5]

1.4 Design demands of the engine mounts

Besides the primary function of engine mounts to support the weight of the engine, in [6] other design requirements for the engine mounts are defined as follows:

1. To prevent fatigue failure of the engine gearbox support points which would occur if they were rigidly attached to the chassis or body structure.
2. To reduce the amplitude of any engine vibration which is being transmitted to the body structure.
3. To reduce noise amplification which would occur if engine vibrations were allowed to be transferred directly to the body structure.
4. To reduce human discomfort and fatigue by partially isolating the engine vibrations from the body by means of an elastic media.
5. To accommodate engine block misalignment and to reduce residual stresses imposed on the engine block and mounting brackets due to chassis or body frame distortion.
6. To prevent road wheel shocks when driving over rough ground imparting excessive rebound movement to the engine.
7. To prevent large engine to body relative movement due to torque reaction, particularly in low gear, which would cause excessive misalignment and strain on components such as the exhaust pipe and silencer system.

8. To restrict engine movement in fore and aft direction of the vehicle due to the inertia of the engine acting in opposition to the accelerating and braking forces.

For fulfilling mentioned targets engineers have developed hydraulic and elastomeric engine mounts.

According to [6] main focus in the design of the engine mounts is to provide large stiffness and large damping for low frequency and large amplitude excitations. Large amplitude excitations are considered excitations with amplitudes larger than 0,3 mm in a frequency range of 1 – 50 Hz. Usually these excitations originate from engine idle, entire drivetrain response in driving condition and engine acceleration. At the same time, the engine mounts should low stiffness and low damping values to provide properly isolation of high frequency and small amplitude excitations.

In figure 4 which shows force transmissibility through typical Voigt mode, the reason for high stiffness and high damping on low engine speeds requirement is shown. Force transmissibility is lower for high damping at low frequencies and for low damping at high frequencies.

Frequency ratio r is defined as a ratio of the input load frequency and natural frequency of the mechanical system, and ordinate F_T/F_I is defined as a ratio of the amplitude value of the transmitted force F_T and input force F_I .

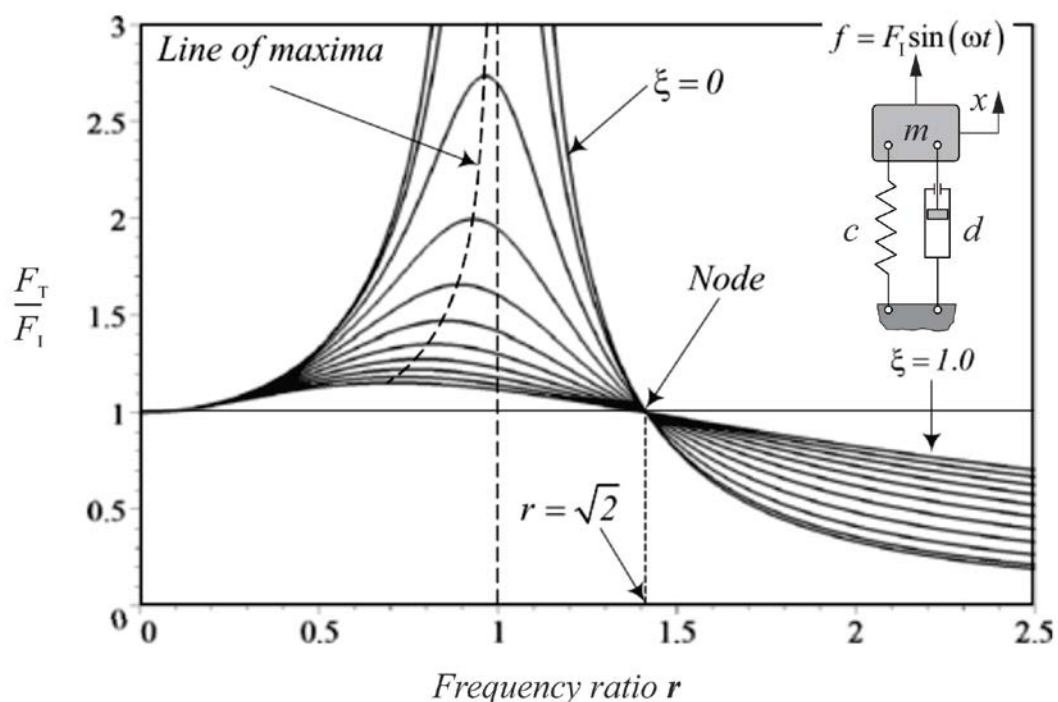


Figure 4. Transmissibility function

According to [7] and [8] ideal dynamic engine mount stiffness is represented in figure 5 and shows that engine mount stiffness should be frequency dependent.

Since lower frequencies usually lead to a larger amplitude of displacement and higher frequencies lead to a smaller amplitude of displacement, the mounting system with an amplitude-dependent characteristic can also meet this requirement. The development of engine mounting systems has mostly concentrated on improvement in such frequency and amplitude dependent properties.

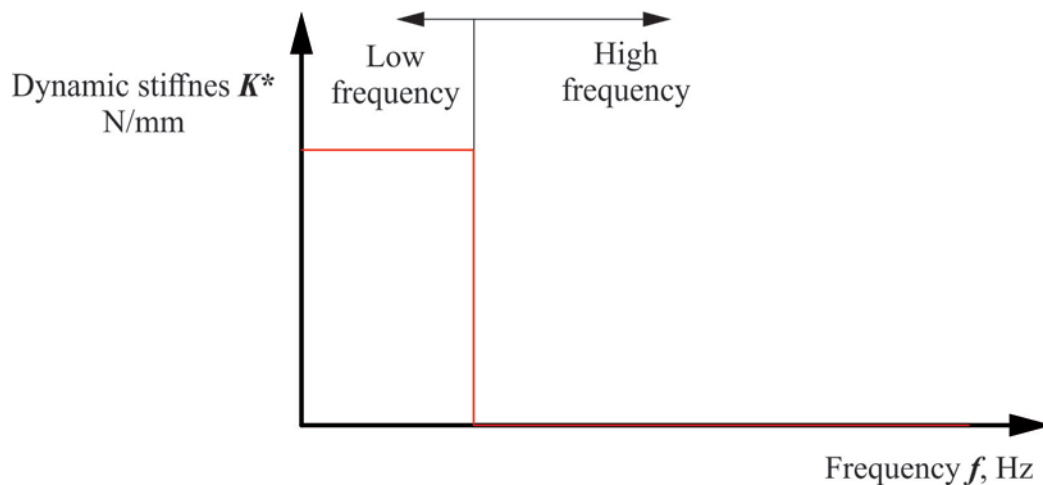


Figure 5. Representation of ideal engine mount

Lightly damped structures can produce high levels of vibration from low level sources if frequency components in the disturbance are close to one of the system's natural frequencies. This means that well designed and manufactured sub-systems, which produce low level disturbing forces, can still create problems when assembled on a vehicle. In order to avoid these problems at the design stage it is necessary to model the system accurately and analyze its response to anticipated disturbances [1].

The general approach to vibration analysis as mentioned in [1] is to:

- a) develop a mathematical model of the system and formulate the equations of motion
- b) analyze the free vibration characteristics (natural frequencies and modes)
- c) analyze the forced vibration response to prescribed disturbances and
- d) investigate methods for controlling undesirable vibration levels if they arise.

1.5 Engine mounting system implementation – example

A practical implementation of an engine mounting system for a four-cylinder diesel engine is shown in figure 6. It comprises two mass carrying mounts and two torque reacting tie bars – tie rods. Hydramount is passive hydraulic mount and hydrabush is elastomeric engine mount which is also passive. The hydramount is linked to the power unit by an aluminum bridge bracket and hydrabush is mounted on the gearbox side.

Both tie bars have a small bush at the power unit, two torque unit ends and a large bush at the body end. The lower tie bar has its power unit end carried by a bracket attached to the sump and its body end attached to a subframe which also carries the vehicle suspension. The vertical stiffnesses of the mass carriers have very little effect on the torque performance of the system and can therefore be tuned for ride. The function of the hydramounts is of course to improve the ride. The tie bar fore and aft rates do not affect ride and can be tuned for the torque loading.

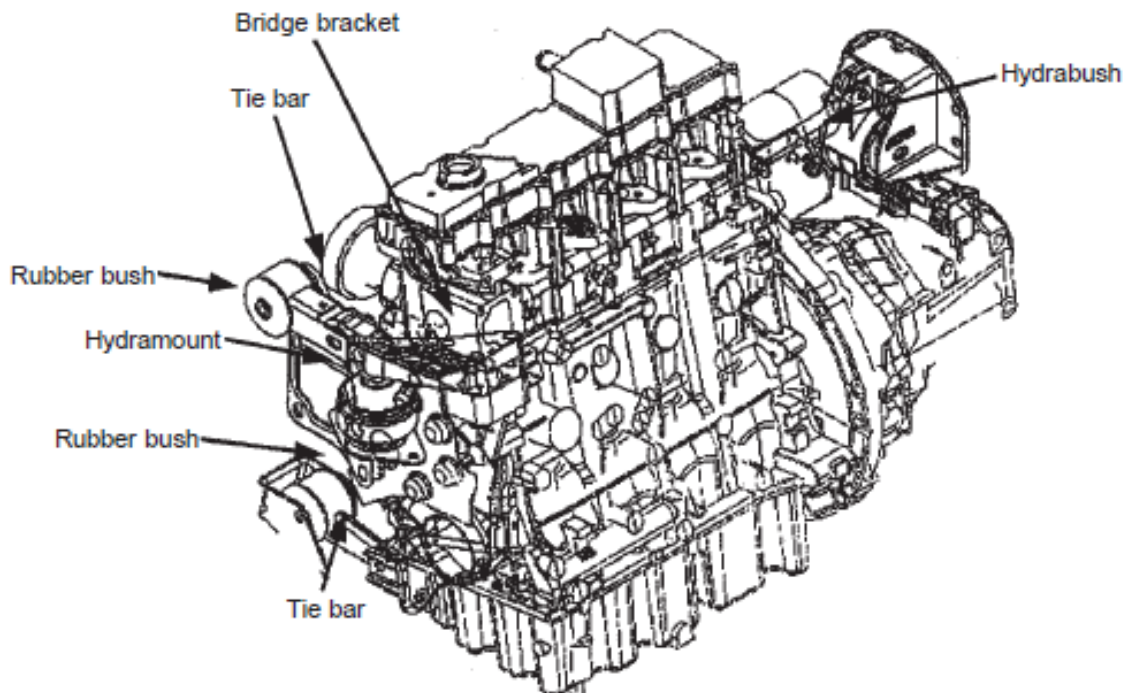


Figure 6. Engine mounting system (courtesy of Rover Group Ltd) [1]

1.5.1 Elastomeric Engine Mounts

Main advantages of elastomeric engine mounts are that they are compact, cost effective, maintenance free and designed to provide vibration isolation in three directions.

In engine mount modeling and simulation for elastomeric engine mount usually the Voigt model is used as shown in figure 7a. Also, elastomer behavior can be described with Maxwell model as shown in figure 7b.

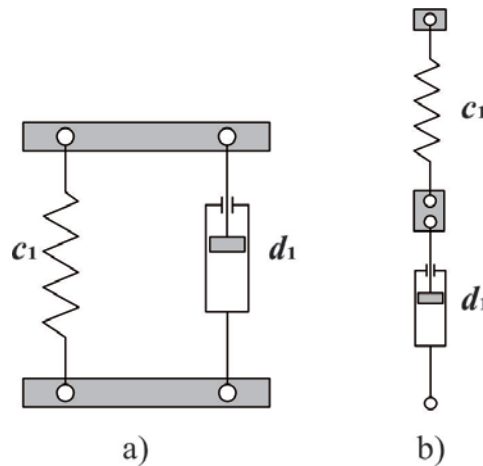


Figure 7. a) Kelvin – Voigt model and b) Maxwell model which are usually used for describing elastomeric engine mount behavior

Main limitations of elastomeric engine mounts is actual behavior of elastomeric mount which gives higher stiffness and higher damping values on higher frequencies which is opposite of earlier defined design target. It is designer's job to make trade – off between low and high frequency behavior of elastomeric engine mount.

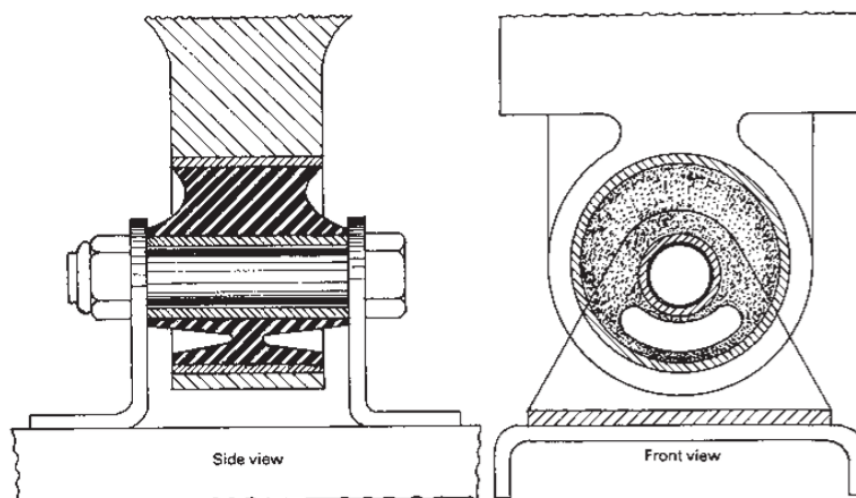


Figure 8. Schematic representation of elastomeric engine mount [6]

1.5.2 Hydraulic engine mount

According to [10] hydraulic engine mounts are divided into passive, semi-active or adaptive and active mounts.

The passive engine mount consists of two chambers filled with fluid which is typically a mixture of ethylene glycol and water. Between two chambers are decoupler and inertia track. Schematic representation of a hydraulic engine mount is shown in figure 9.

Upper chamber is bound with elastomeric structure and on the bottom by a steel plate on which the inertia track and decoupler are fixed. Elastomeric structure carries engine weight and acts as the main load carrying component, and an actuator of the fluid motion within the engine mount.

Decoupler plate oscillates in a small intervals. Hydraulic mount limits the volume of fluids that can pass with low resistance between upper and lower chamber. When the decoupler plate touches the lower bottom in the cage, the fluid is restricted to pass through the inertia track which is the path with higher resistance.

During small amplitude excitations the fluid passes through the decoupler, giving the mount low damping and stiffness characteristics which is good for high frequency excitations. For large amplitude excitations, the resistance and mass of the fluid passing through the inertia track increases the mount's stiffness and damping characteristics which is good for low frequency excitations. In general the decoupler causes the mount to have the desired amplitude dependency.

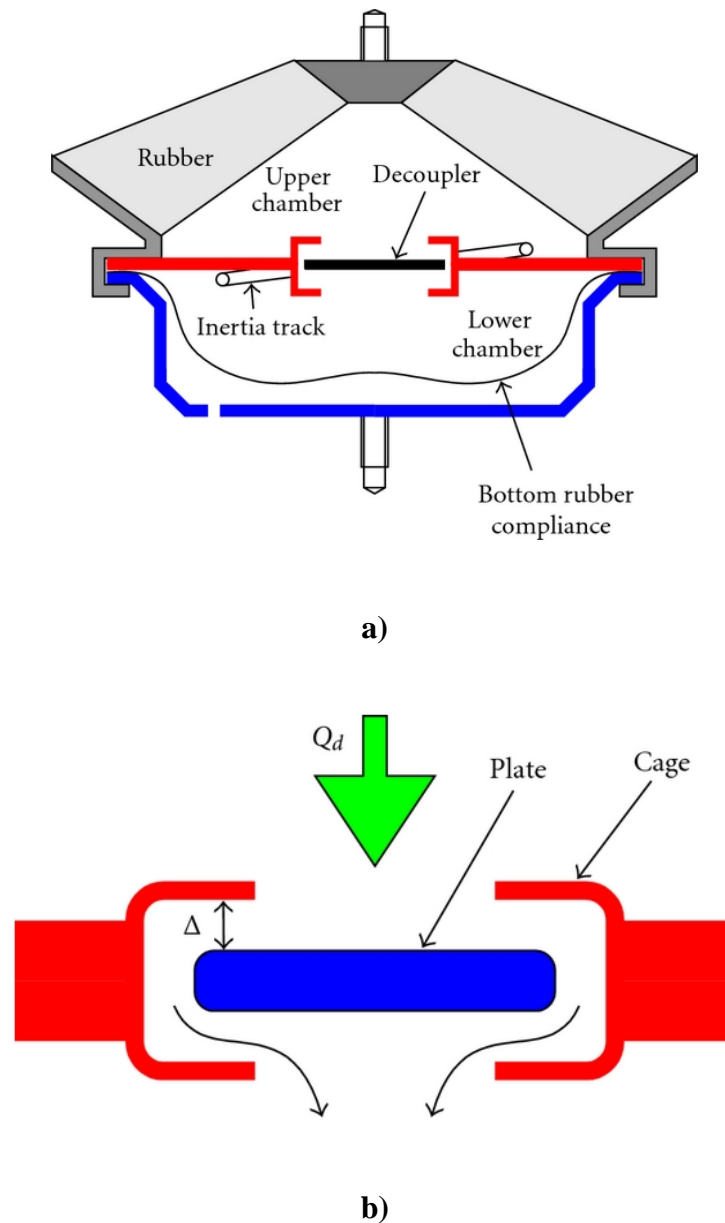


Figure 9. a) Schematic representation of hydraulic engine mount
b) Decoupler mechanism

Semi active or adaptive engine mounts control hydraulic engine mount properties by using electromechanical devices. Changing properties such as the chamber compliance and inertia track length alter the dynamic characteristics of the mount [10].

Active hydraulic engine mount create counteracting dynamic force to suppress transmission of the system disturbance forces. A typical active mount consists of a passive mount (elastomer or hydraulic), force generating actuator, a structural vibration sensor and an electronic controller. Passive mounts are used to support the engine in the event of an actuator failure [10].

1.6 Frequency response functions

Frequency response function (**FRF**) is a mathematical representation of the relationship between the input and the output of a system and it is used to characterize dynamic behavior of the mechanical system. In the vibration and acoustic analysis different kind of frequency response functions are used as shown in table 2.

For example, to measure response of engine mounting system dynamic stiffness is usually used and for performing modal analysis of some mechanical system accelerance frequency response function is usually used.

Table 1. FRF commonly used in vibration and acoustic analysis

| <i>Quantity</i> | <i>Input quantities</i> | <i>Relation</i> |
|--|---|---|
| Dynamic flexibility or Receptance $H(\omega)$ | Displacement $x(\omega)$ Force $F(\omega)$ | $H(\omega) = \frac{x(\omega)}{F(\omega)}$ |
| Mobility or mechanical admittance $Y(\omega)$ | Velocity $v(\omega)$ Force $F(\omega)$ | $Y(\omega) = \frac{v(\omega)}{F(\omega)}$ |
| Accelerance $A(\omega)$ | Acceleration $a(\omega)$ Force $F(\omega)$ | $A(\omega) = \frac{a(\omega)}{F(\omega)}$ |
| Dynamic stiffness $K(\omega)$ | Displacement $x(\omega)$ Force $F(\omega)$ | $K(\omega) = \frac{F(\omega)}{x(\omega)}$ |
| Mechanical impedance $Z(\omega)$ | Velocity $v(\omega)$ Force $F(\omega)$ | $Z(\omega) = \frac{F(\omega)}{v(\omega)}$ |
| Acoustic impedance $Z(\omega)$ | Acoustic volume flow rate $Q(\omega)$ Acoustic pressure $p(\omega)$ | $Z(\omega) = \frac{p(\omega)}{Q(\omega)}$ |
| Specific impedance $Z(\omega)$ | Acoustic particle velocity $u(\omega)$ Acoustic pressure $p(\omega)$ | $Z(\omega) = \frac{p(\omega)}{u(\omega)}$ |

Frequency response function used in this study is dynamic stiffness described in section 1.7.

1.7 Dynamic stiffness

Two types of dynamic stiffness are used in measurements and they are shown in figure 10:

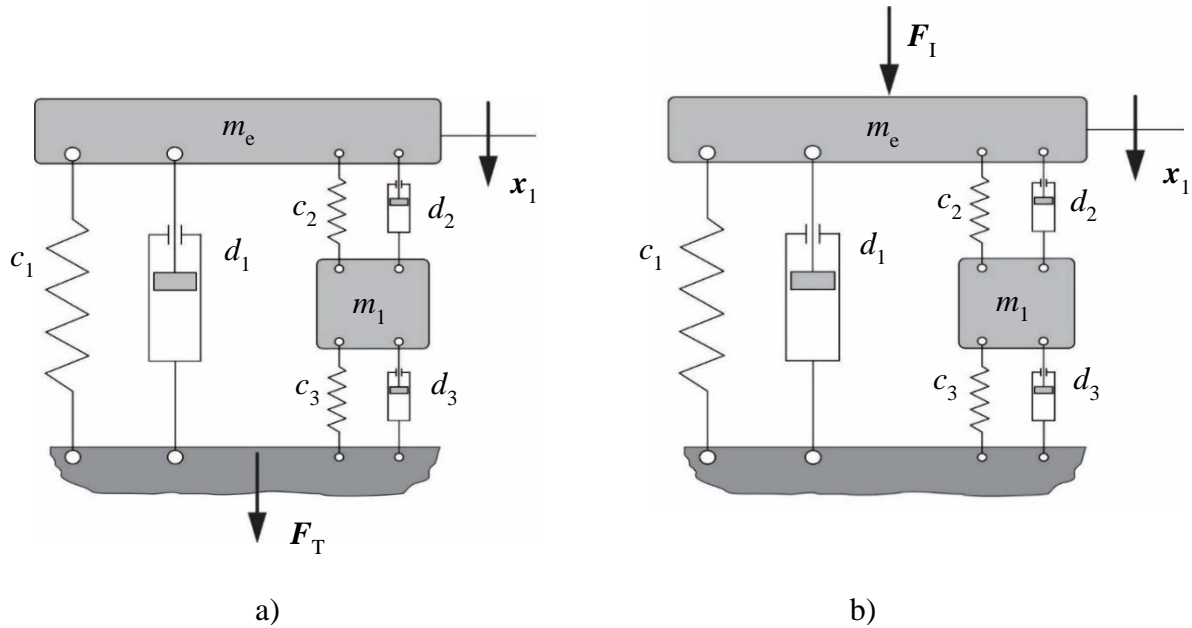


Figure 10. a) Cross point and b) input point dynamic stiffness

Main differences between cross point and input point dynamic stiffness is position where the force is measured. For determining cross point dynamic stiffness transmitted force is measured at ground which represents car chassis and for determining input point dynamic stiffness input force is measured. This results with major difference that input point dynamic stiffness is a function of an engine mass.

Equation to calculate cross point dynamic stiffness:

$$K_{CP} = \frac{F_T}{\hat{X}_1} \quad (1)$$

Equation to calculate input point dynamic stiffness:

$$K_{IP} = \frac{F_1}{\hat{X}_1} \quad (2)$$

Transmitted force for cross point stiffness is written in equation (10) and input force for input point stiffness is equal to:

$$F_1 = m_e \cdot \ddot{x}_1 + d_1 \cdot \dot{x}_1 + d_2 \cdot (\dot{x}_1 - \dot{x}_2) + c_1 \cdot x_1 + c_2 \cdot (x_1 - x_2) \quad (3)$$

Engine mass dependency of input dynamic stiffness is shown in equation (3).

All calculated dynamic stiffness of the mathematical models and dynamic stiffness obtained from measurements data is **cross point dynamic stiffness**.

1.8 Engine mount measurement procedure

Dynamic stiffness properties of engine mounts in frequency domain can be determined by using servo controlled hydraulic rate machine [11], as shown in figure 11.

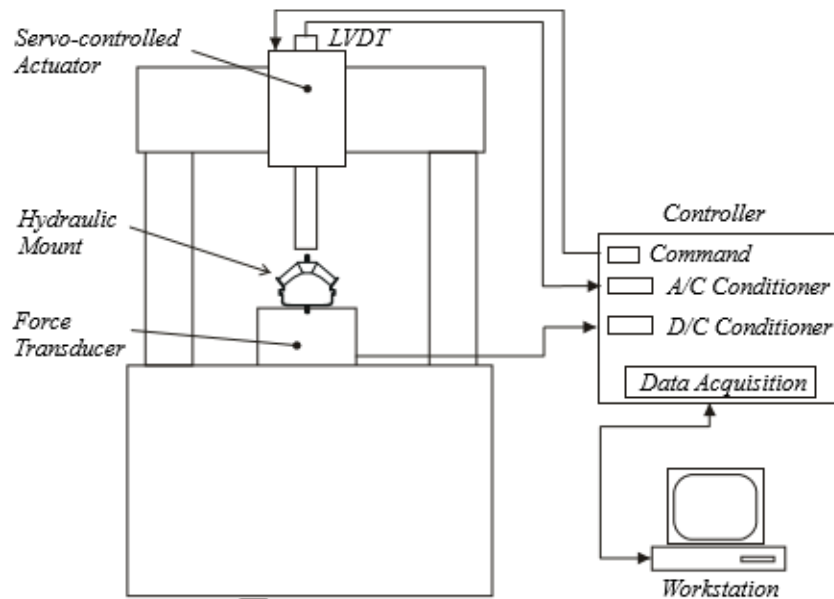


Figure 11. Measurement procedure of dynamic stiffness [13]

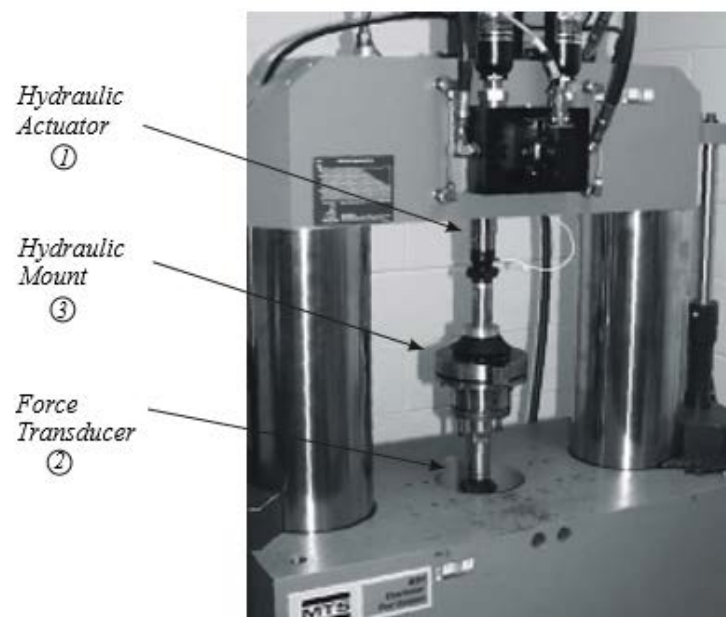


Figure 12. Illustration of MTS 1000-Hz rate machine that can be used to measure cross point dynamic stiffness [13]

Before starting of dynamic testing procedure, a static preload, or mean force, is applied to represent the static mass of the engine. During the testing procedure engine mount is excited with displacement excitation which is defined as sine wave at a predetermined amplitude and frequency. The transmitted force at the mount base is measured using a force transducer. After digital data processing, collected and processed data is used to determine amplitude of cross point dynamic stiffness K^* and phase ϕ . In figure 13 collected and processed data in a complex plane is shown.

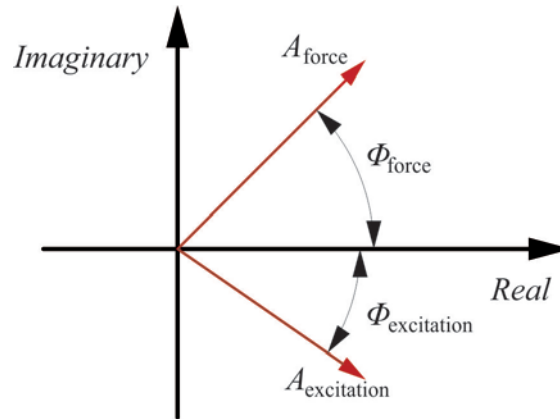


Figure 13. Measurement data shown in complex plane

$$K^* = \frac{A_{\text{force}}}{A_{\text{excitation}}} \quad (4)$$

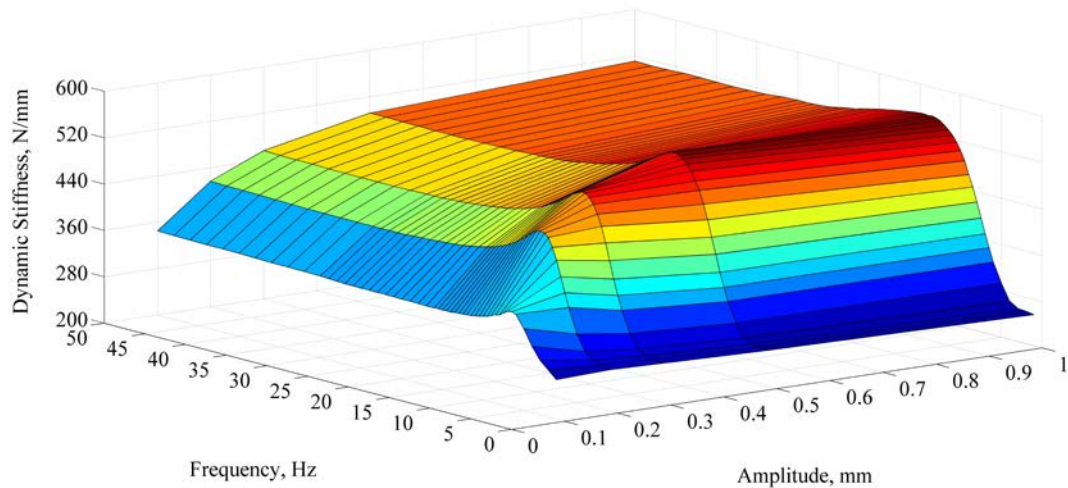
$$\phi = \phi_{\text{force}} - \phi_{\text{excitation}} \quad (5)$$

It is possible to calculate real and imaginary part of measured cross point dynamic stiffness.

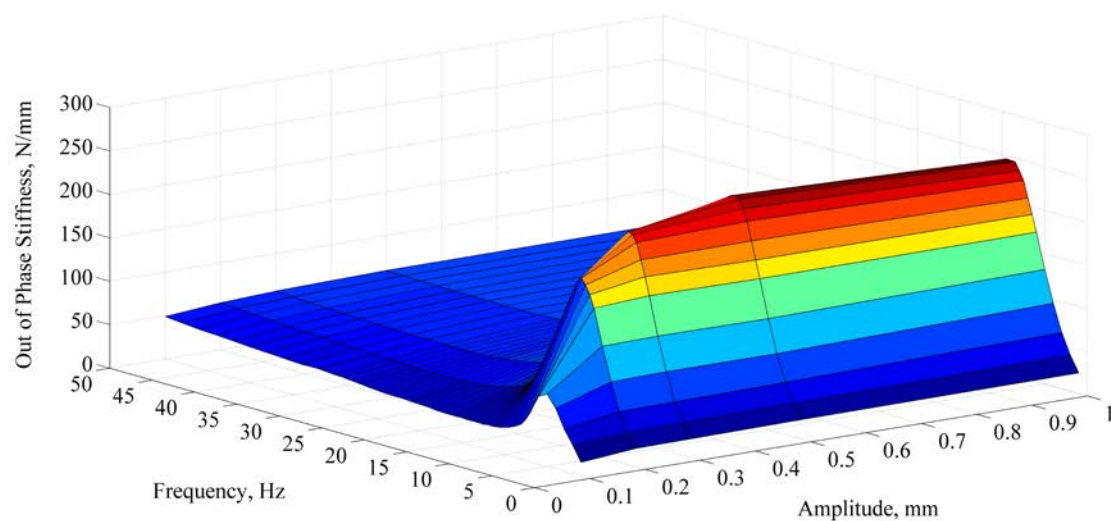
$$K_{\text{real}} = K^* \cdot \cos(\phi) \quad (6)$$

$$K_{\text{imag}} = K^* \cdot \sin(\phi) \quad (7)$$

In figure 14 the measurement data of cross point dynamic stiffness is shown. Measured dynamic stiffness is amplitude and frequency dependent. Measurement data is provided by engine mount manufacturer.



a)



b)

Figure 14. Cross point dynamic stiffness measurement (frequency and amplitude dependency)
a) real part and b) imaginary part

1.9 Idle speed vibration problem definition

In this study low frequency vibration response is also analyzed. This is important because idle speeds for four cylinder engines are in the range of 8–20 Hz producing dominant frequency components in the range of 16–40 Hz (2nd order). Since the primary bending mode of the passenger car can be less than 20 Hz it is obvious that it is easy to excite car body resonance at idle if engine mounts are not carefully designed and analyzed.

1.10 Thesis outcome

Main objective of this thesis is the contribution to the better understanding of hydraulic and elastomeric engine mount behavior and modeling. One of the main target of the thesis is to describe hydraulic and elastomeric engine mounts dynamic stiffness with the same mathematical model on low and high frequencies. For that purpose different mathematical models that are able to describe frequency dependency of the engine mount dynamic stiffness are considered. Amplitude and temperature dependency of dynamic stiffness were not considered in this study. For the mathematical modeling purposes the optimization procedure is also developed. Optimization procedure is based on the minimization of the norm of differences between transmitted load calculated from the mathematical model and measured transmitted load.

After studying different mathematical models, one mathematical model is chosen based on optimization results.

Chosen mathematical model is used to implement measurements data from frequency domain into time domain in *AVL Excite Power Unit* [1] and to make a numerical simulation of a gasoline internal combustion engine. Engine mounts vibration response measurements data of simulated engine are available and simulation results are compared with the measurements. Also, one of the targets is to set workflow for hydraulic and elastomeric engine mount usage in the internal combustion engine simulation.

2. Engine mounts mathematical model

The first step in vibration analysis is to develop mathematical model. Developing of mathematical model provide the basis of all vibration studies at the design stage. The general aim of the mathematical model is to represent the dynamics of a system by one or more differential equations. In this study the aim is to represent the behavior of elastomeric and hydraulic engine mounts.

2.1 Modeling frequency dependency of the engine mount dynamic stiffness

As mentioned earlier, hydraulic and rubber engine mounts are frequency, amplitude and temperature dependent. Describing frequency dependency can be achieved by using simple mass, spring and damper model as shown in figure 15.

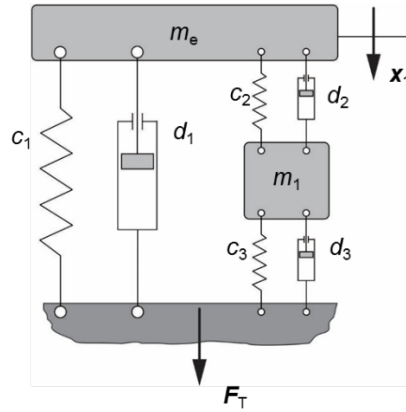


Figure 15. Single mass oscillator

The first step is to define the equations of motion for the single mass oscillator dynamic system shown in figure 15.

$$m_e \cdot \ddot{x}_1 + d_1 \cdot \dot{x}_1 + d_2 \cdot (\dot{x}_1 - \dot{x}_2) + c_1 \cdot x_1 + c_2 \cdot (x_1 - x_2) = 0 \quad (8)$$

$$m_1 \cdot \ddot{x}_2 + d_3 \cdot \dot{x}_2 - d_2 \cdot (\dot{x}_1 - \dot{x}_2) + c_3 \cdot x_2 - c_2 \cdot (x_1 - x_2) = 0 \quad (9)$$

The equations (5) and (6) can be converted to frequency domain using equations:

$$x(t) = \hat{X} \cdot e^{i\omega t} \quad (10)$$

$$\dot{x}(t) = i\omega \cdot \hat{X} \cdot e^{i\omega t} \quad (11)$$

$$\ddot{x}(t) = -\omega^2 \cdot \hat{X} \cdot e^{i\omega t}, \quad (12)$$

where ω is the angular frequency and is equal to:

$$\omega = 2 \cdot \pi \cdot f \tag{13}$$

Transmitted force F_T to ground is equal to:

$$F_T = c_1 \cdot \hat{X}_1 + i\omega \cdot d_1 \cdot \hat{X}_1 + c_3 \cdot \hat{X}_2 + i\omega \cdot d_3 \cdot \hat{X}_2 \tag{14}$$

X_1 can be expressed as a function of X_2 :

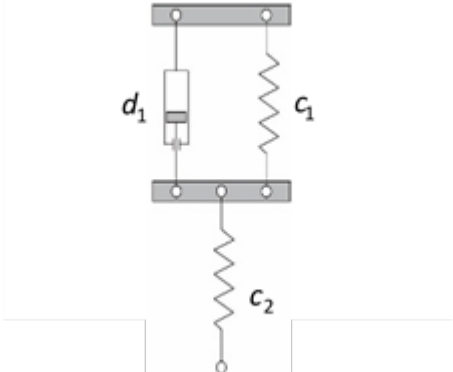
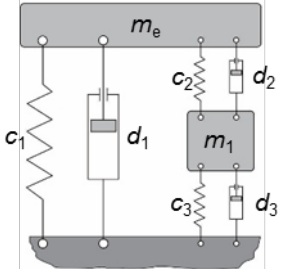
$$F_T = c_1 \cdot \hat{X}_1 + i\omega \cdot d_1 \cdot \hat{X}_1 + c_3 \cdot \hat{X}_2 + i\omega \cdot d_3 \cdot \hat{X}_2 \tag{15}$$

Cross point dynamic stiffness now is equal to:

$$K = \frac{F_T}{\hat{X}_1} \tag{16}$$

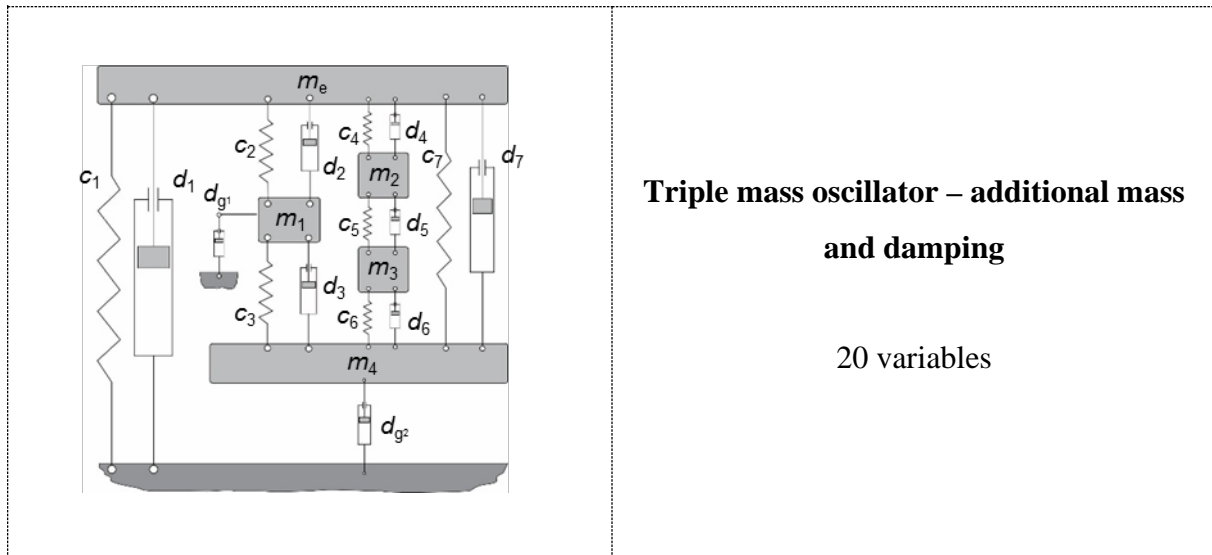
During the study 10 different mathematical models with different number of variables were considered as described in table 2.

Table 2. Considered mathematical models during study

| | |
|---|--|
|  | <p>Standard linear solid (SLS) joint</p> <p>3 variables</p> |
|  | <p>Single mass oscillator</p> <p>7 variables</p> |

| | |
|--|--|
| | <p>Dual mass oscillator</p> <p>10 variables</p> |
| | <p>Triple mass oscillator – series connection</p> <p>13 variables</p> |
| | <p>Triple mass oscillator – parallel connection</p> <p>15 variables</p> |
| | <p>Quad mass oscillator</p> <p>18 variables</p> |

| | |
|--|--|
| | <p>Penta mass oscillator</p> <p>23 variables</p> |
| | <p>Single mass oscillator – additional mass and damping</p> <p>12 variables</p> |
| | <p>Dual mass oscillator –additional mass and damping</p> <p>16 variables</p> |



2.2 Parameter identification

For all mentioned mathematical models in table 2 it is necessary to determine parameters of mathematical models ($c_1, d_1, c_2, d_2, m_1, c_3, d_3, c_4, d_4 \dots$).

Optimization procedure to determine parameter values in each presented mathematical model is established. Optimization procedure involves finding the difference between the transmitted force computed by the theoretical models and the measured force [11].

Objective function is written as:

$$\|F_{\text{theory}} - F_{\text{measure}}\|, \quad (17)$$

where F_{theory} is the time history of the transmitted force to the calculated from the theoretical model and F_{measure} the time history of the measured force for a specified input. The Euclidian norm of the difference between the time history of the two forces is minimized, which results in finding the relevant parameters of the corresponding models [11].

Force is equal to:

$$F = k \cdot x \quad (18)$$

If we assume that displacement x is 1 mm, then equation (17) can be written as:

$$\|k_t - k_m\|, \quad (19)$$

where k_t is the theoretical calculated stiffness and k_m is measured stiffness.

Only constraints in optimization process is that mathematical model parameters cannot have negative value.

The Sequential Quadratic Programming (SQP) algorithm is used to the optimization problem. The '*fmincon*' function in MATLAB® is used to minimize the function in equation (19).

2.3 Results of the mathematical model parameter optimization

During this study all mentioned mathematical models for describing hydraulic and elastomeric engine mounts were considered. Because of the large number of the mathematical models with which measured engine mount dynamic stiffness can be described, only some of the results are shown.

SLS joint, single and dual mass oscillators are shown in results for describing low frequency behavior of elastomeric engine mounts because with more complicated models it is not possible to obtain better results. High frequency behavior of elastomeric engine mounts can be successfully described with triple mass oscillator.

Single, dual and triple mass oscillators are shown for describing low frequency behavior of hydraulic engine mounts. For high frequency behavior more complicated models were used and shown in results.

Low frequency behavior is up to 50 Hz, depends on available measurements data and high frequency behavior is with frequencies larger than 50 Hz. Usually, measurements for high frequency response are up to 400 Hz, but during this study some high frequency measurements are up to 700 Hz.

2.3.1 Measurement data

All measurement data available for elastomeric and hydraulic engine mounts shown in this section are provided by engine mounts manufacturer.

7 different measurements sets for 2 different engines are available – 4 measurements sets (2 low frequency and 2 high frequency) for elastomeric engine mounts and 3 measurements sets (2 low frequency and 1 high frequency) for hydraulic engine mount. Measurement set for gasoline engine that is studied in this thesis is detailed described in section 4. Results shown in this section are measurements set for gasoline engine that is not studied in this thesis. Also, to present results of describing high frequency behavior of hydraulic engine mounts, some results that are presented later in section 4 are included in this section. In figure 16 hydraulic and

elastomeric engine mount coordinate system is defined. All results shown in this section are results in axial direction Z.

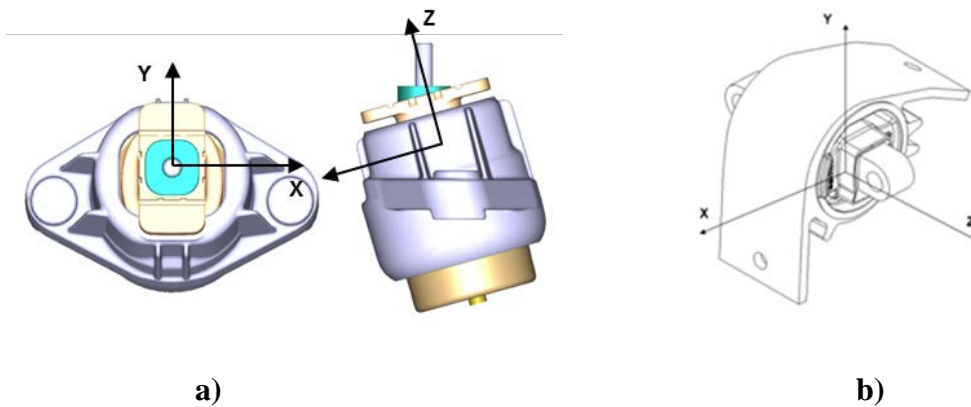


Figure 16. Schematic representation of a) hydraulic and b) elastomeric engine mount and definition of engine mount coordinate system

2.3.2 Elastomeric engine mount – Low frequency behavior optimization



Standard Linear Solid (SLS) joint

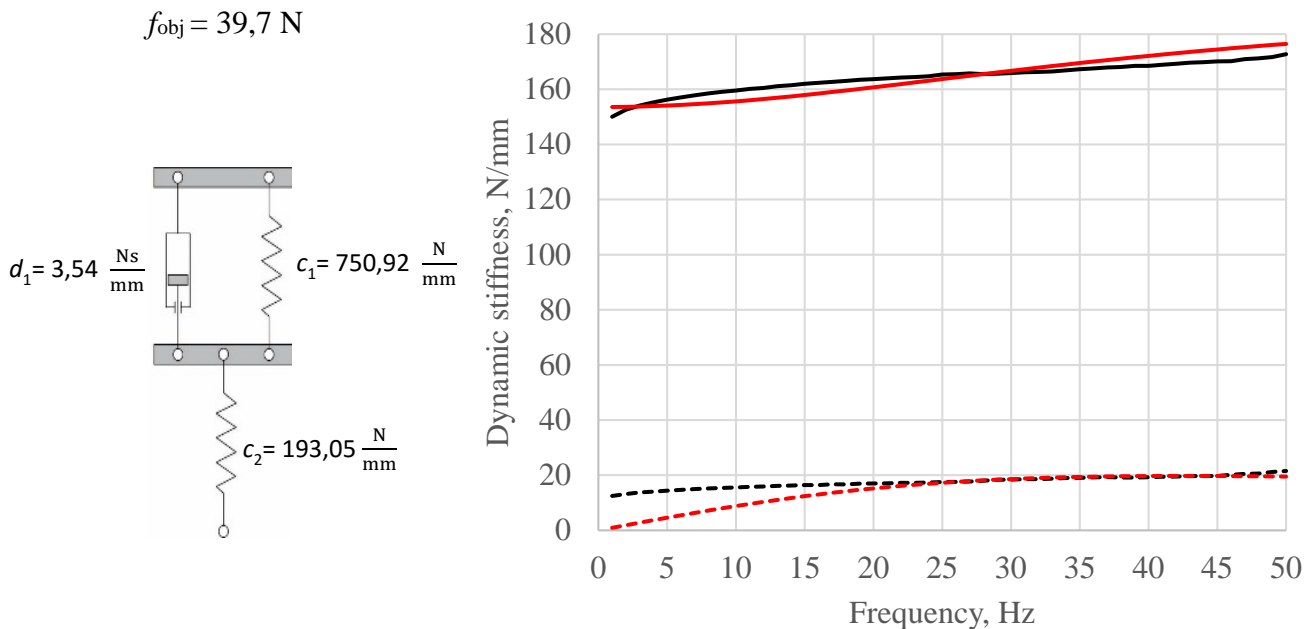


Figure 17. Describing low frequency behavior of **elastomeric engine mount** dynamic stiffness by using SLS joint

— Measurement -- Real - - - - Measurement -- Imaginary
 — Mathematical model -- Real - - - - Mathematical model -- Imaginary

Single mass oscillator

$f_{obj} = 21,68 \text{ N}$
 $c_1 = 104,5 \text{ N/mm}$
 $d_1 = 0 \text{ Ns/mm}$
 $c_2 = 66 \text{ N/mm}$
 $d_2 = 0,061 \text{ Ns/mm}$
 $m_1 = 3,2 \text{ kg}$
 $c_3 = 118 \text{ N/mm}$
 $d_3 = 3,56 \text{ Ns/mm}$

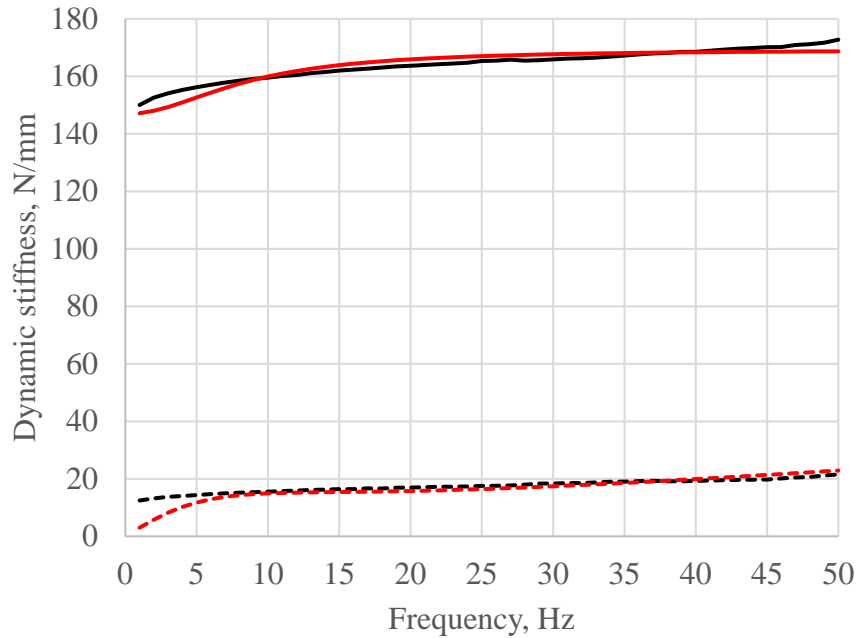


Figure 18. Describing low frequency behavior of **elastomeric engine mount** dynamic stiffness by using single mass oscillator

Dual mass oscillator

$f_{obj} = 11,2 \text{ N}$
 $c_1 = 0 \text{ N/mm}$
 $d_1 = 0,1565 \text{ Ns/mm}$
 $c_2 = 0 \text{ N/mm}$
 $d_2 = 272,54 \text{ Ns/mm}$
 $m_1 = 394 \text{ kg}$
 $c_3 = 154,9 \text{ N/mm}$
 $d_3 = 0,393 \text{ Ns/mm}$
 $m_2 = 149,7 \text{ kg}$
 $c_4 = 3842 \text{ N/mm}$
 $d_4 = 109,16 \text{ Ns/mm}$

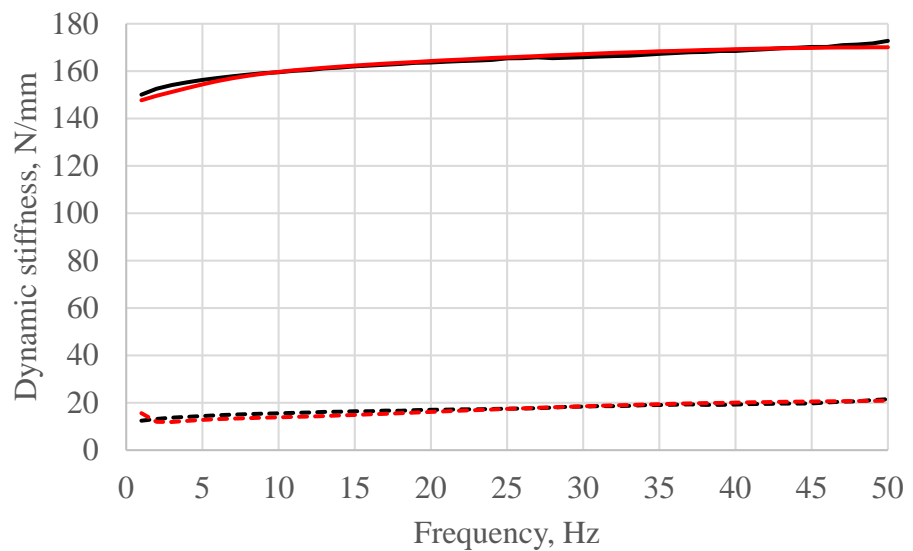


Figure 19. Describing low frequency behavior of **elastomeric engine mount** dynamic stiffness by using dual mass oscillator

To describe low frequency behavior of **elastomeric engine mount** by using SLS joint with single degree of freedom which is usually used in this purposes generate satisfying results as shown in figure 17.

For more accurate description of elastomeric mount low frequency behavior it is recommended to use single or dual mass oscillator which low frequency behavior is shown in figures 18 and 19.

Optimization of single or dual mass oscillator is robust, so it is possible to use them without any difficulties.

2.3.3 Hydraulic engine mounts – Low frequency behavior optimization

— Measurement -- Real - - - - Measurement -- Imaginary
 — Mathematical model -- Real - - - - Mathematical model -- Imaginary

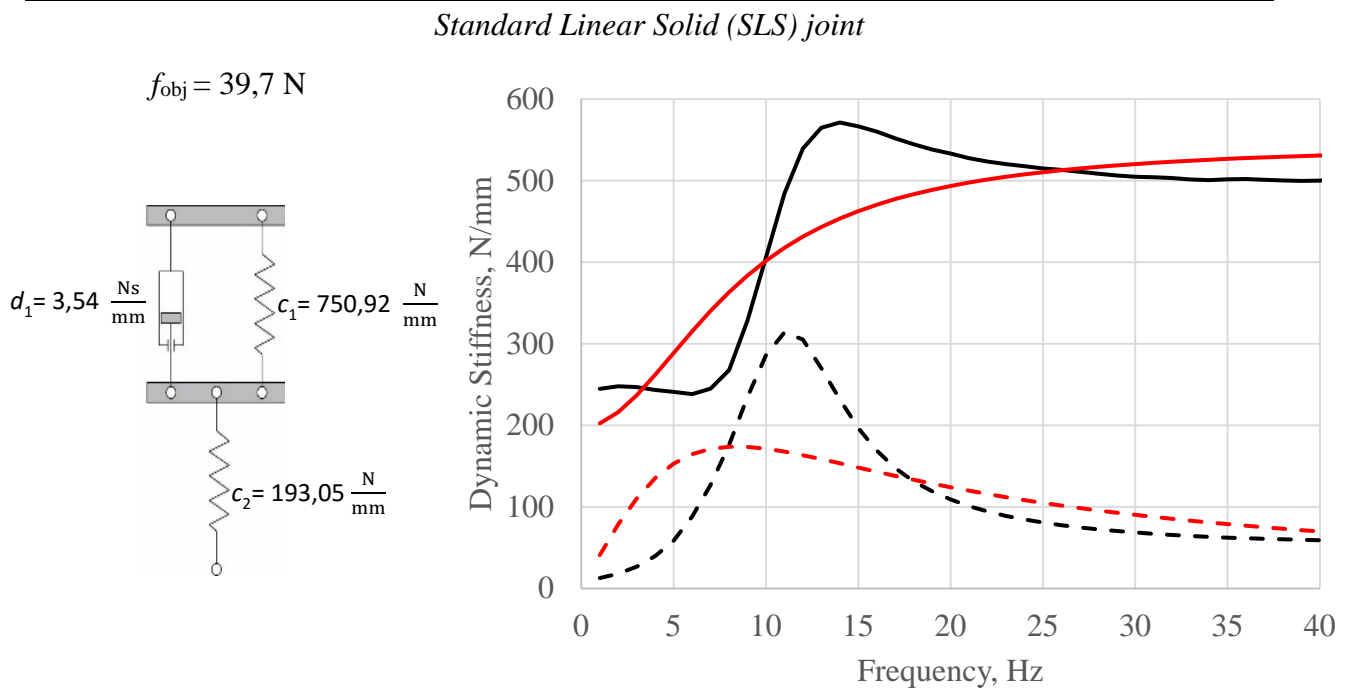


Figure 20. Describing low frequency behavior of **hydraulic engine mount** dynamic stiffness by using SLS joint

— Measurement -- Real - - - - Measurement -- Imaginary
 — Mathematical model -- Real - - - - Mathematical model -- Imaginary

Single mass oscillator

$f_{obj} = 166,6 \text{ N}$
 $c_1 = 269,07 \text{ N/mm}$
 $d_1 = 0 \text{ Ns/mm}$
 $c_2 = 216,64 \text{ N/mm}$
 $d_2 = 0,212 \text{ Ns/mm}$
 $m_1 = 43,7 \text{ kg}$
 $c_3 = 0 \text{ N/mm}$
 $d_3 = 2,077 \text{ Ns/mm}$

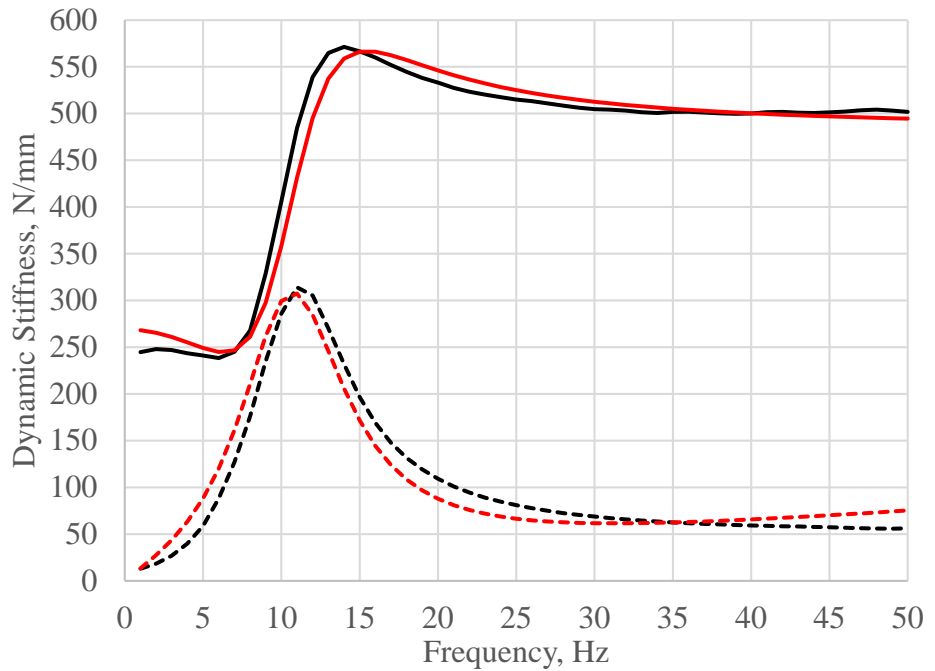


Figure 21. Describing low frequency behavior of **hydraulic engine mount** dynamic stiffness by using single mass oscillator

Dual mass oscillator

$f_{obj} = 207 \text{ N}$
 $c_1 = 244 \text{ N/mm}$
 $d_1 = 0,705 \text{ Ns/mm}$
 $c_2 = 5521,3 \text{ N/mm}$
 $d_2 = 13 \text{ Ns/mm}$
 $m_1 = 58,6 \text{ kg}$
 $c_3 = 0 \text{ N/mm}$
 $d_3 = 2,8 \text{ Ns/mm}$
 $m_2 = 200 \text{ kg}$
 $c_4 = 1370,6 \text{ N/mm}$
 $d_4 = 11,81 \text{ Ns/mm}$

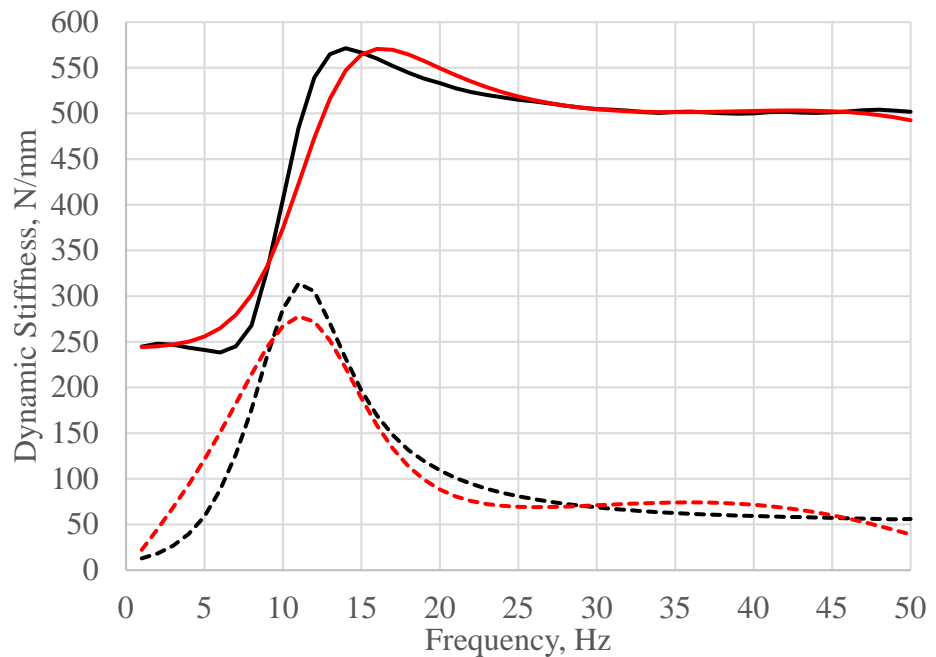


Figure 22. Describing low frequency behavior of **hydraulic engine mount** dynamic stiffness by using dual mass oscillator

— Measurement -- Real - - - - Measurement -- Imaginary
 — Mathematical model -- Real - - - - Mathematical model -- Imaginary

Triple mass oscillator – parallel connection

$f_{obj} = 185,1 \text{ N}$
 $c_1 = 224,3 \text{ N/mm}$
 $d_1 = 0,871 \text{ Ns/mm}$
 $c_2 = 46,2 \text{ N/mm}$
 $d_2 = 0 \text{ Ns/mm}$
 $m_1 = 3,02 \text{ kg}$
 $c_3 = 360,2 \text{ N/mm}$
 $d_3 = 0,273 \text{ Ns/mm}$
 $c_4 = 12,06 \text{ N/mm}$
 $d_4 = 0,8 \text{ Ns/mm}$
 $m_2 = 2,2 \text{ kg}$
 $c_5 = 154,3 \text{ N/mm}$
 $d_5 = 0,952 \text{ Ns/mm}$
 $m_3 = 36,6 \text{ kg}$
 $c_6 = 137,35 \text{ N/mm}$
 $d_6 = 8,97 \text{ Ns/mm}$

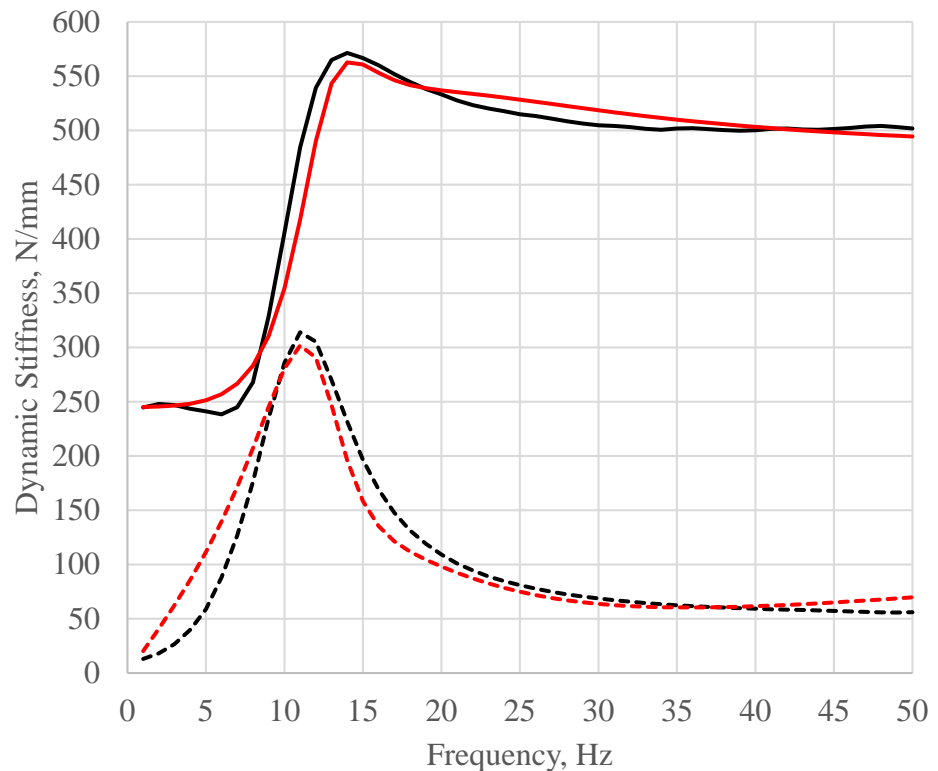


Figure 23. Describing low frequency behavior of **hydraulic engine mount** dynamic stiffness by using triple mass oscillator

To describe low frequency behavior it is not enough to use SLS joint with single degree of freedom as shown in figure 20. When low frequency response of engine mount is studied it is necessary to accurately describe damping. Damping values on each frequency is contained in imaginary part of dynamic stiffness. As mentioned, idle speeds for four cylinder engines are in the range of 8 – 20 Hz producing dominant frequency components in the range of 16 – 40 Hz (2nd order excitation) and car body bending mode is often under 20 Hz, so it is necessary to describe low frequency damping as accurately as possible to predict behavior of entire vehicle structure for optimum vehicle design. Low frequency dynamic stiffness of engine mount can be described by using single mass oscillator 21. Using more complicated models with more variables does not obtain better results as shown in figures 22 and 23 for dual and triple mass oscillators.

2.3.4 Elastomeric engine mounts – High frequency behavior optimization

— Measurement -- Real - - - - Measurement -- Imaginary
 — Mathematical model -- Real - - - - Mathematical model -- Imaginary

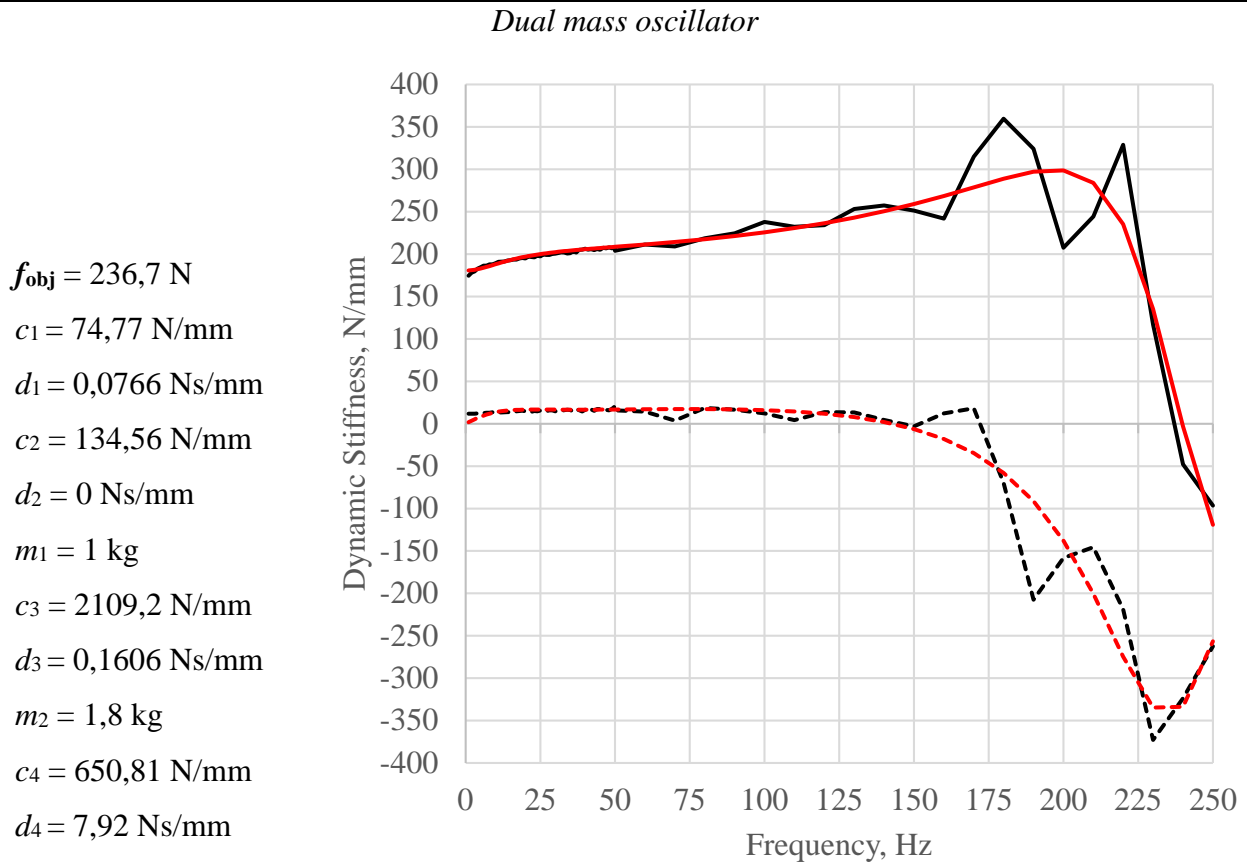


Figure 24. Describing high frequency behavior of **elastomeric engine mount** dynamic stiffness by using dual mass oscillator

— Measurement -- Real - - - - Measurement -- Imaginary
 — Mathematical model -- Real - - - - Mathematical model -- Imaginary

Triple mass oscillator – parallel connection

$f_{obj} = 128,8 \text{ N}$
 $c_1 = 38,4 \text{ N/mm}$
 $d_1 = 0,071 \text{ Ns/mm}$
 $c_2 = 127,9 \text{ N/mm}$
 $d_2 = 0,0467 \text{ Ns/mm}$
 $m_1 = 0,208 \text{ kg}$
 $c_3 = 297,41 \text{ N/mm}$
 $d_3 = 0,0075 \text{ Ns/mm}$
 $c_4 = 457,86 \text{ N/mm}$
 $d_4 = 2,375 \text{ Ns/mm}$
 $m_2 = 3,2 \text{ kg}$
 $c_5 = 594,9 \text{ N/mm}$
 $d_5 = 0,0129 \text{ Ns/mm}$
 $m_3 = 0,468 \text{ kg}$
 $c_4 = 71,76 \text{ N/mm}$
 $d_4 = 0,0327 \text{ Ns/mm}$

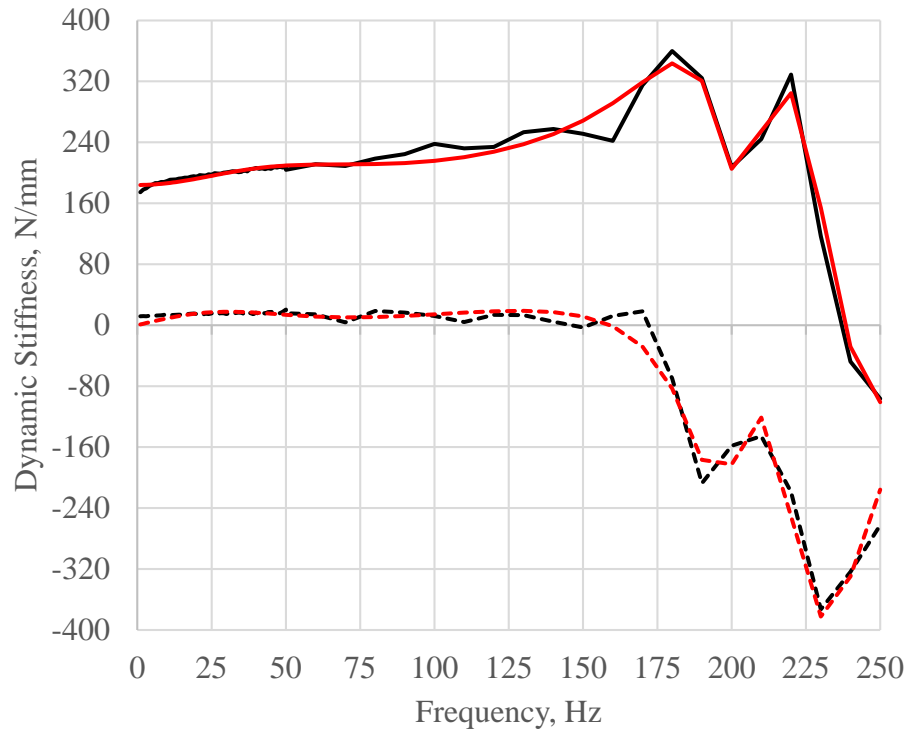


Figure 25. Describing high frequency behavior of **elastomeric engine mount** dynamic stiffness by using triple mass oscillator

To describe high frequency behavior of elastomeric engine mount it is recommended to use triple mass oscillator as shown in figure 25.

Main difference between dual mass oscillator and triple mass oscillator mathematical model for describing high frequency behavior of elastomeric engine mounts is that with triple mass oscillator it is possible to describe more resonant peaks that occur on some frequencies due to engine mount excitation.

2.3.5 Hydraulic engine mount – High frequency behavior

— Measurement -- Real - - - - Measurement -- Imaginary
 — Mathematical model -- Real - - - - Mathematical model -- Imaginary

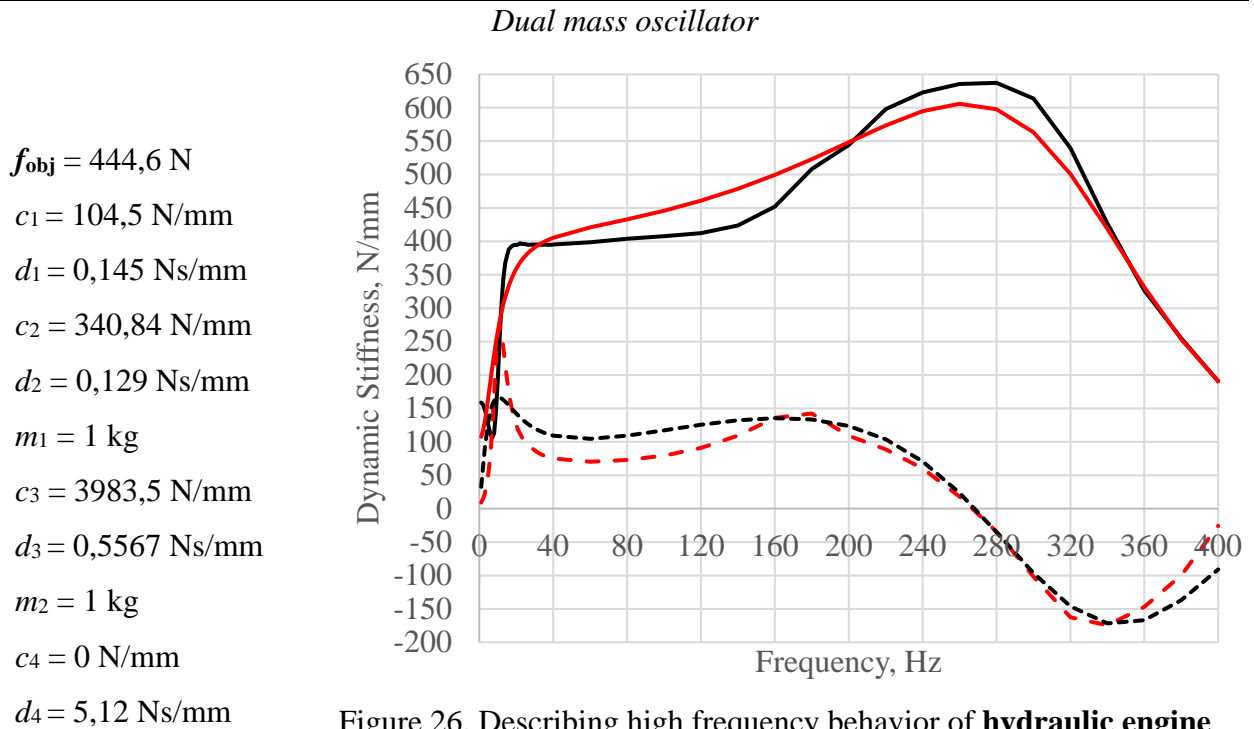


Figure 26. Describing high frequency behavior of **hydraulic engine mount** dynamic stiffness by using dual mass oscillator

— Measurement -- Real - - - - Measurement -- Imaginary
 — Mathematical model -- Real - - - - Mathematical model -- Imaginary

Triple mass oscillator – parallel connection

$f_{obj} = 128,8 \text{ N}$
 $c_1 = 54,18 \text{ N/mm}$
 $d_1 = 0,1 \text{ Ns/mm}$
 $c_2 = 0 \text{ N/mm}$
 $d_2 = 2,087 \text{ Ns/mm}$
 $m_1 = 200 \text{ kg}$
 $c_3 = 1545,4 \text{ N/mm}$
 $d_3 = 13,82 \text{ Ns/mm}$
 $c_4 = 28838 \text{ N/mm}$
 $d_4 = 7,18 \text{ Ns/mm}$
 $m_2 = 7,23 \text{ kg}$
 $c_5 = 217,1 \text{ N/mm}$
 $d_5 = 0,0209 \text{ Ns/mm}$
 $m_3 = 0,01 \text{ kg}$
 $c_4 = 99,51 \text{ N/mm}$
 $d_4 = 1,815 \text{ Ns/mm}$

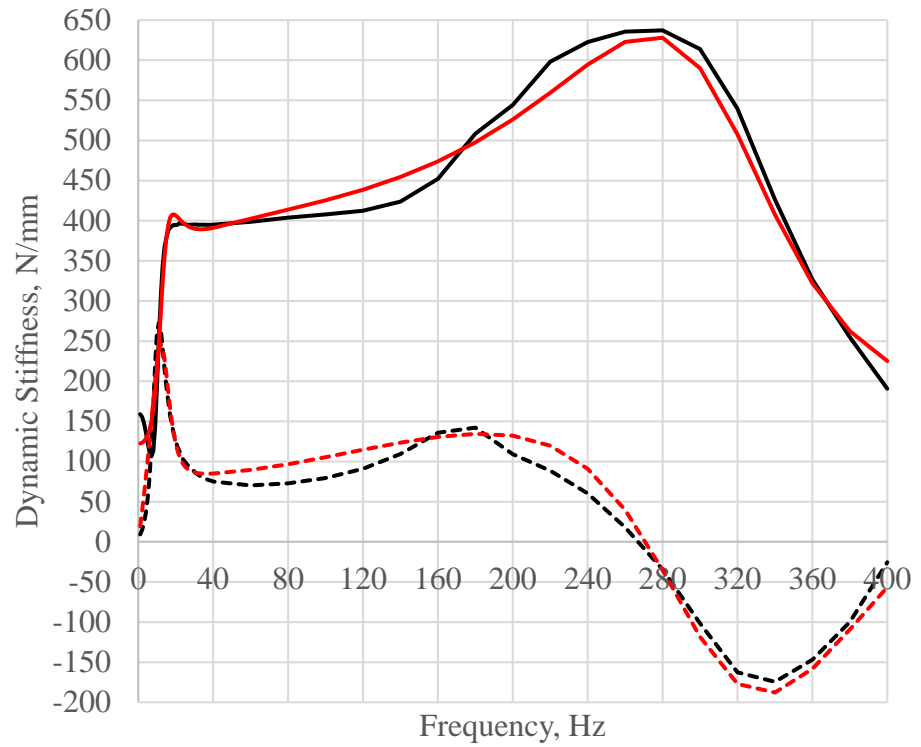


Figure 27. Describing high frequency behavior of **hydraulic engine mount** dynamic stiffness up to 400 Hz by using triple mass oscillator

— Measurement -- Real - - - - Measurement -- Imaginary
 — Mathematical model -- Real - - - - Mathematical model -- Imaginary

Triple mass oscillator – parallel connection

$f_{obj} = 128,8 \text{ N}$
 $c_1 = 54,18 \text{ N/mm}$
 $d_1 = 0,1 \text{ Ns/mm}$
 $c_2 = 0 \text{ N/mm}$
 $d_2 = 2,087 \text{ Ns/mm}$
 $m_1 = 200 \text{ kg}$
 $c_3 = 1545,4 \text{ N/mm}$
 $d_3 = 13,82 \text{ Ns/mm}$
 $c_4 = 28838 \text{ N/mm}$
 $d_4 = 7,18 \text{ Ns/mm}$
 $m_2 = 7,23 \text{ kg}$
 $c_5 = 217,1 \text{ N/mm}$
 $d_5 = 0,0209 \text{ Ns/mm}$
 $m_3 = 0,01 \text{ kg}$
 $c_4 = 99,51 \text{ N/mm}$
 $d_4 = 1,815 \text{ Ns/mm}$

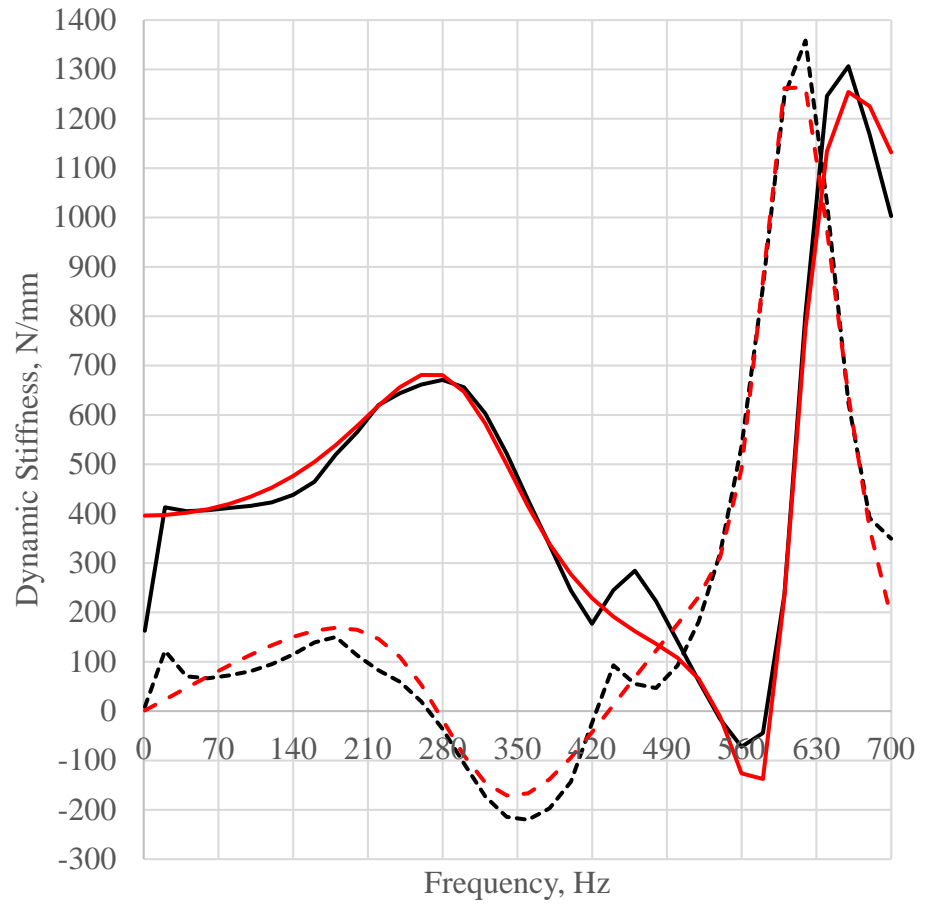


Figure 28. Describing high frequency behavior of **hydraulic engine mount** dynamic stiffness up to 700 Hz by using triple mass oscillator

— Measurement -- Real - - - - Measurement -- Imaginary
 — Mathematical model -- Real - - - - Mathematical model -- Imaginary

Penta mass oscillator

$$f_{obj} = 287,4 \text{ N}$$

$$c_1 = 200,2 \text{ N/mm}$$

$$d_1 = 0 \text{ Ns/mm}$$

$$c_2 = 519,45 \text{ N/mm}$$

$$d_2 = 0 \text{ Ns/mm}$$

$$m_1 = 0,05 \text{ kg}$$

$$c_3 = 17,2 \text{ N/mm}$$

$$d_3 = 0,2 \text{ Ns/mm}$$

$$c_4 = 47,93 \text{ N/mm}$$

$$d_4 = 0,005 \text{ Ns/mm}$$

$$m_2 = 0,015 \text{ kg}$$

$$c_5 = 0 \text{ N/mm}$$

$$d_5 = 0,0104 \text{ Ns/mm}$$

$$c_6 = 26,11 \text{ N/mm}$$

$$d_6 = 0,0016 \text{ Ns/mm}$$

$$m_3 = 13,1 \text{ kg}$$

$$m_4 = 0,01 \text{ kg}$$

$$c_7 = 71,97 \text{ N/mm}$$

$$d_7 = 8,582 \text{ Ns/mm}$$

$$c_8 = 126,55 \text{ N/mm}$$

$$d_8 = 0,0069 \text{ Ns/mm}$$

$$m_5 = 0,01 \text{ kg}$$

$$c_9 = 22,97 \text{ N/mm}$$

$$d_9 = 1,51 \text{ Ns/mm}$$

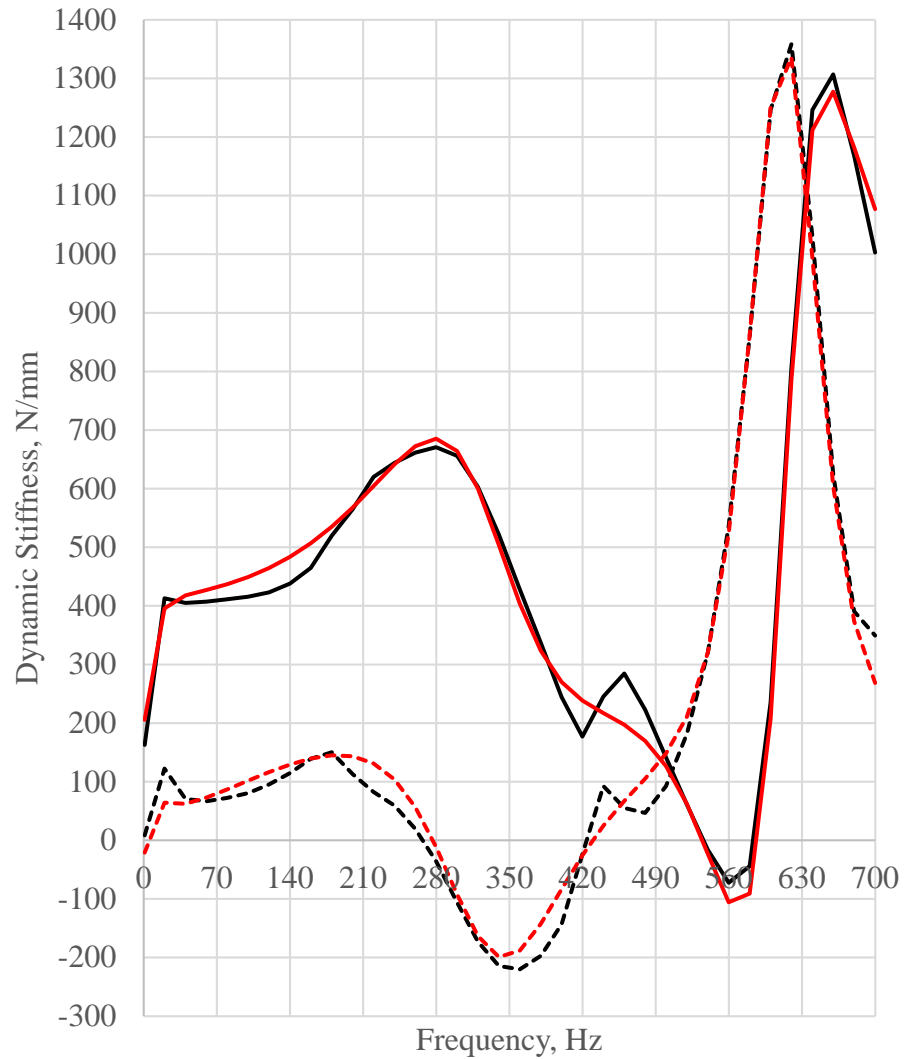


Figure 29. Describing high frequency behavior of **hydraulic engine mount** dynamic stiffness by using penta mass oscillator

To describe low and high frequency behavior for vibration analysis with only single set of mathematical model variables, it is recommended to use triple mass oscillator model because it is possible to successfully describe dynamic stiffness up to 400 Hz as shown 27.

Penta mass oscillator can successfully describe dynamic stiffness on low and high frequencies with single set of mathematical model parameters if the highest considered frequency is 700 Hz as shown in figure 29.

Optimization of penta mass oscillator mathematical model parameters is not robust and it is sensitive on boundary condition, so it is not easy to optimize these mathematical models and to implement them.

2.3.6 Conclusion

Based on the work done in this section triple mass oscillator with parallel mass connection is chosen for further investigation and implementation in *AVL Excite* environment because by using triple mass oscillator it is possible to describe frequency dependency of the engine mount dynamic stiffness on low and high frequencies.

Mathematical models with additional damping d_g that are presented in table 2 are also giving satisfying results with relatively small number of variables but since these are already implemented in *AVL Excite* as *EMO1 joint* they are not taken in further consideration.

3. Mathematical model verification

After choosing mathematical model it is necessary to make verification of the mathematical model by using available computer software that are used for numerical simulations: *AVL Excite*, *MSC Adams* and *MSC Nastran* (SOL 108).

First step is to formulate equations of motion and to calculate cross point dynamic stiffness analytically. Then next step is to make models in mentioned software with optimized parameter values and compare results with analytical solution.

Verification process diagram is shown in figure 30.

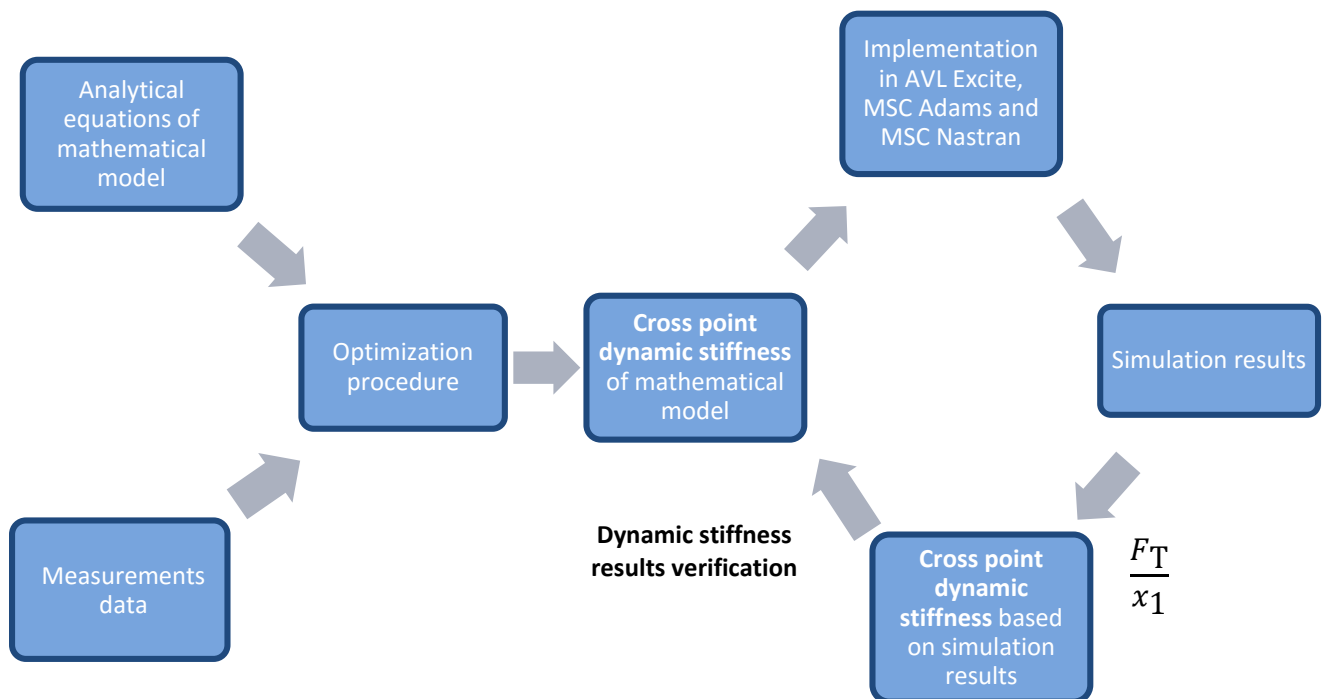


Figure 30. Mathematical model verification process

3.1 Triple mass oscillator mathematical model equations of motion (EOM)

The first step in the formulation of the equations of motion is to assign a set of generalized coordinates (a minimum set of independent coordinates) to the model which describes the general motion. For three mass oscillator shown in figure 31 the equations of motion can be determined from a set of free-body diagrams (FBDs) of the masses. The equation of motion can then be determined by applying Newton's second law to each free-body [1].

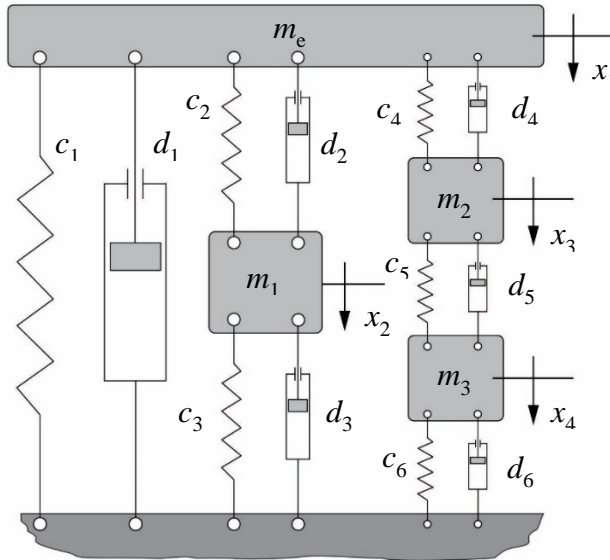


Figure 31. Triple mass oscillator with masses connected in parallel

EOM for 4 DOF dynamic system shown in figure 31:

$$m_e \cdot \ddot{x}_1 + d_1 \cdot \dot{x}_1 + d_2 \cdot (\dot{x}_1 - \dot{x}_2) + d_4 \cdot (\dot{x}_1 - \dot{x}_3) + c_1 \cdot x_1 + c_2 \cdot (x_1 - x_2) + c_4 \cdot (x_1 - x_3) = 0 \quad (20)$$

$$m_1 \cdot \ddot{x}_2 - d_2 \cdot (\dot{x}_1 - \dot{x}_2) + d_3 \cdot \dot{x}_2 - c_2 \cdot (x_1 - x_2) + c_3 \cdot x_2 = 0 \quad (21)$$

$$m_2 \cdot \ddot{x}_3 - d_4 \cdot (\dot{x}_1 - \dot{x}_3) + d_5 \cdot (\dot{x}_3 - \dot{x}_4) - c_4 \cdot (x_1 - x_3) + c_5 \cdot (x_3 - x_4) = 0 \quad (22)$$

$$m_3 \cdot \ddot{x}_4 - d_5 \cdot (\dot{x}_3 - \dot{x}_4) + d_6 \cdot \dot{x}_4 - c_5 \cdot (x_3 - x_4) + c_6 \cdot x_4 = 0 \quad (23)$$

Transmitted force to ground is equal to:

$$F_T = c_1 \cdot x_1 + d_1 \cdot \dot{x}_1 + c_3 \cdot x_2 + d_3 \cdot \dot{x}_2 + c_6 \cdot x_4 + d_6 \cdot \dot{x}_4 \quad (24)$$

Transform equations (20) to (23) into frequency domain using equations (8), (9) and (10).

Equations of motion in frequency domain:

$$-\omega^2 \cdot m_e \cdot \hat{X}_1 + i\omega \cdot d_1 \cdot \hat{X}_1 + i\omega \cdot d_2 \cdot (\hat{X}_1 - \hat{X}_2) + i\omega \cdot d_4 \cdot (\hat{X}_1 - \hat{X}_3) + c_1 \cdot \hat{X}_1 + c_2 \cdot (\hat{X}_1 - \hat{X}_2) + c_4 \cdot (\hat{X}_1 - \hat{X}_3) = 0 \quad (25)$$

$$-\omega^2 \cdot m_1 \cdot \hat{X}_2 - i\omega \cdot d_2 \cdot (\hat{X}_1 - \hat{X}_2) + i\omega \cdot d_3 \cdot \hat{X}_2 - c_2 \cdot (\hat{X}_1 - \hat{X}_2) + c_3 \cdot \hat{X}_2 = 0 \quad (26)$$

$$-\omega^2 \cdot m_2 \cdot \hat{X}_3 - i\omega \cdot d_4 \cdot (\hat{X}_1 - \hat{X}_3) + i\omega \cdot d_5 \cdot (\hat{X}_3 - \hat{X}_4) - c_4 \cdot (\hat{X}_1 - \hat{X}_3) + c_5 \cdot (\hat{X}_3 - \hat{X}_4) = 0 \quad (27)$$

$$-\omega^2 \cdot m_3 \cdot \hat{X}_4 - i\omega \cdot d_5 \cdot (\hat{X}_3 - \hat{X}_4) + i\omega \cdot d_6 \cdot \hat{X}_4 - c_5 \cdot (\hat{X}_3 - \hat{X}_4) + c_6 \cdot \hat{X}_4 = 0 \quad (28)$$

To describe cross point stiffness it is necessary to express all mass displacement with engine mass displacement x_1 .

$$\hat{X}_2 = \frac{i\omega \cdot d_2 + c_2}{-\omega^2 \cdot m_1 + i\omega \cdot (d_2 + d_3) + c_2 + c_3} \cdot \hat{X}_1 \quad (29)$$

Transfer function y_1 is equal to:

$$y_1 = \frac{i\omega \cdot d_2 + c_2}{-\omega^2 \cdot m_1 + i\omega \cdot (d_2 + d_3) + c_2 + c_3} \quad (30)$$

Expressing x_4 with x_3 :

$$\hat{X}_4 = \frac{i\omega \cdot d_5 + c_5}{-\omega^2 \cdot m_3 + i\omega \cdot (d_5 + d_6) + c_5 + c_6} \cdot \hat{X}_3 \quad (31)$$

Transfer function y_2 is equal to:

$$y_2 = \frac{i\omega \cdot d_5 + c_5}{-\omega^2 \cdot m_3 + i\omega \cdot (d_5 + d_6) + c_5 + c_6} \quad (32)$$

Expressing x_3 with x_1 :

$$\hat{X}_3 = \frac{i\omega \cdot d_4 + c_4}{-\omega^2 \cdot m_2 + i\omega \cdot [d_4 + d_5 \cdot (1 - y_2)] + c_4 + c_5 \cdot (1 - y_2)} \cdot \hat{X}_1 \quad (33)$$

Transfer function y_3 is equal to:

$$y_3 = \frac{i\omega \cdot d_4 + c_4}{-\omega^2 \cdot m_2 + i\omega \cdot [d_4 + d_5 \cdot (1 - y_2)] + c_4 + c_5 \cdot (1 - y_2)} \quad (34)$$

Displacement express:

$$\hat{X}_2 = y_1 \cdot \hat{X}_1 \quad (35)$$

$$\hat{X}_3 = y_3 \cdot \hat{X}_1 \quad (36)$$

$$\hat{X}_4 = y_2 \cdot \hat{X}_3 = y_2 \cdot y_3 \cdot \hat{X}_1 \quad (37)$$

Transmitted force to ground is equal to:

$$F_T = (c_1 + y_1 \cdot c_3 + y_2 \cdot y_3 \cdot c_6) \cdot \hat{X}_1 + i\omega \cdot (d_1 + y_1 \cdot d_3 + y_2 \cdot y_3 \cdot d_6) \cdot \hat{X}_1 \quad (38)$$

Cross point stiffness is equal to:

$$K_{CP} = \frac{F_T}{\hat{X}_1} = c_1 + y_1 \cdot c_3 + y_2 \cdot y_3 \cdot c_6 + i\omega \cdot (d_1 + y_1 \cdot d_3 + y_2 \cdot y_3 \cdot d_6) \quad (39)$$

Equation (39) is used for optimization procedure.

3.2 Triple mass oscillator verification

Analytical equation (39) for cross point dynamic stiffness is used for an optimization procedure in MatLab® as described in paragraph 2.2.

Hydraulic engine mount dynamic stiffness on low frequencies was considered in verification process. Cross point dynamic stiffness is shown in figure 32.

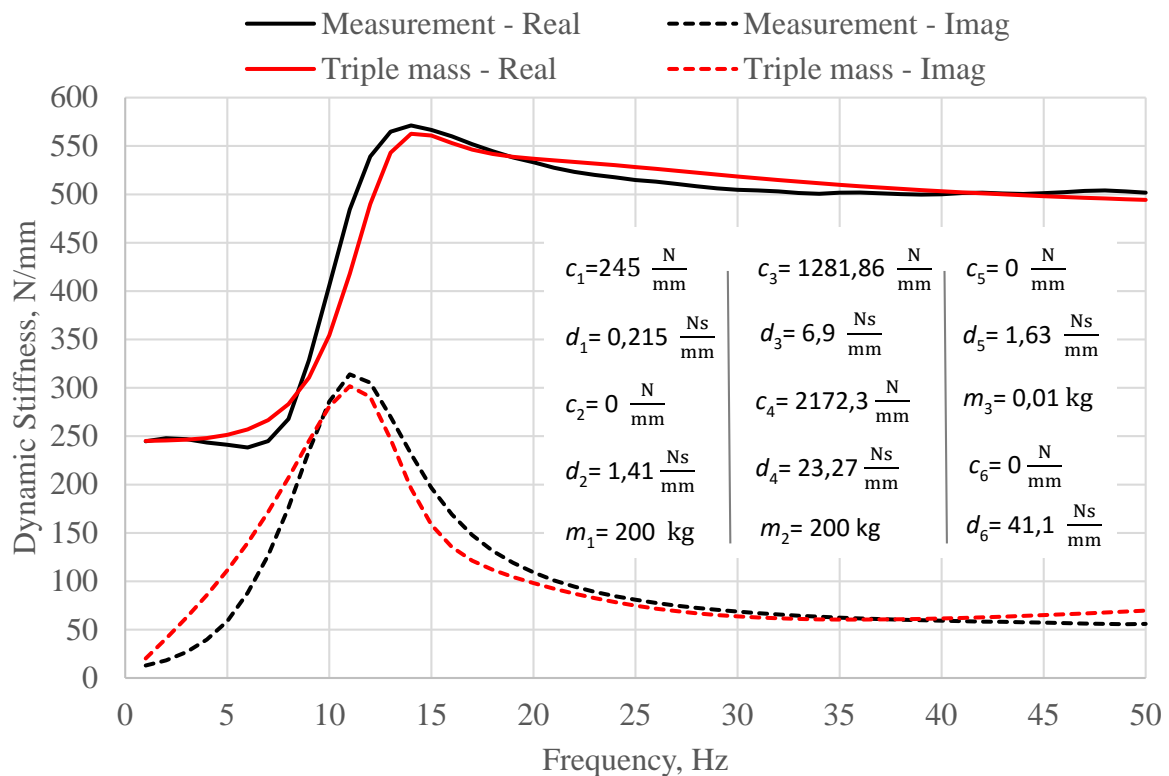


Figure 32. Cross point dynamic stiffness used for verification process

After determining parameter values, triple mass oscillator is analyzed in *AVL Excite*, *MSC Adams* and *MSC Nastran*. Aim of verification procedure is to confirm frequency behavior of triple mass oscillator in simulation software and to confirm that it can be used in powertrain simulation.

Simulation load input is **sinusoidal force with 100 N amplitude**. Mass, stiffness and damping values of mathematical model shown in figure 31 values are defined in figure 3234.

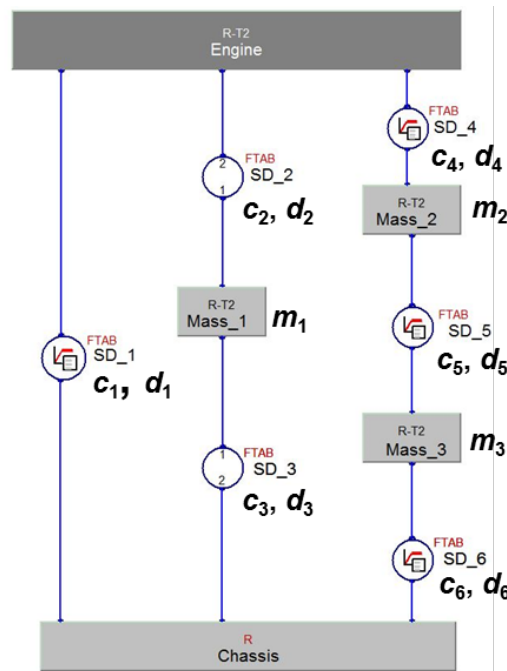


Figure 33. Triple mass oscillator model in AVL Excite

In *AVL Excite* vibration analysis is made in time domain and results were processed into frequency domain using FFT. Simulation model is shown in figure 33.

In *MSC Nastran* direct frequency response analysis (SOL 108) is used and code is shown in Appendix A.

In *MSC Adams* vibration toolbox is used to make analysis in frequency domain.

Table 3. Calculated engine mass displacement x_1

| f [Hz] | Analytical | | MSC Nastran | | AVL Excite | | MSC Adams | |
|-------------|-------------------|-----------|-------------------|-----------|-------------------|-----------|-------------------|-----------|
| | Displacement [mm] | | Displacement [mm] | | Displacement [mm] | | Displacement [mm] | |
| | Real | Imaginary | Real | Imaginary | Real | Imaginary | Real | Imaginary |
| 5 | -0.3644 | -0.6746 | -0.3653 | -0.6750 | -0.3644 | -0.6746 | -0.3656 | -0.6753 |
| 10 | -0.0787 | -0.034 | -0.0787 | -0.0340 | -0.0787 | -0.0340 | -0.0787 | -0.0340 |
| 12 | -0.0492 | -0.0243 | -0.0492 | -0.0243 | -0.0492 | -0.0243 | -0.0492 | -0.0243 |
| 15 | -0.0284 | -0.019 | -0.0285 | -0.0190 | -0.0284 | -0.0190 | -0.0285 | -0.0190 |
| 17 | -0.0215 | -0.0173 | -0.0216 | -0.0173 | -0.0215 | -0.0173 | -0.0215 | -0.0173 |
| 20 | -0.0158 | -0.0155 | -0.0158 | -0.0155 | -0.0158 | -0.0155 | -0.0158 | -0.0155 |
| 25 | -0.0114 | -0.013 | -0.0114 | -0.0130 | -0.0114 | -0.0130 | -0.0114 | -0.0130 |
| 30 | -0.0094 | -0.0107 | -0.0094 | -0.0107 | -0.0094 | -0.0107 | -0.0094 | -0.0107 |
| 40 | -0.0073 | -0.0071 | -0.0073 | -0.0071 | -0.0073 | -0.0071 | -0.0073 | -0.0071 |

Table 4. Calculated transmitted force F_T to ground (chassis) node

| f [Hz] | Analytical | | MSC Nastran | | AVL Excite | | MSC Adams | |
|-------------|--------------------------|-----------|--------------------------|-----------|--------------------------|-----------|--------------------------|-----------|
| | Transmitted force [N] | | Transmitted force [N] | | Transmitted force [N] | | Transmitted force [N] | |
| | Real | Imaginary | Real | Imaginary | Real | Imaginary | Real | Imaginary |
| 5 | -16.5 | -210.1 | -16.7 | -210.3 | -16.5 | -210.1 | -16.9 | -210.3 |
| 10 | -18.3 | -34.1 | -18.4 | -34.1 | -18.3 | -34.1 | -18.3 | -34.1 |
| 12 | -17.0 | -26.2 | -17.1 | -26.2 | -17.0 | -26.2 | -17.0 | -26.1 |
| 15 | -12.9 | -15.2 | -13.0 | -15.1 | -12.9 | -15.2 | -12.9 | -15.1 |
| 17 | -9.7 | -12.1 | -9.7 | -12.0 | -9.7 | -12.1 | -9.7 | -12.1 |
| 20 | -6.9 | -9.9 | -7.0 | -9.8 | -6.9 | -9.9 | -6.9 | -9.9 |
| 25 | -5.0 | -7.7 | -5.1 | -7.7 | -5.0 | -7.7 | -5.0 | -7.7 |
| 30 | -4.2 | -6.2 | -4.2 | -6.2 | -4.2 | -6.2 | -4.2 | -6.2 |
| 40 | -3.3 | -4.0 | -3.3 | -4.0 | -3.3 | -4.0 | -3.3 | -4.0 |

From results in table (3) and (4) it is possible to calculate cross point dynamic stiffness.

$$K_{CP} = \frac{F_T}{x_1} \quad (40)$$

Table 5. Calculated cross point dynamic stiffness K_{CP}

| f [Hz] | Analytical | | MSC Nastran | | AVL Excite | | MSC Adams | |
|-------------|---|-----------|---|-----------|---|-----------|---|-----------|
| | Cross point dynamic stiffness [N/mm] | | Cross point dynamic stiffness [N/mm] | | Cross point dynamic stiffness [N/mm] | | Cross point dynamic stiffness [N/mm] | |
| | Real | Imaginary | Real | Imaginary | Real | Imaginary | Real | Imaginary |
| 5 | 251.3 | 111.4 | 251.4 | 111.1 | 251.3 | 111.4 | 251.3 | 111.1 |
| 10 | 354.4 | 280.7 | 354.6 | 280.2 | 354.4 | 280.6 | 354.1 | 279.8 |
| 12 | 490.0 | 290.7 | 490.1 | 289.8 | 489.5 | 290.3 | 488.8 | 289.7 |
| 15 | 560.8 | 158.4 | 560.1 | 157.5 | 561.3 | 157.9 | 559.0 | 158.5 |
| 17 | 546.3 | 121.4 | 545.3 | 120.7 | 547.2 | 121.1 | 546.4 | 121.3 |
| 20 | 536.8 | 98.1 | 535.5 | 97.5 | 535.8 | 98.4 | 534.8 | 98.7 |
| 25 | 528.3 | 74.9 | 527.3 | 73.2 | 527.8 | 74.4 | 527.4 | 74.8 |
| 30 | 518.5 | 63.7 | 520.0 | 62.4 | 520.0 | 63.4 | 520.0 | 63.4 |
| 40 | 503.2 | 61.6 | 503.4 | 58.4 | 504.7 | 59.8 | 504.0 | 59.1 |

3.3 Verification procedure results

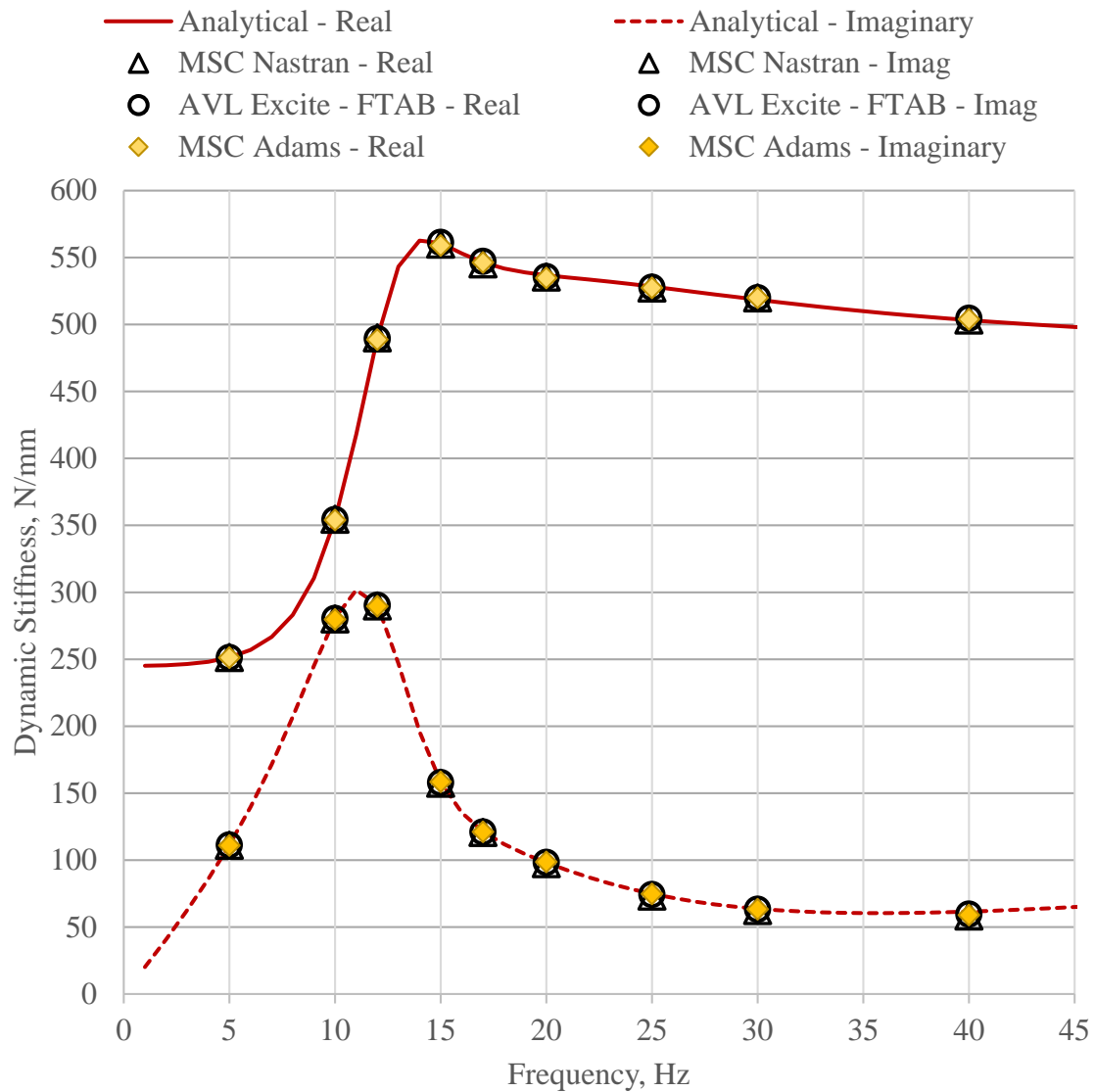


Figure 34. Cross point dynamic stiffness verification results

Based on cross point dynamic stiffness verification results shown in figure 34 conclusion can be made that frequency dependency of engine mounts can be described by triple mass oscillator. More important, this behavior is also possible to achieve in numerical simulations software that are used to make dynamic models for vibration analysis of IC engine.

4. Gasoline IC engine simulation

In this section verified triple mass oscillator with masses in parallel mathematical model is implemented in powertrain simulation model in *AVL Excite Power Unit* [1]. For the simulated IC engine measurements of the engine mounts velocities are available and obtain simulation results are compared with measurements data. Simulation model is made for vibration and acoustic analysis purposes. In scope of this study only vibration analysis is done.

4.1 IC engine data

Simulated IC engine data is turbocharged 1,8 dm³, 4 cylinder inline gasoline engine with direct gasoline injection. Engine emission certificate is EU6.

More engine information cannot be provided due to confidentiality agreement.

Powertrain mounting system consists of 2 hydraulic engine mounts and 1 elastomeric gearbox mount as shown in figure 35. Also, engine coordinate system is defined. Origin of the engine coordinate system is in the center of the third main bearing.

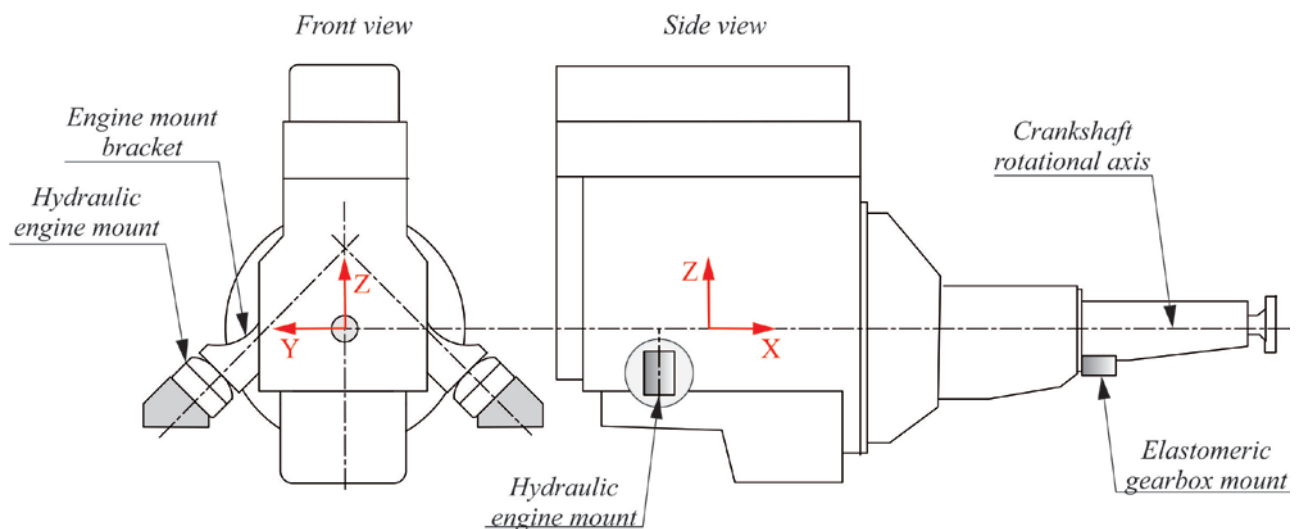


Figure 35. Simulated longitudinal IC engine defined coordinate system and mounting brackets

In figure 36 car coordinate system is shown. Layout of the simulated engine is longitudinal (north – south) and Z axis is coincident with vehicle Z axis. Engines X and Y axes are opposite direction compared with vehicle coordinate system. Engine mount coordinate system is defined in figure 16.

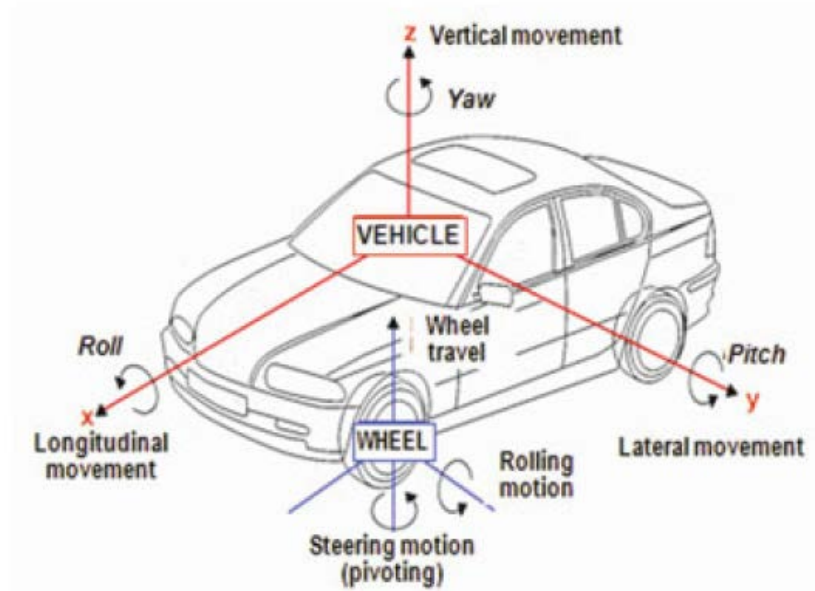


Figure 36. Vehicle coordinate system as defined by ISO 8855 / DIN 70000 [14]

4.2 Mounting system dynamic stiffness optimization

Engine and gearbox mounts dynamic stiffness measurements are available from the engine mount manufacturer. Cross point dynamic stiffness is described with triple mass oscillator explained in section 3.1.

For hydraulic engine mounts measurements for X and Y directions are available up to 200 Hz and for Z direction is up to 400 Hz.

For elastomeric gearbox mounts for X and Y directions are available up to 250 Hz and for Z direction up to 400 Hz.

Amplitude of engine mount displacement during the measurements is 0,1 mm.

4.2.1 Hydraulic engine mount dynamic stiffness



$c_1 = 0$ N/mm
 $d_1 = 0$ Ns/mm
 $c_2 = 194,1$ N/mm
 $d_2 = 2,087$ Ns/mm
 $m_1 = 200$ kg
 $c_3 = 1545,4$ N/mm
 $d_3 = 13,82$ Ns/mm
 $c_4 = 28838$ N/mm
 $d_4 = 7,18$ Ns/mm
 $m_2 = 7,23$ kg
 $c_5 = 217,1$ N/mm
 $d_5 = 0,0209$ Ns/mm
 $m_3 = 0,01$ kg
 $c_4 = 99,51$ N/mm
 $d_4 = 1,815$ Ns/mm

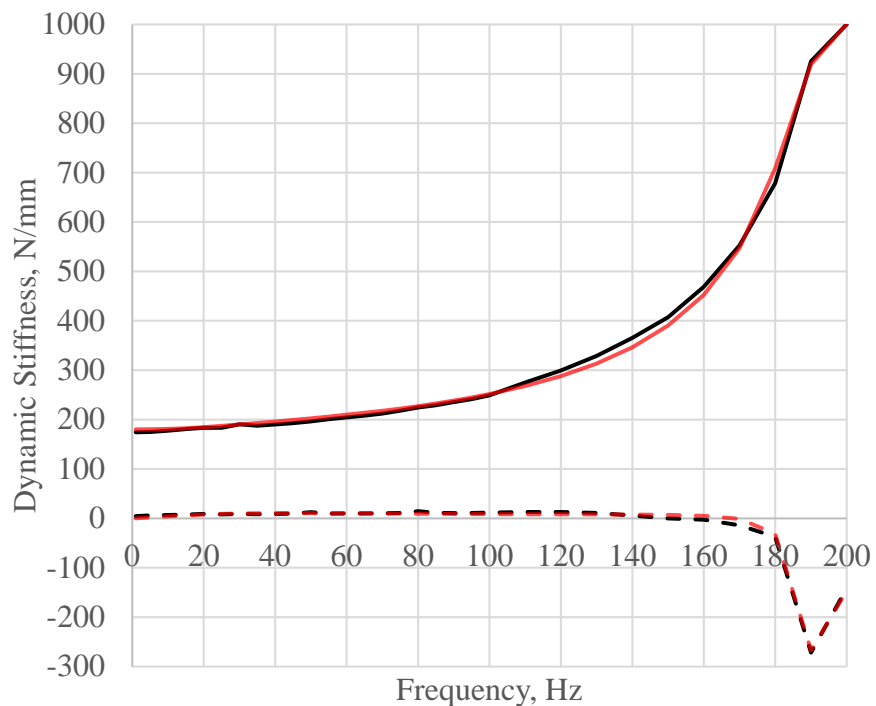


Figure 37. Engine mount dynamic stiffness – X direction

— Measurement – Real - - - Measurement – Imaginary
— Optimization – Real - - - Optimization – Imaginary

$c_1 = 0 \text{ N/mm}$
 $d_1 = 0 \text{ Ns/mm}$
 $c_2 = 127,9 \text{ N/mm}$
 $d_2 = 0,053 \text{ Ns/mm}$
 $m_1 = 0,67 \text{ kg}$
 $c_3 = 980,56 \text{ N/mm}$
 $d_3 = 0 \text{ Ns/mm}$
 $c_4 = 76,06 \text{ N/mm}$
 $d_4 = 0 \text{ Ns/mm}$
 $m_2 = 0,712 \text{ kg}$
 $c_5 = 1151,3 \text{ N/mm}$
 $d_5 = 0,31 \text{ Ns/mm}$
 $m_3 = 3,96 \text{ kg}$
 $c_4 = 1188,8 \text{ N/mm}$
 $d_4 = 21,85 \text{ Ns/mm}$

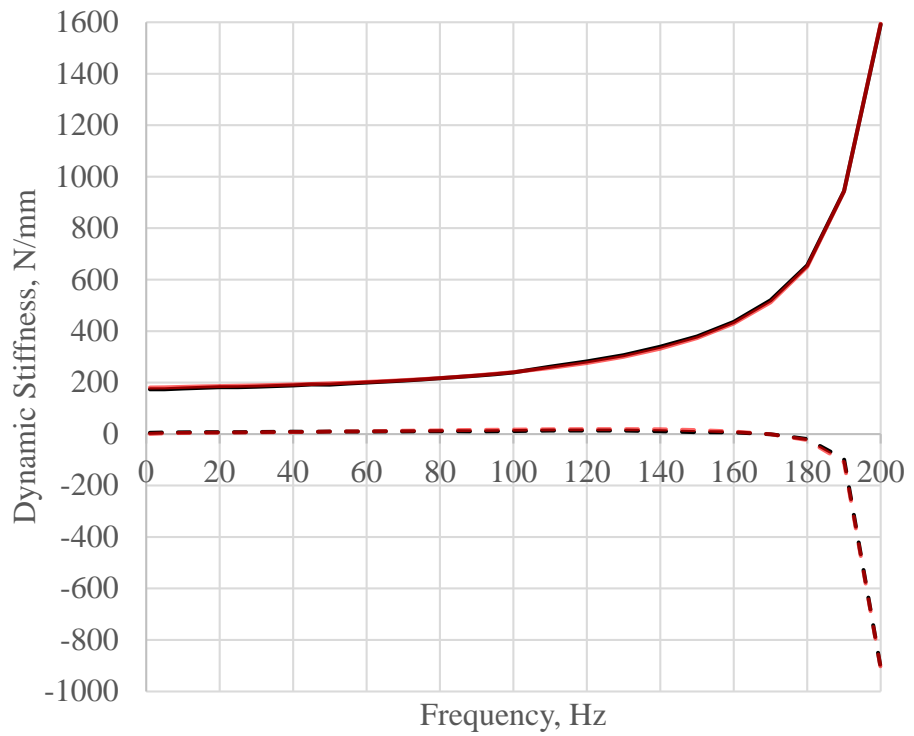


Figure 38. Engine mount dynamic stiffness – **Y direction**

$c_1 = 54,18 \text{ N/mm}$
 $d_1 = 0,1 \text{ Ns/mm}$
 $c_2 = 0 \text{ N/mm}$
 $d_2 = 2,087 \text{ Ns/mm}$
 $m_1 = 200 \text{ kg}$
 $c_3 = 1545,4 \text{ N/mm}$
 $d_3 = 13,82 \text{ Ns/mm}$
 $c_4 = 28838 \text{ N/mm}$
 $d_4 = 7,18 \text{ Ns/mm}$
 $m_2 = 7,23 \text{ kg}$
 $c_5 = 217,1 \text{ N/mm}$
 $d_5 = 0,0209 \text{ Ns/mm}$
 $m_3 = 0,01 \text{ kg}$
 $c_4 = 99,51 \text{ N/mm}$
 $d_4 = 1,815 \text{ Ns/mm}$

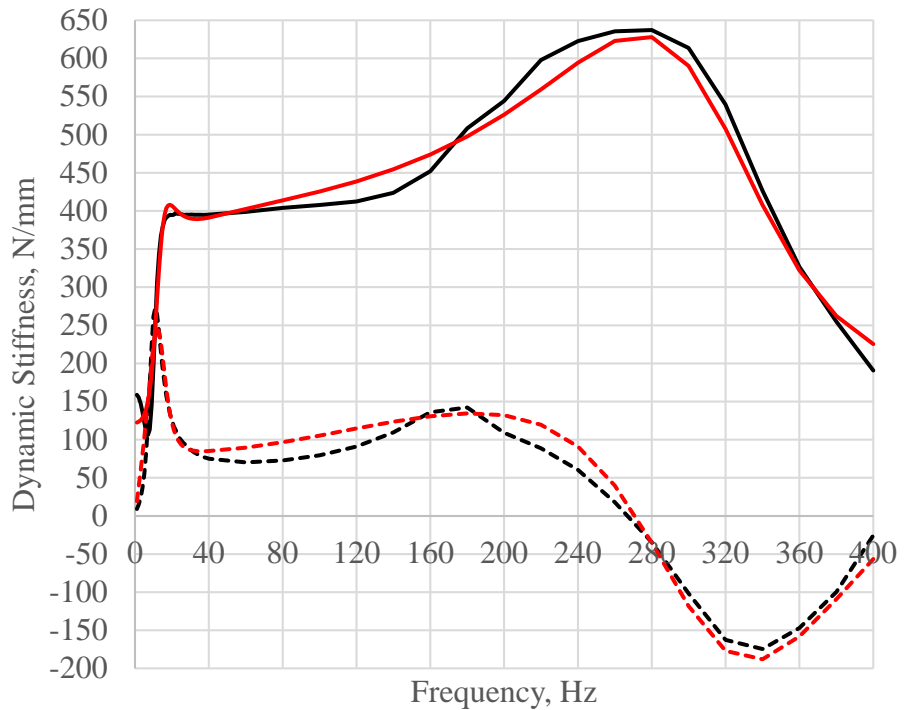


Figure 39. Engine mount dynamic stiffness – **Z direction**

4.2.2 Elastomeric gearbox mount stiffness

— Measurement – Real - - - Measurement – Imaginary
— Optimization – Real - - - Optimization – Imaginary

$c_1 = 54,18 \text{ N/mm}$
 $d_1 = 0,1 \text{ Ns/mm}$
 $c_2 = 0 \text{ N/mm}$
 $d_2 = 2,087 \text{ Ns/mm}$
 $m_1 = 200 \text{ kg}$
 $c_3 = 1545,4 \text{ N/mm}$
 $d_3 = 13,82 \text{ Ns/mm}$
 $c_4 = 28838 \text{ N/mm}$
 $d_4 = 7,18 \text{ Ns/mm}$
 $m_2 = 7,23 \text{ kg}$
 $c_5 = 217,1 \text{ N/mm}$
 $d_5 = 0,0209 \text{ Ns/mm}$
 $m_3 = 0,01 \text{ kg}$
 $c_4 = 99,51 \text{ N/mm}$
 $d_4 = 1,815 \text{ Ns/mm}$

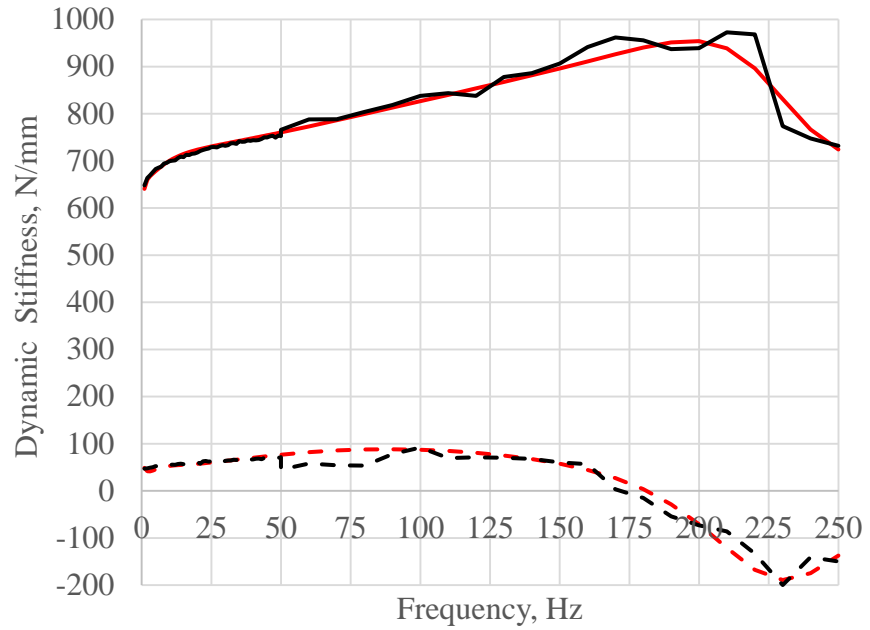


Figure 40. Gearbox mount dynamic stiffness – X direction

$c_1 = 0 \text{ N/mm}$
 $d_1 = 0,068 \text{ Ns/mm}$
 $c_2 = 54113,6 \text{ N/mm}$
 $d_2 = 33,06 \text{ Ns/mm}$
 $m_1 = 20 \text{ kg}$
 $c_3 = 90,4 \text{ N/mm}$
 $d_3 = 0 \text{ Ns/mm}$
 $c_4 = 34,84 \text{ N/mm}$
 $d_4 = 0 \text{ Ns/mm}$
 $m_2 = 0,824 \text{ kg}$
 $c_5 = 185,1 \text{ N/mm}$
 $d_5 = 0,664 \text{ Ns/mm}$
 $m_3 = 0,698 \text{ kg}$
 $c_4 = 30,67 \text{ N/mm}$
 $d_4 = 3,28 \text{ Ns/mm}$

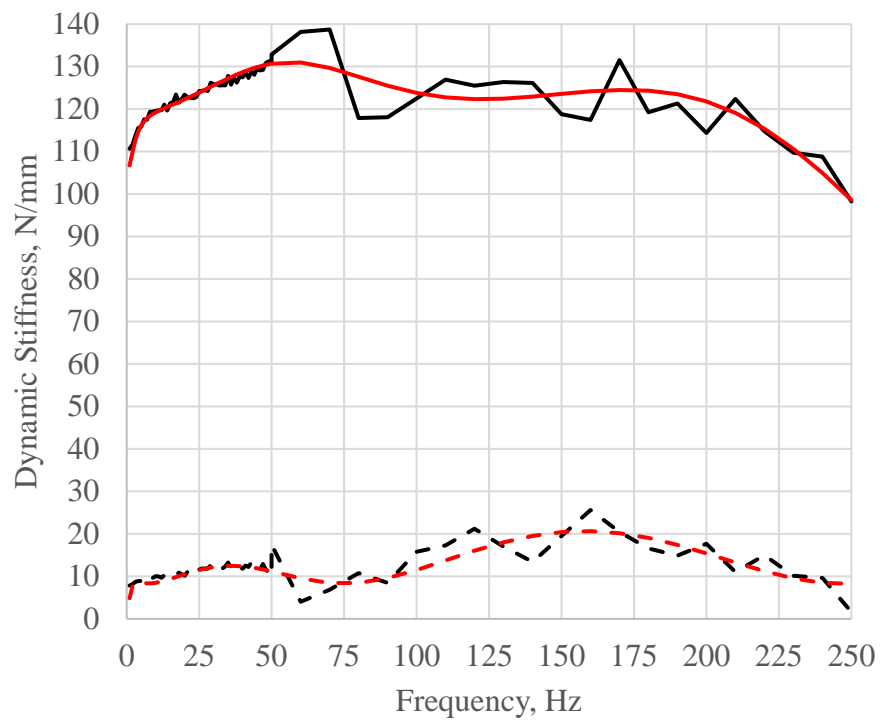


Figure 41. Gearbox mount dynamic stiffness – Y direction

— Measurement – Real - - - Measurement – Imaginary
 — Optimization – Real - - - Optimization – Imaginary

$c_1 = 0 \text{ N/mm}$
 $d_1 = 0 \text{ Ns/mm}$
 $c_2 = 73,66 \text{ N/mm}$
 $d_2 = 0 \text{ Ns/mm}$
 $m_1 = 0,157 \text{ kg}$
 $c_3 = 0,132 \text{ N/mm}$
 $d_3 = 15,35 \text{ Ns/mm}$
 $c_4 = 624 \text{ N/mm}$
 $d_4 = 0,42 \text{ Ns/mm}$
 $m_2 = 0,00758 \text{ kg}$
 $c_5 = 790,6 \text{ N/mm}$
 $d_5 = 7,67 \text{ Ns/mm}$
 $m_3 = 0,00637 \text{ kg}$
 $c_4 = 403,4 \text{ N/mm}$
 $d_4 = 0 \text{ Ns/mm}$

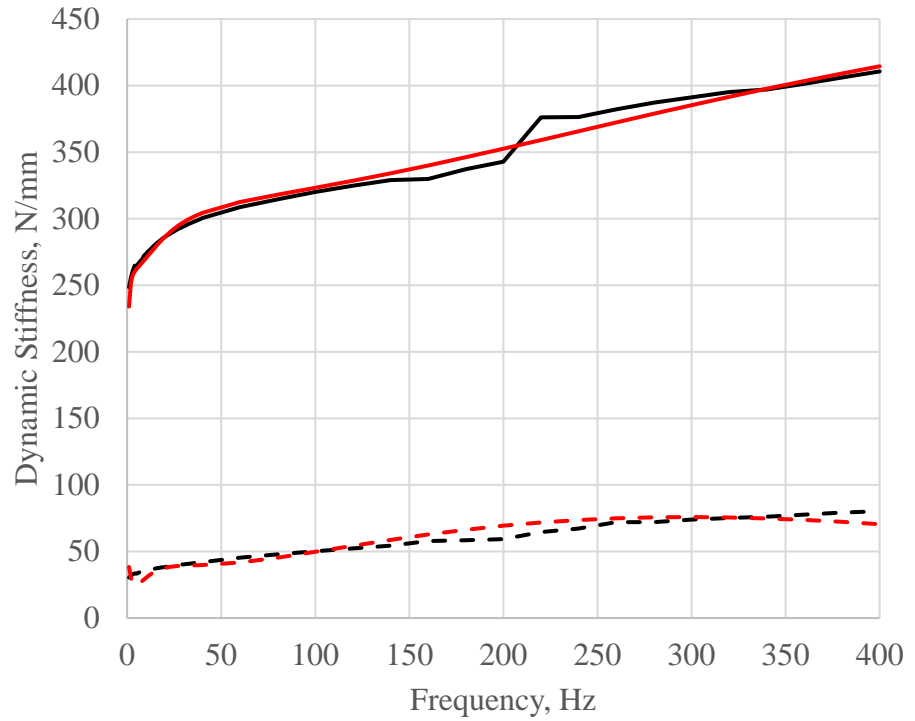


Figure 42. Gearbox mount dynamic stiffness – Z direction

4.3 Simulation model

Due to confidentiality agreement it is not allowed to show *AVL Excite* simulation model details, but some model setup can be shown. Whole model is described with 4 064 429 nodes and 2 572 854 elements. Each body, except chassis, has some internal Rayleigh damping value defined. Geometry and properties of the crankshaft, connecting rods, pistons, balancing shafts are defined. Some geometry and property information are from the CAD model and some information are based on the AVL assumptions. Also, as mentioned each engine mount is described with triple mass oscillator mathematical model.

In *AVL Excite* powetrain model is separated in several bodies as shown in figure 43 and in figure 44 simulation model in *AVL Excite Power Unit* is shown. In figure 44 is also shown that each mount dynamic stiffness is defined separately in each direction. For 3 different mounts 9 triple mass oscillators were used to define dynamic stiffness in each direction for each mount.

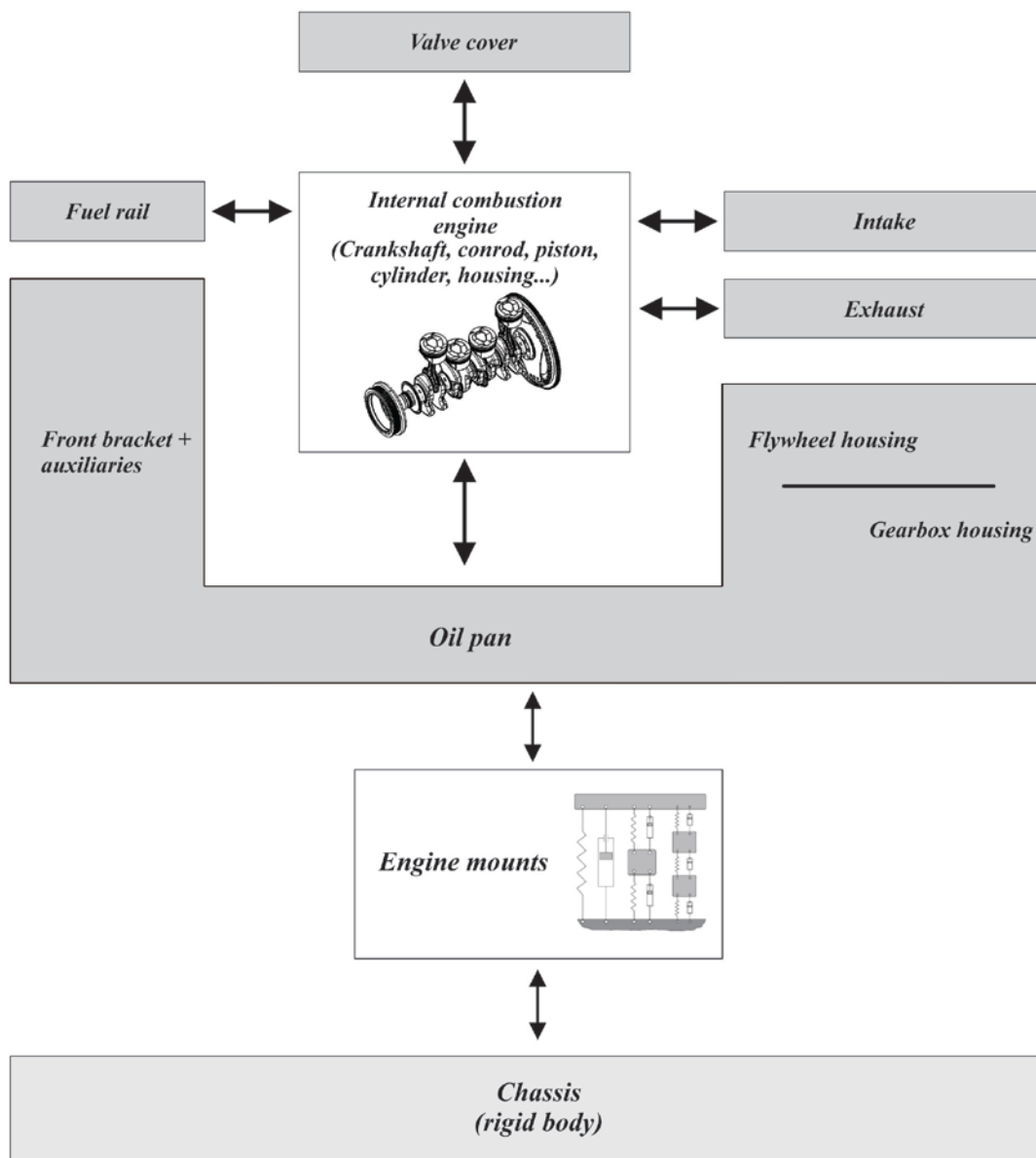


Figure 43. Simplified simulation model topology

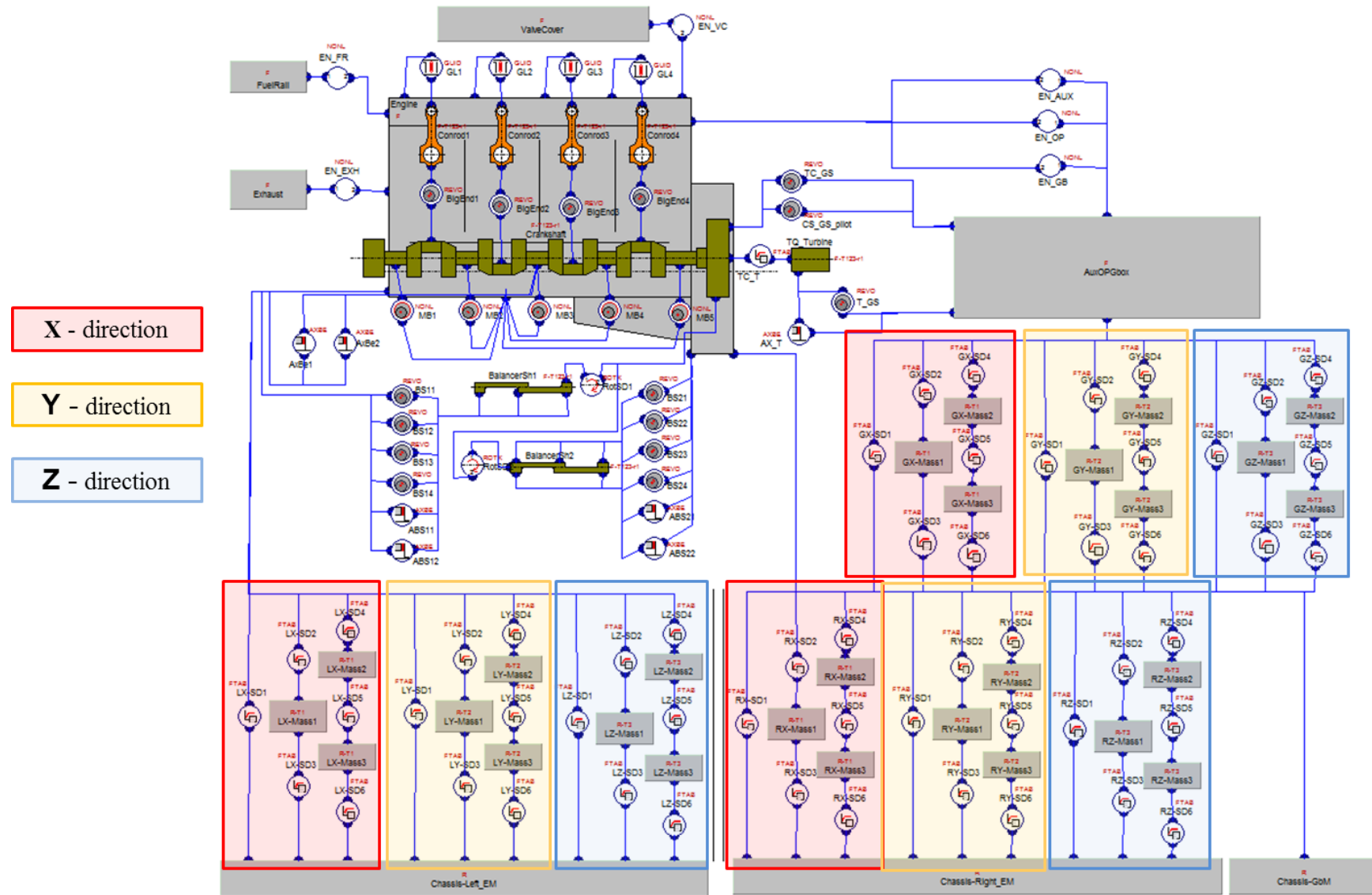


Figure 44. Powertrain simulation model topology in AVL Excite Power Unit

4.4 Simulation results

Measurement data is processed up to frequency value of 800 Hz. All measurement and simulation results of the engine mounts response are shown in form of the **velocities**. For comparison only 2nd and 4th order are shown because they have the biggest influence on transmitted vibration value. Also, sum of all orders (synthesis) is shown up to 8 order. All results are considered as RMS (root mean square).

Engine mount response is measured in the transient state during the *engine run-up* process from 0 rpm to 6300 rpm. Results are processed from 1000 rpm to 6000 rpm.

Simulation is run with 500 rpm step from 1000 rpm to 6000 rpm.

Load boundary conditions are in form of gas pressure for each cylinder. Simulation is run in 6 cycles and last 2 cycles were processed and used for results comparison. In first 4 cycle steady state is reached for each examined engine speed.

Measurement and simulation results are shown in the **engine coordinate system** defined in figure 35.

4.4.1 Left engine mount – X direction

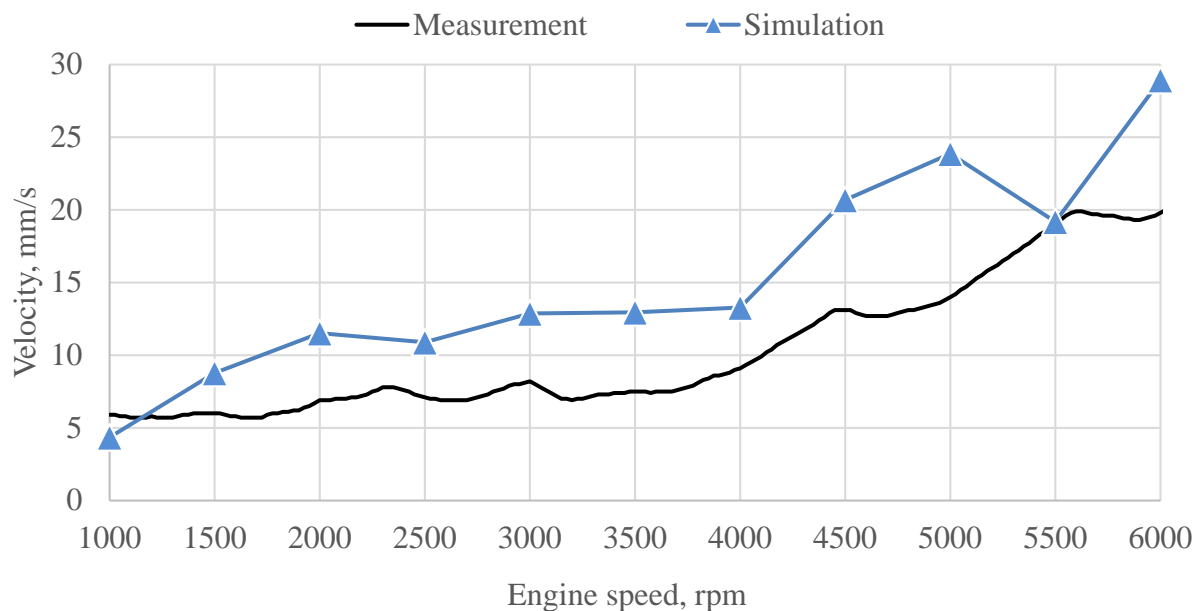


Figure 45. Left engine mount - X direction - synthesis

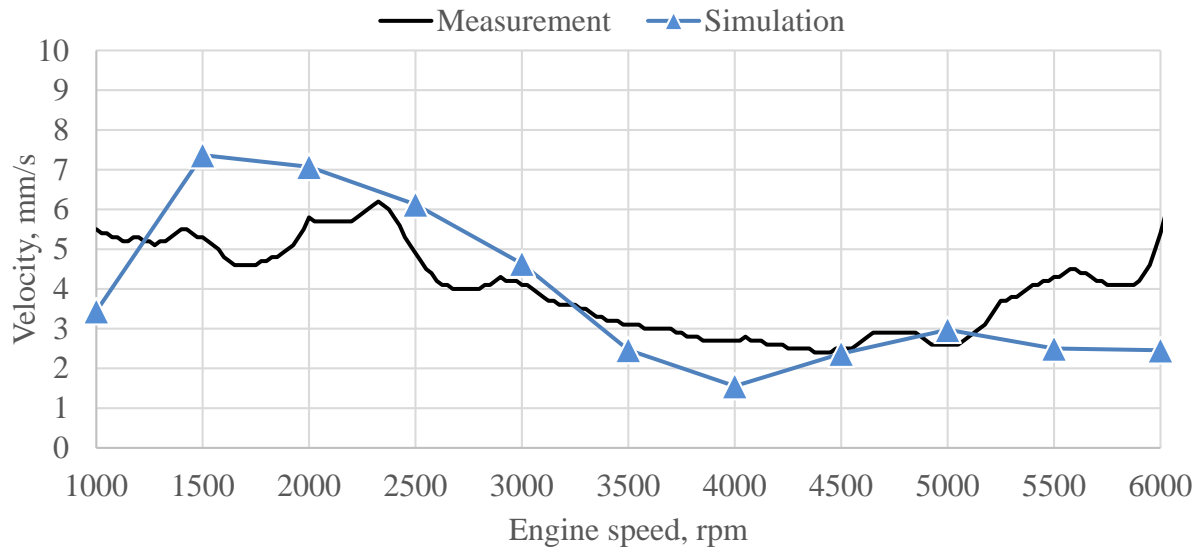


Figure 46. Left engine mount - X direction – 2nd order

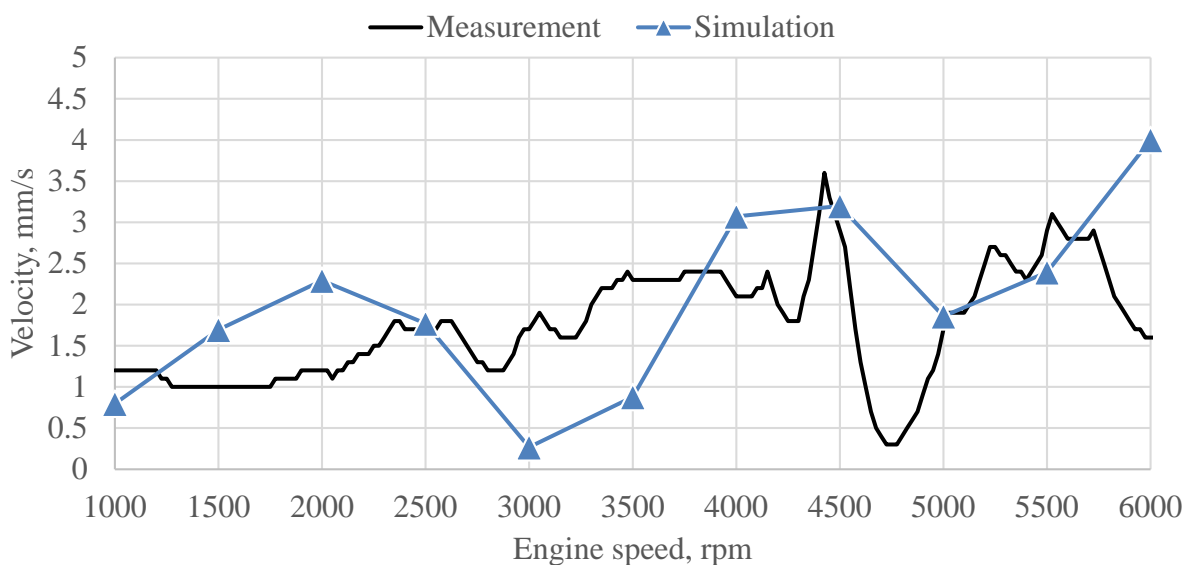


Figure 47. Left engine mount - X direction - 4th order

As shown in figure 45 sum value of all analyzed orders (synthesis) is higher than synthesis value obtain from measurement results. On simulation results influence of higher frequencies is larger and this is shown in figure 46 and figure 47 where simulation results curve is following measurement curve. From that it can be concluded that simulation model is more influenced by high frequency vibration.

4.4.2 Left engine mount – Y direction

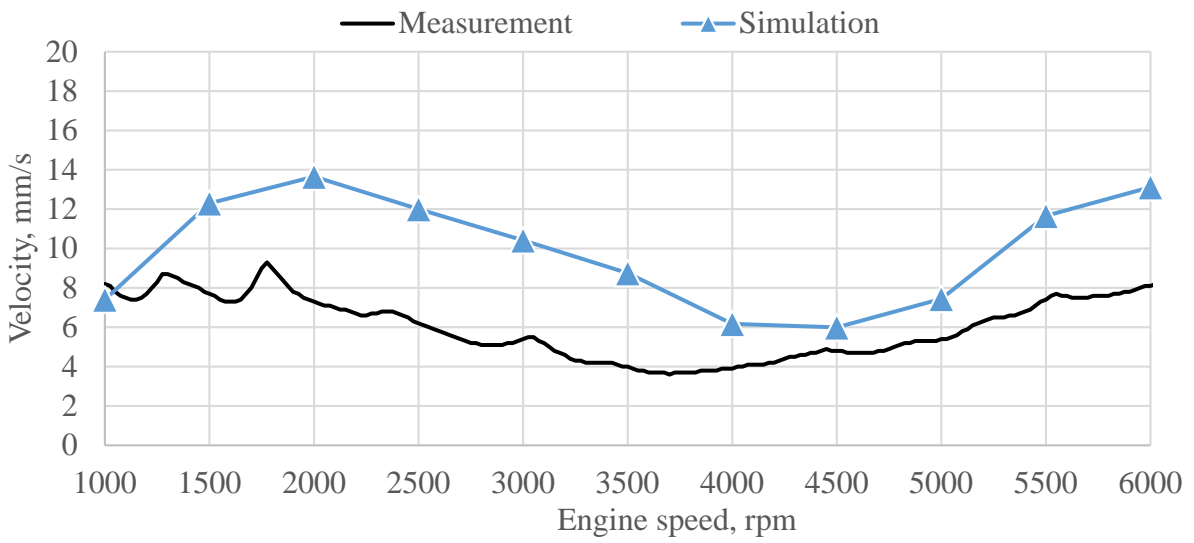


Figure 48. Left engine mount - Y direction – synthesis

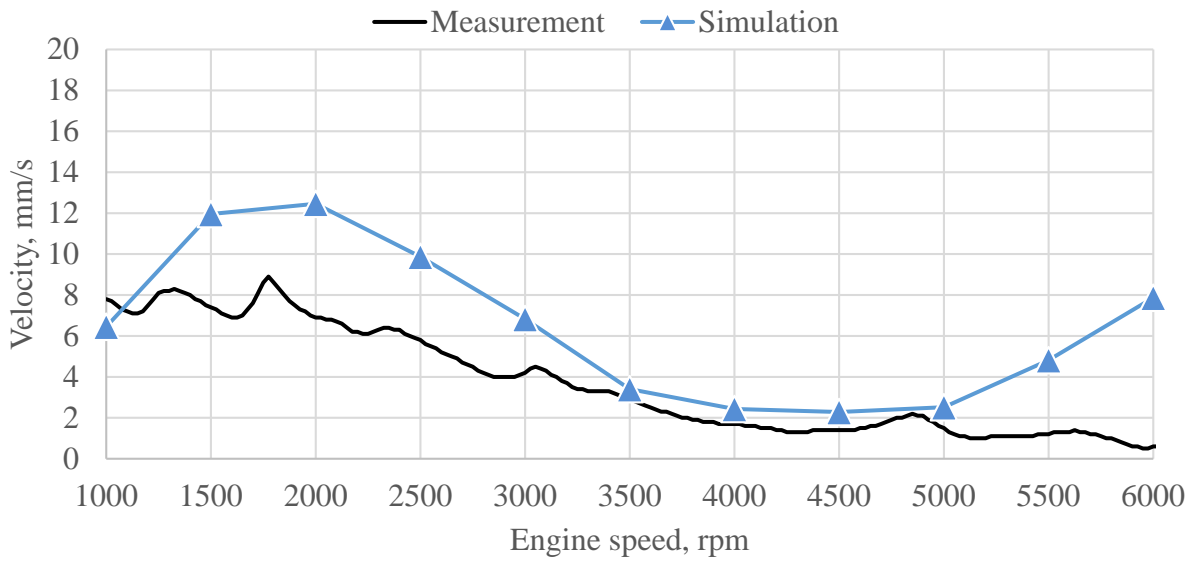


Figure 49. Left engine mount - Y direction – 2nd order

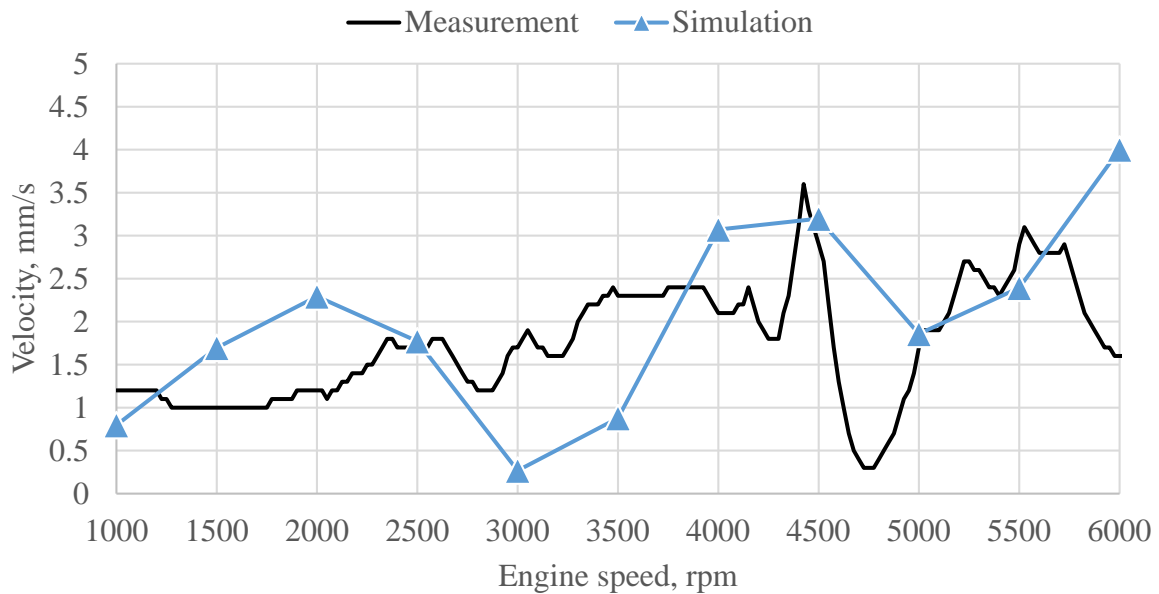


Figure 50. Left engine mount - Y direction – 4th order

In Y direction, on engine speed below 3000 rpm and above 5000 rpm, 2nd order has higher value in simulation than in measurements as shown in figure 49. This influences on synthesis values which have higher values on entire engine speed range as shown in figure 48.

4.4.3 Left engine mount – Z direction

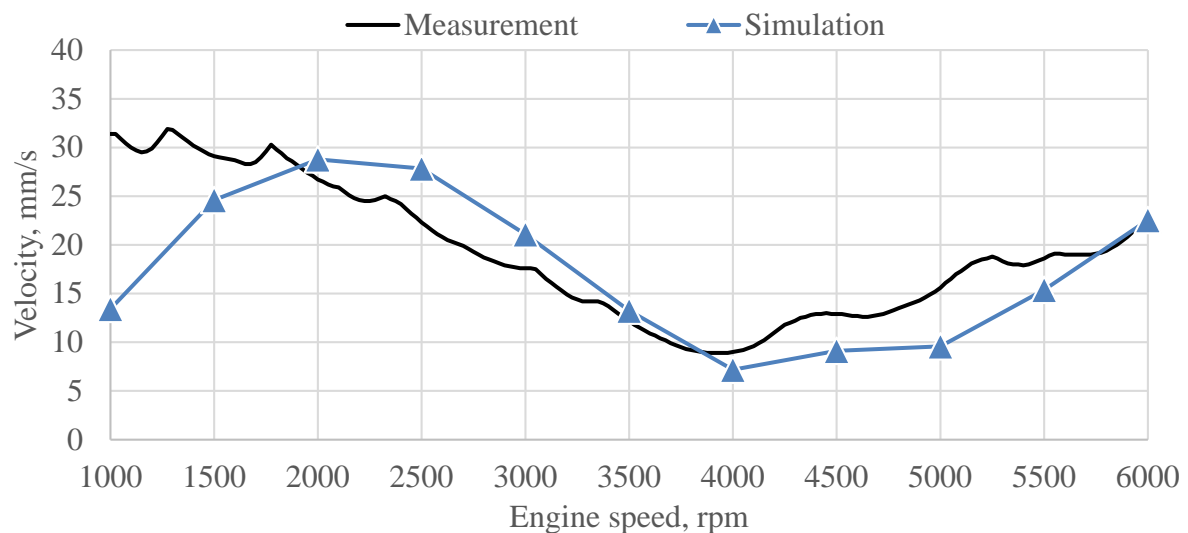


Figure 51. Left engine mount - Z direction – synthesis

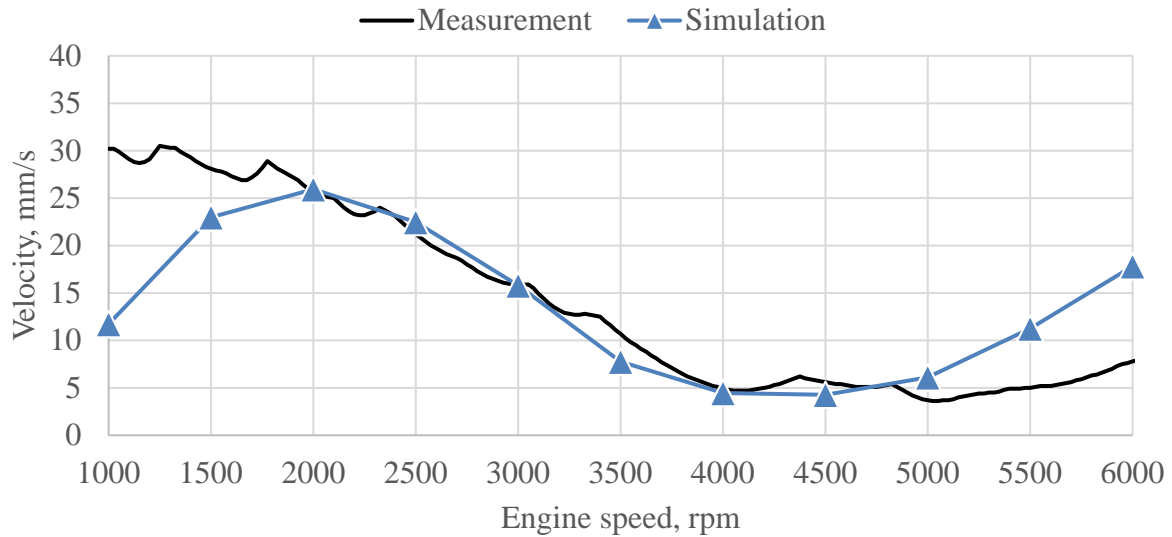


Figure 52. Left engine mount - Z direction – 2nd order

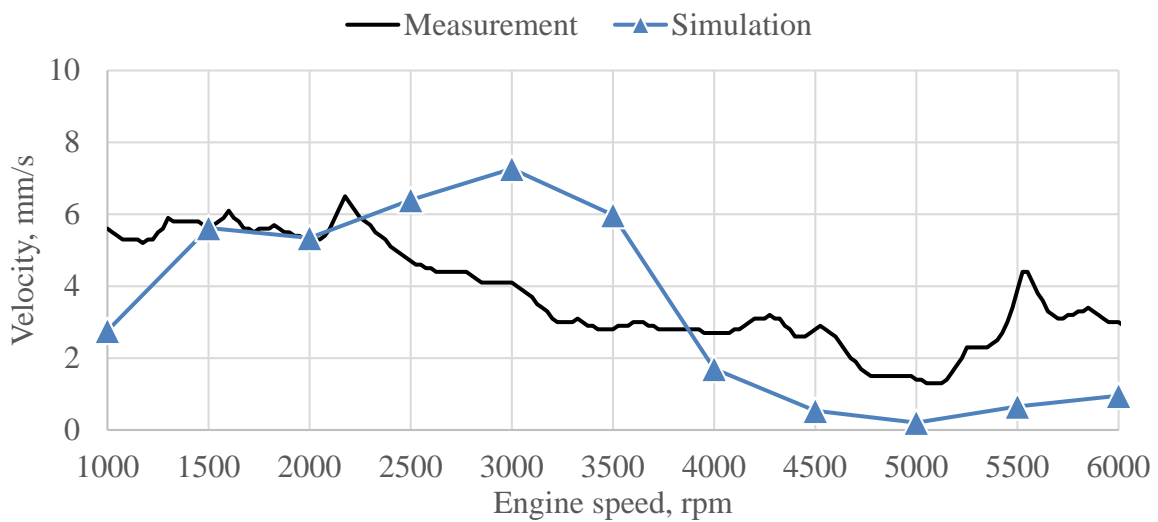


Figure 53. Left engine mount - Z direction – 4th order

In figure 51 satisfying results are above 2000 rpm. For 2nd order results satisfying results are between 2000 rpm and 5000 rpm as shown in figure 52. 4th order results vary and because of smaller values of velocities it is hard to simulate exact measurement response.

4.4.4 Right engine mount – X direction

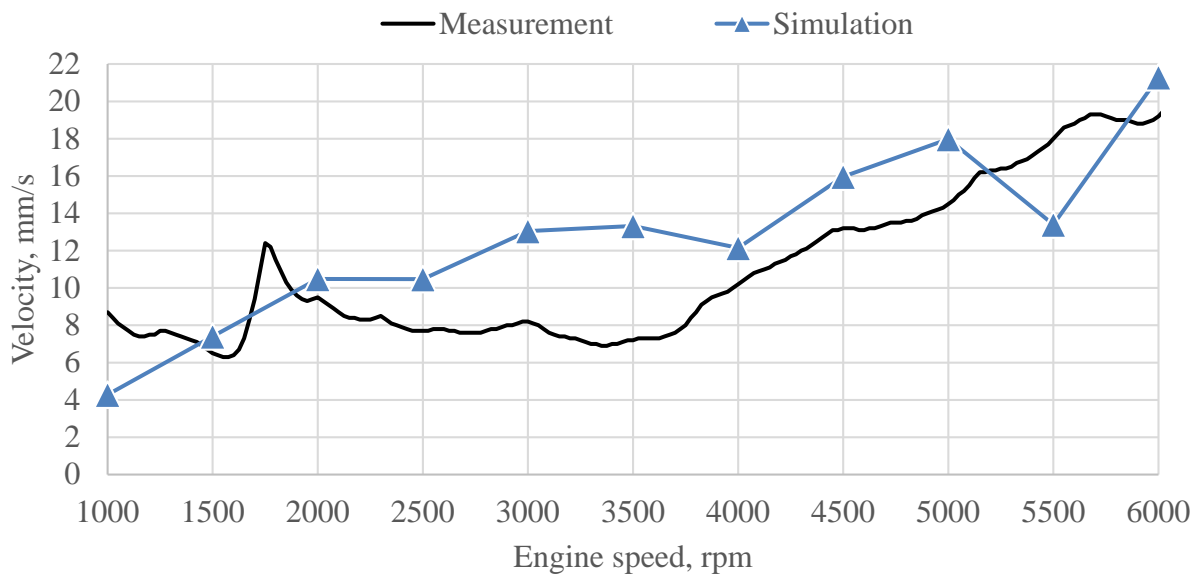


Figure 54. Right engine mount – X direction – synthesis

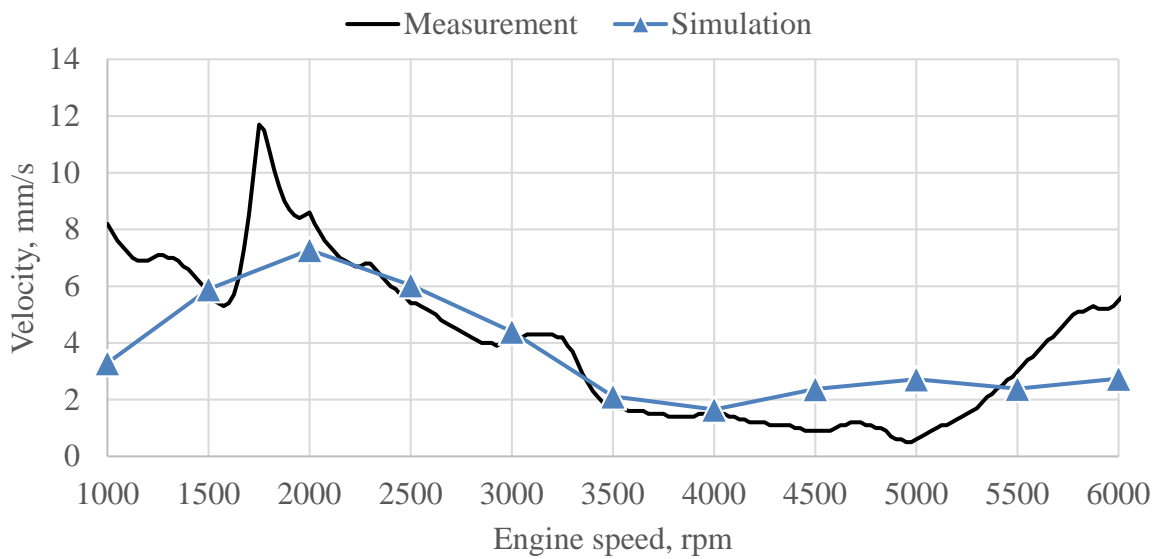


Figure 55. Right engine mount – X direction – 2nd order

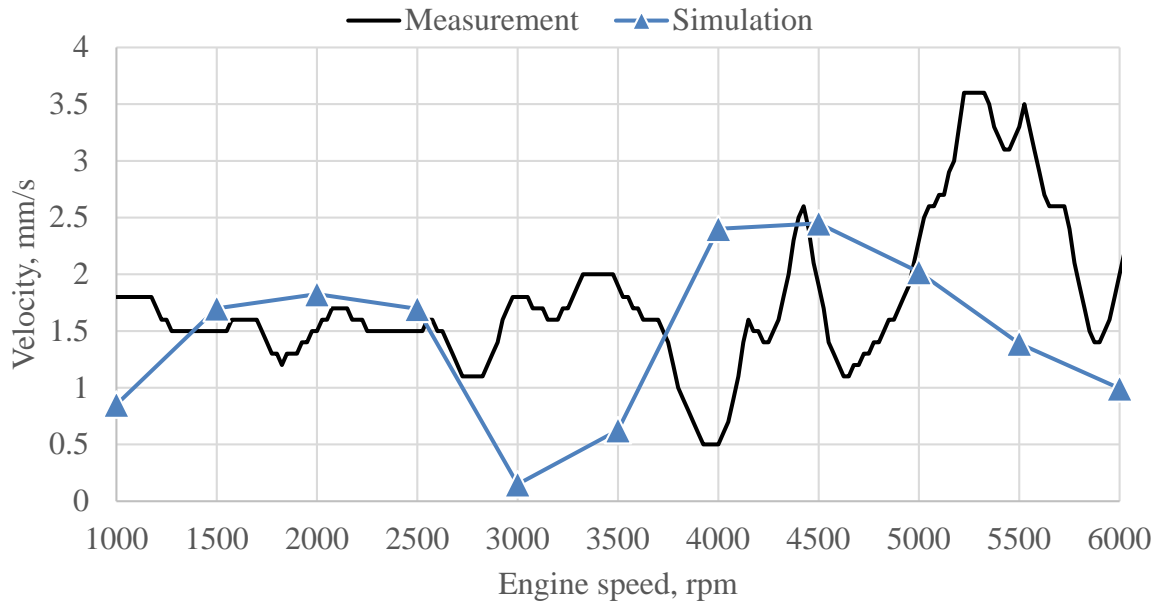


Figure 56. Right engine mount – X direction – 4th order

Right engine mount simulation synthesis values are satisfying close to the measurement values as shown in figure 54. This also refers to 2nd order values as shown in figure 55 and 4th order velocity results varies.

4.4.5 Right engine mount – Y direction

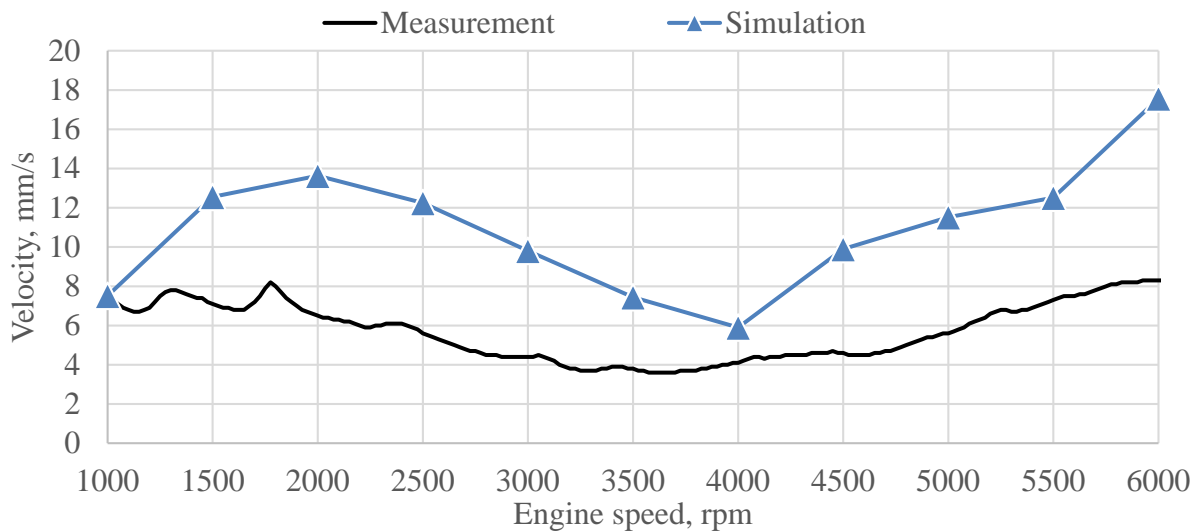
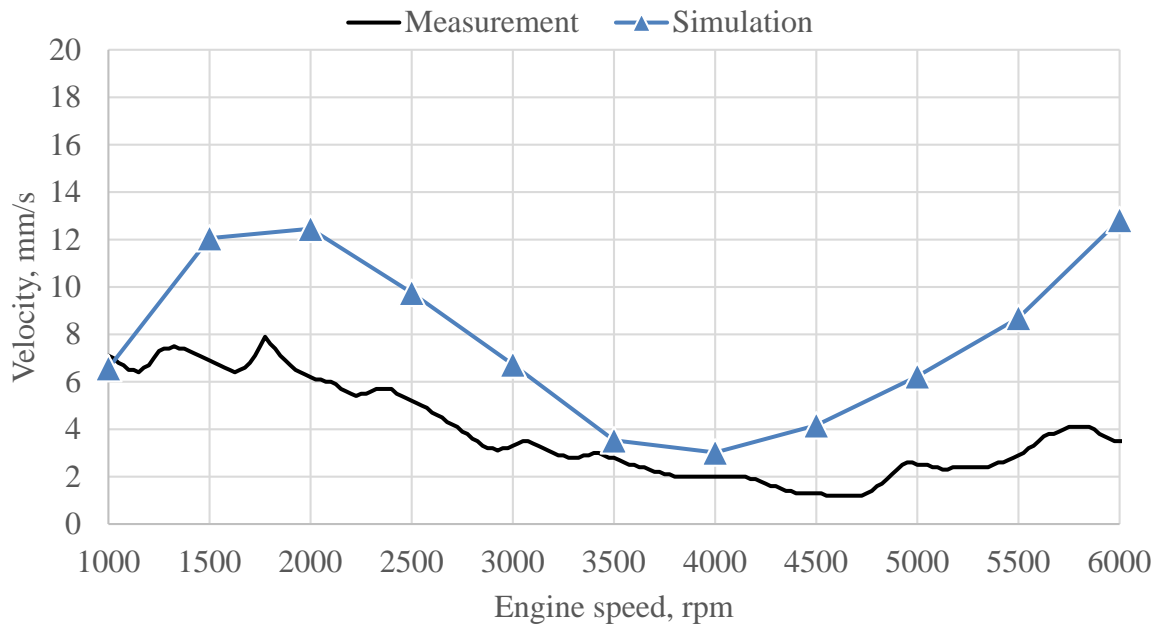
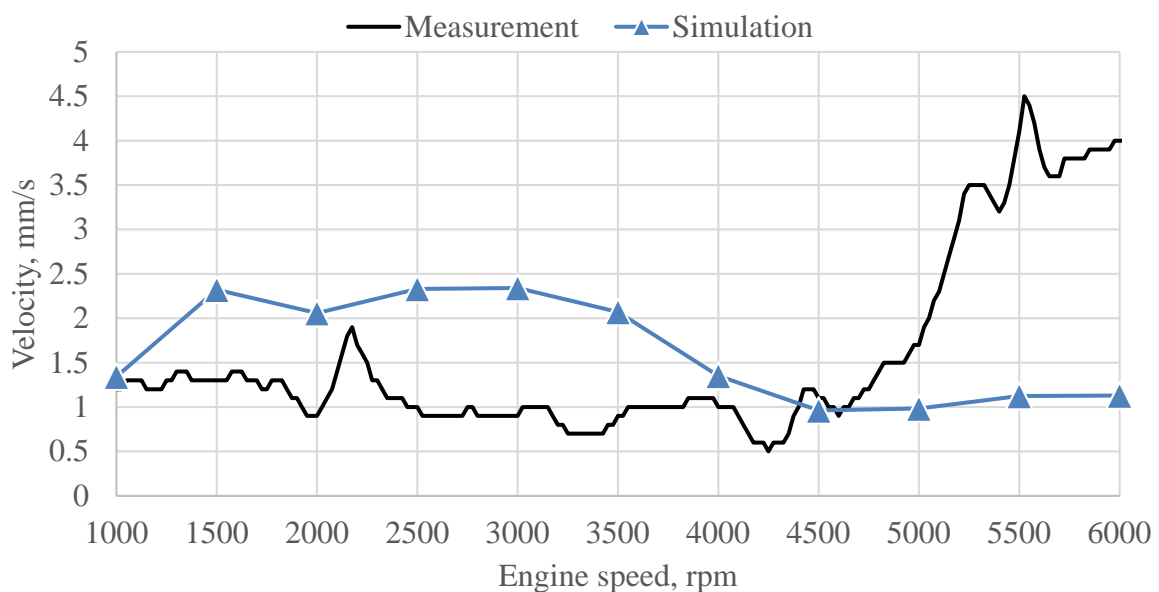


Figure 57. Right engine mount – Y direction – synthesis

Figure 58. Right engine mount – Y direction – 2nd orderFigure 59. Right engine mount – Y direction – 4th order

Right engine mount Y direction simulation values are not satisfying for synthesis, 2nd order and 4th order. Only satisfying results for 2nd order are for engine speed 1000 rpm, 3500 rpm, 4000 rpm and 4500 rpm. For all other engine speed velocities obtain from simulation are overestimated compared with measurements results. It is worth to mention that for 1000 rpm, which is close to engine idle engine speed, all results matches with measurement data.

4.4.6 Right engine mount – Z direction

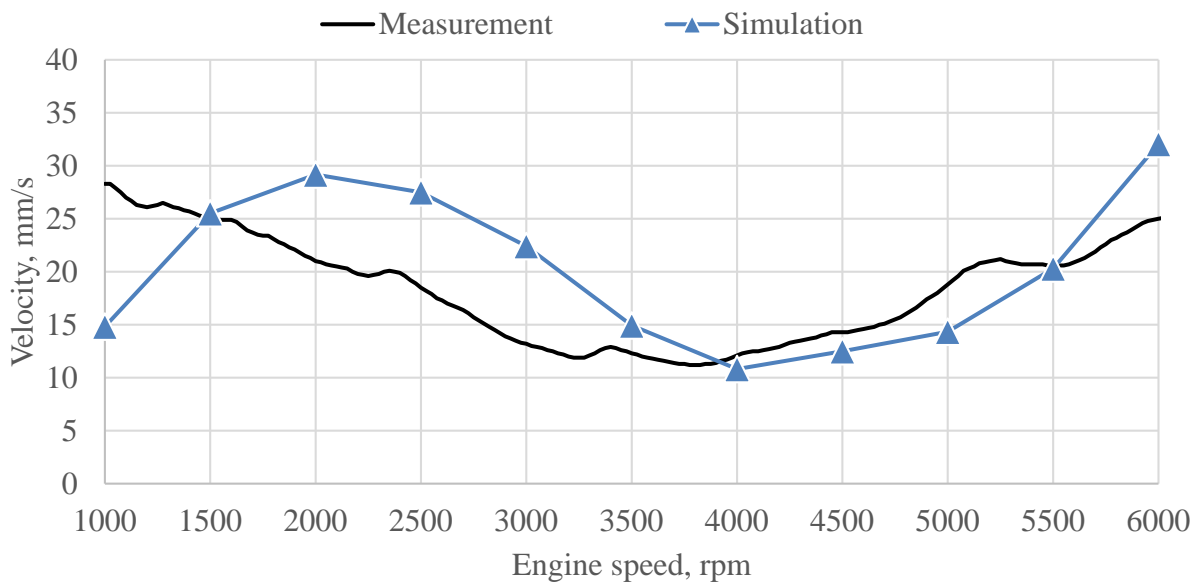


Figure 60. Right engine mount – Z direction – synthesis

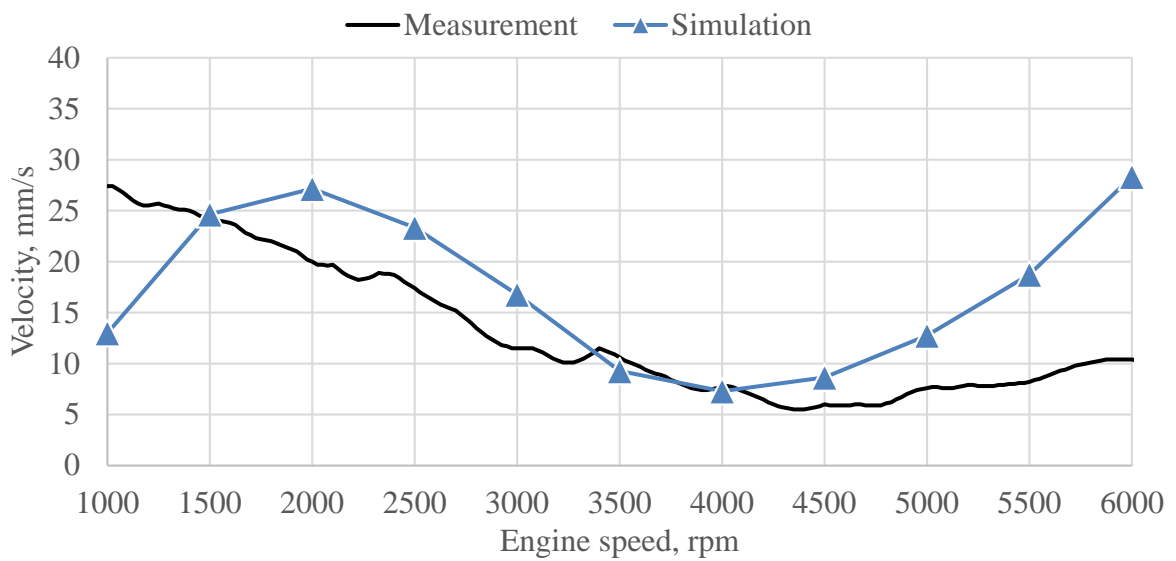


Figure 61. Right engine mount – Z direction – 2nd order

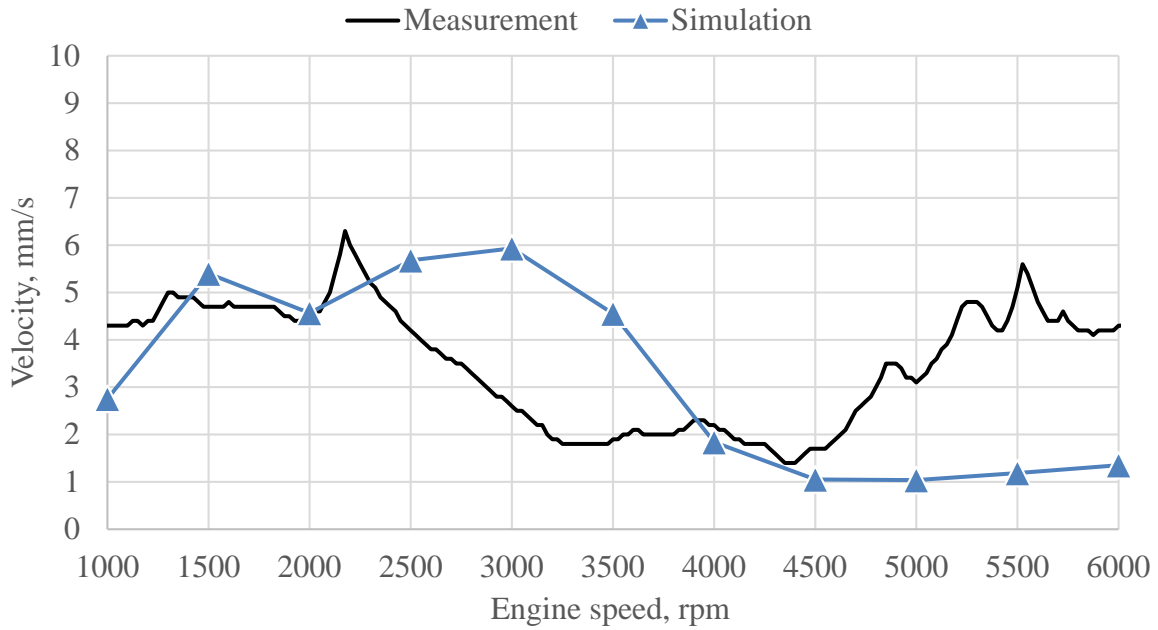


Figure 62. Right engine mount – Z direction – 4th order

As for left engine mount, simulation results are satisfying in middle range engine speed where velocity values are very close to measurement data.

4.4.7 Gearbox mount – X direction

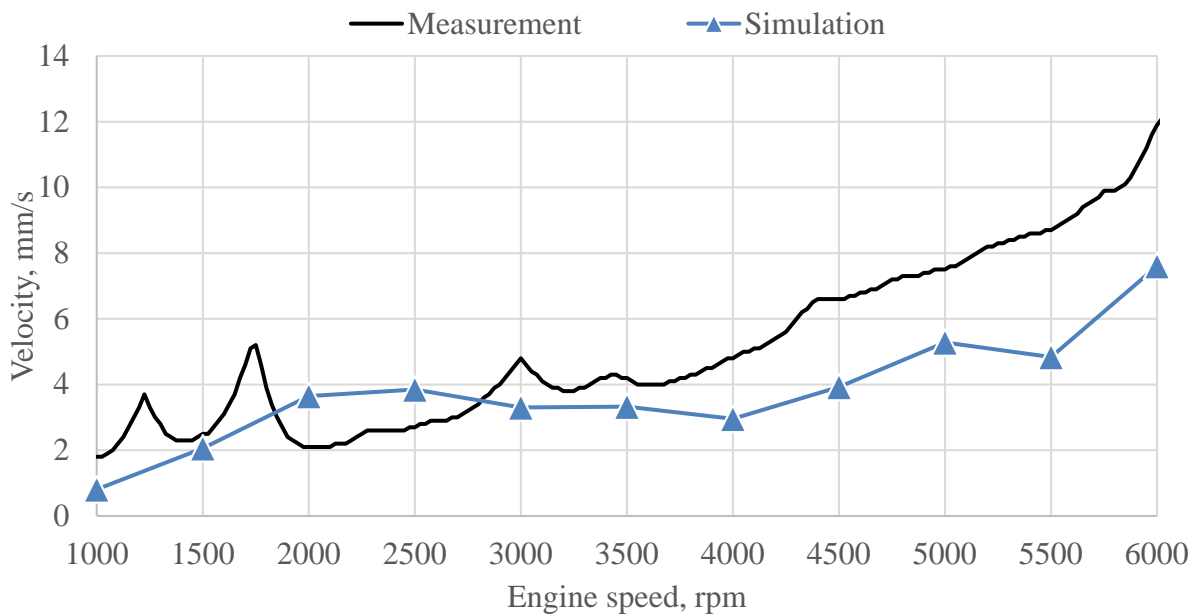


Figure 63. Gearbox mount – X direction – synthesis

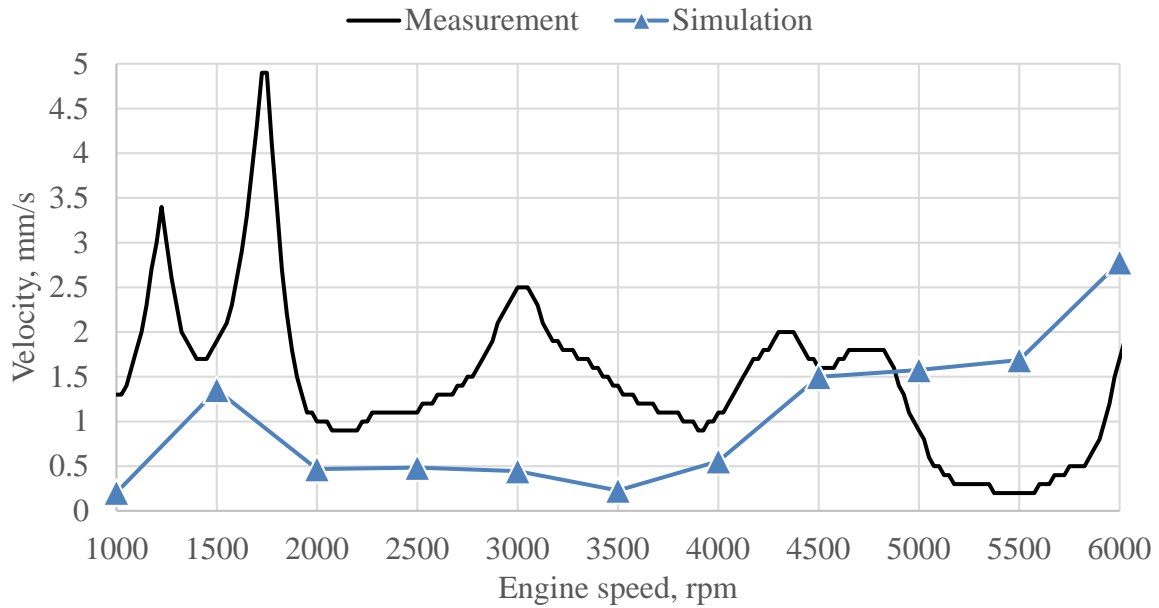


Figure 64. Gearbox mount – X direction – 2nd order

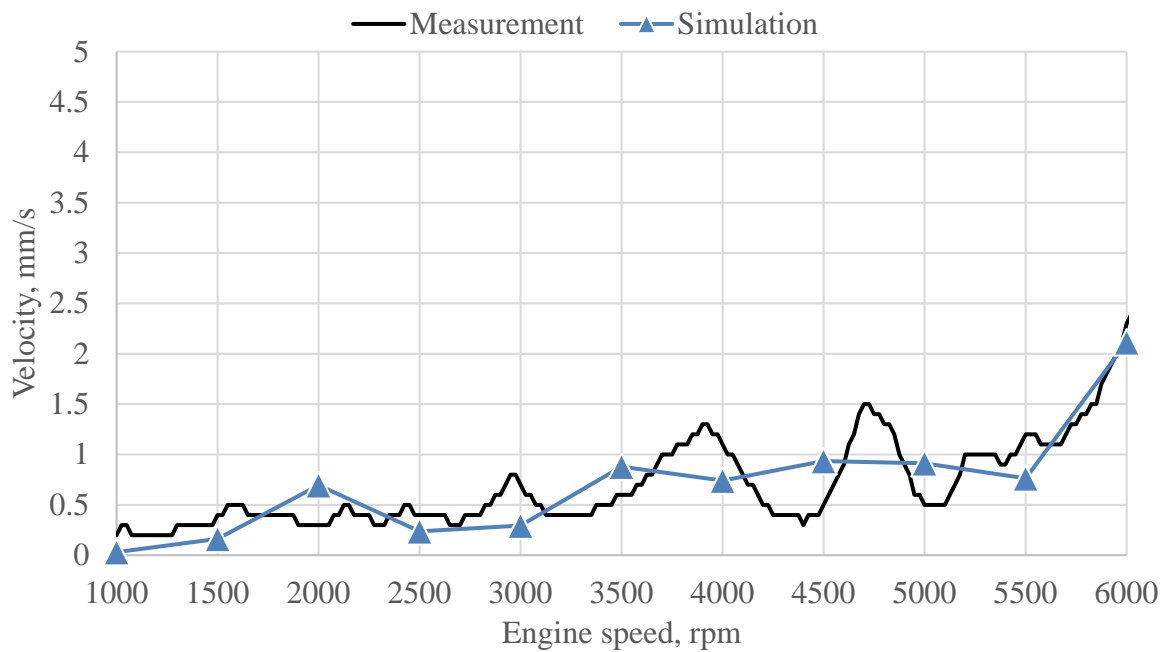


Figure 65. Gearbox mount – X direction – 4th order

Elastomeric gearbox mount synthesis values of all considered orders are lower than synthesis obtain from measurement for higher engine speeds as shown in figure 63. This means that for gearbox mount X direction in simulation higher frequencies vibration does not appear as during the measurement. In figure 65 is shown that 4th order simulation results curve follows measurement curve trend.

4.4.8 Gearbox mount – Y direction

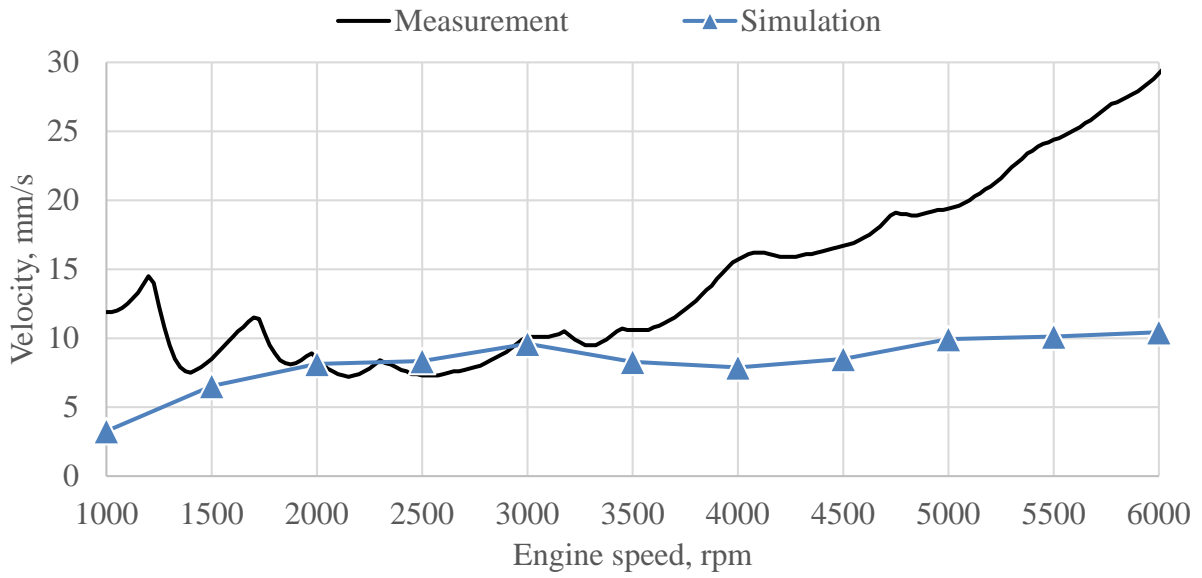


Figure 66. Gearbox mount – Y direction – synthesis

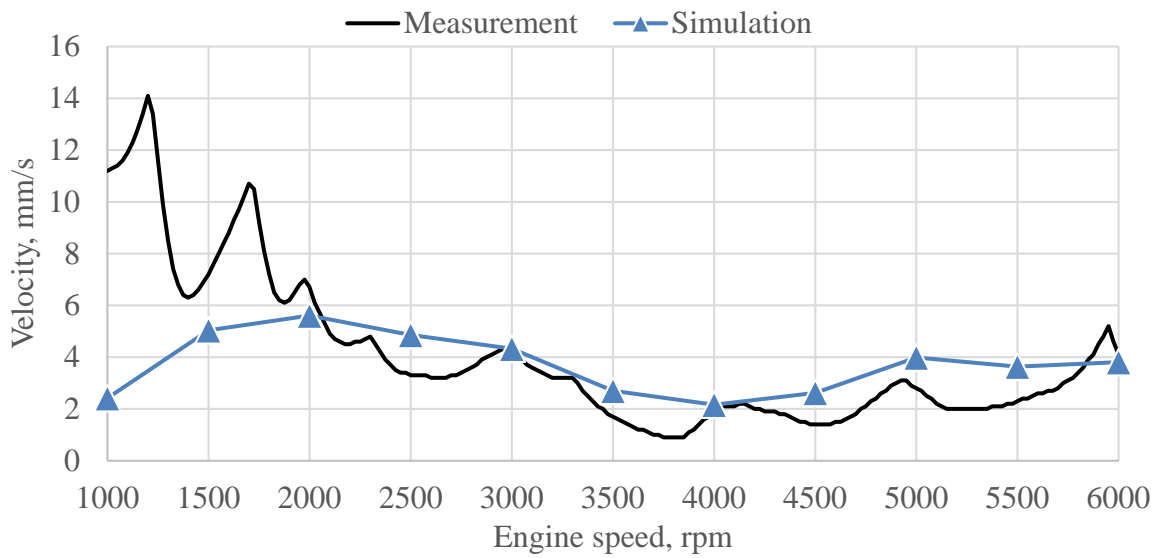


Figure 67. Gearbox mount – Y direction – 2nd order

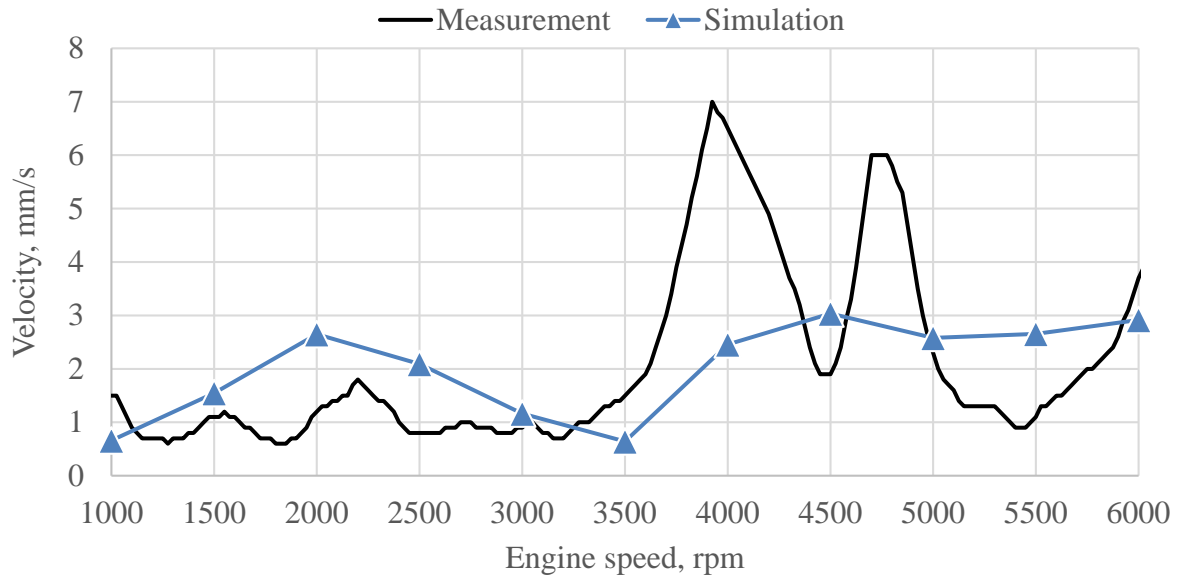


Figure 68. Gearbox mount – Y direction – 4th order

In Y direction for gearbox mount influence of higher frequency vibration could not be calculated in simulation model as can be seen in figure 66 where from 3000 rpm to 6000 rpm simulation synthesis values are lower than in measurement. 2nd order for mentioned speed range is satisfying so it can be concluded that higher order have influence on synthesis results. In figure 68 it can be seen that 4th order is under estimated on middle speed range.

4.4.9 Gearbox mount – Z direction

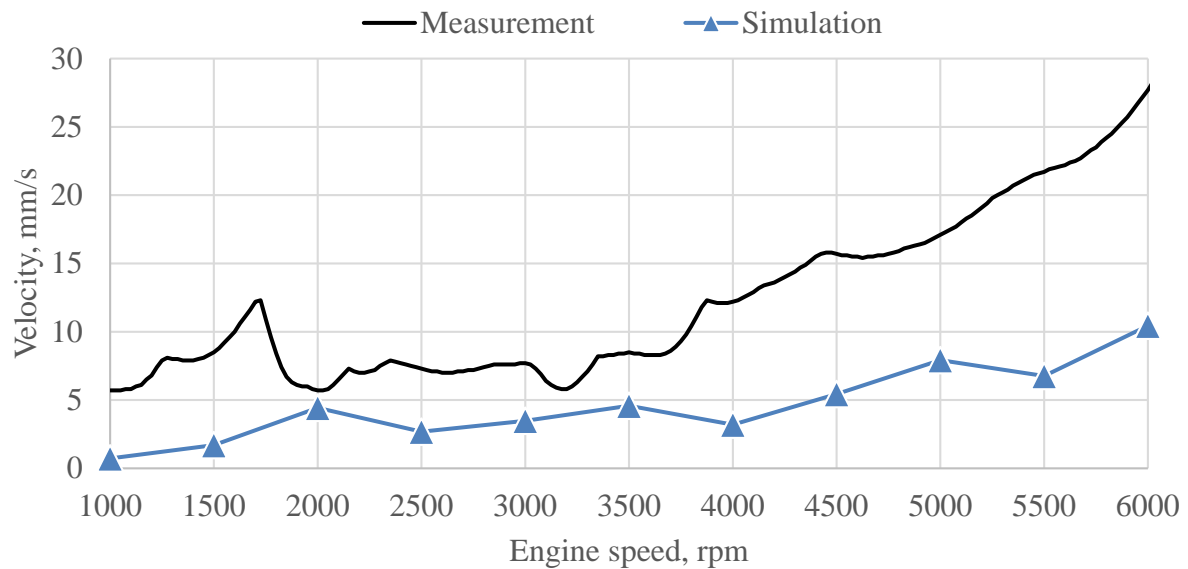
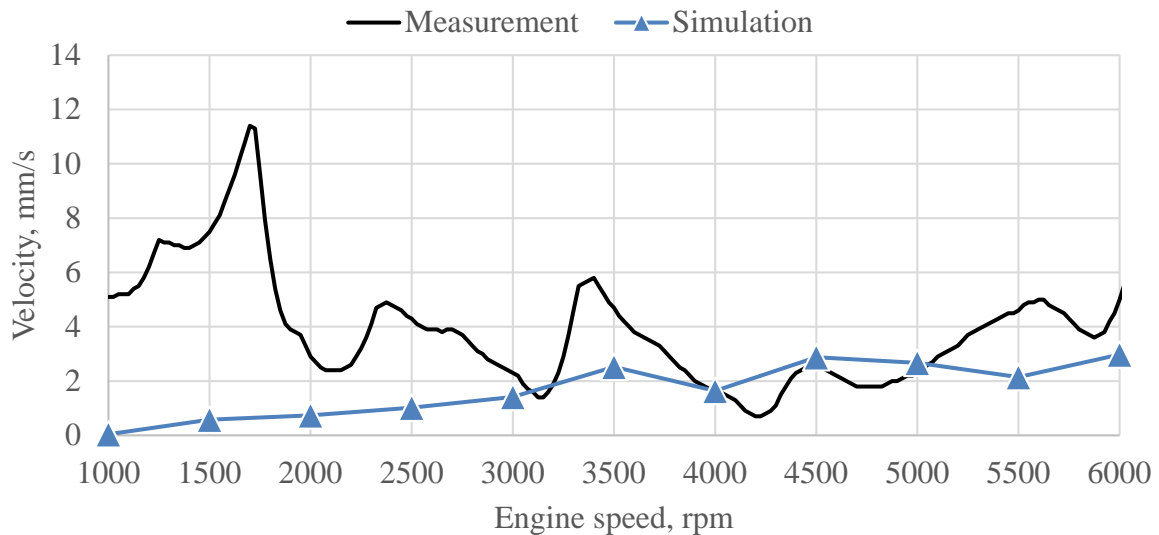
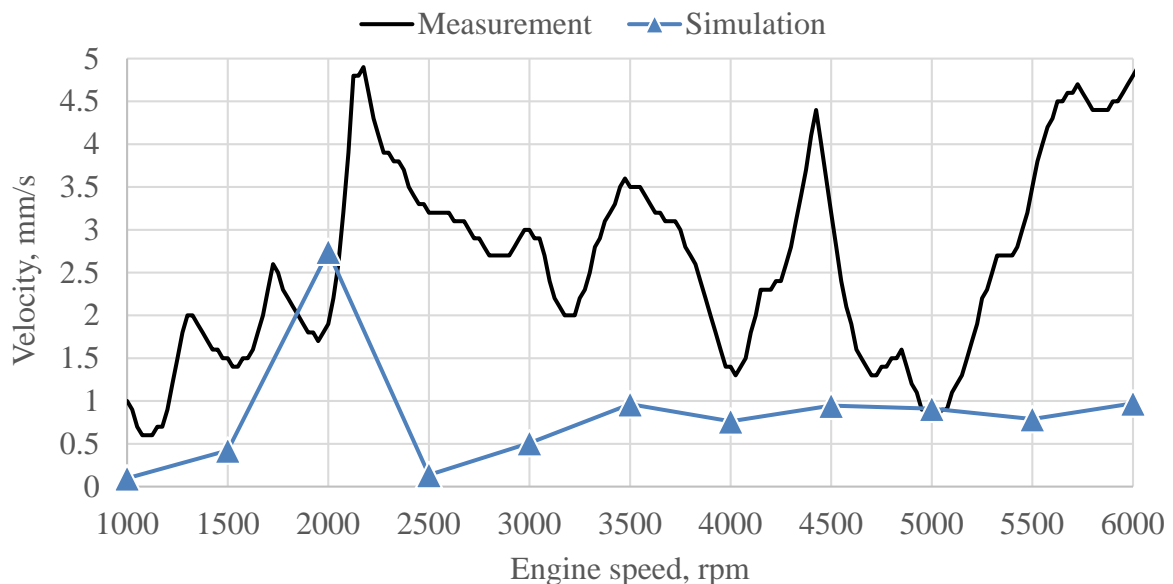


Figure 69. Gearbox mount – Z direction – synthesis

Figure 70. Gearbox mount – Z direction – 2nd orderFigure 71. Gearbox mount – Z direction – 4th order

Gearbox mount in Z direction is underestimated on synthesis values and in 4th order values as shown in figures 69 and 71. As for Y direction, in simulation model higher frequency vibration influence could not be calculated which results in lower synthesis values. 2nd order from 3000 rpm has relatively satisfying results with exception of describing peaks at 3500 rpm and 5500 rpm as shown in figure 70.

4.5 Conclusion

Measurement of the engine mount dynamic stiffness can be successfully described using triple mass oscillator as shown in section 4.2. Implementation of triple mass oscillator in *AVL Excite* can be done using *FTAB joint* in which linear mass, stiffness and damping values can be defined. This is shown in figure 33.

After preparing and defining entire engine model, simulation is run and response of engine mounts measurement points were examined.

Conclusion after comparing simulation results with measurements is that simulation model with engine mounts described as triple mass oscillators can successfully simulate IC engine response at measurement points. Some deviations between results do exist with an emphasis on engine mount *Y* direction and gearbox mount *Z* direction.

Some results deviations can be explained in the way that chassis is considered as rigid, but in reality chassis has some compliance which influences on measurement results because measurements of the engine mount response were conducted on the vehicle.

5. Conclusions and Recommendations

The main goal of this thesis was to develop mathematical model that can describe frequency dependency of the passive hydraulic and elastomeric engine mount cross point dynamic stiffness. Also, method of mathematical model parameter optimization is developed.

Suggested mathematical model was implemented in the IC engine simulation and engine mount response results were compared with the measurements results in terms of engine mount velocities. The work done in this thesis is based on published articles and PhD thesis that are listed in the literature section.

5.1 Conclusions

Based on the examined literature and results of this thesis some conclusions can be made:

- The ideal engine mounts should isolate engine vibration caused by engine disturbances in the engine working speed range and prevent engine bounce from shock excitation like for example road load input or abrupt vehicle acceleration and braking. This implies that the dynamic stiffness and damping of the engine mount should be **frequency and amplitude dependent**.
- Passive hydraulic mounts can provide better performance than elastomeric mounts, especially in the low frequency range, but the advantage of the elastomeric mounts lies in its properties, e.g. compactness, cost-effectiveness, and low maintenance requirement.
- By using mass, spring and damper mathematical model it is possible to get nonlinear behavior in frequency domain with linear coefficients.
- By using 4 DOF triple mass oscillator with 15 variables described in section 3.1 it is possible to describe low and high frequency behavior of the elastomeric and passive hydraulic engine mount.
- It is possible to use triple mass oscillator in numerical simulation software to successfully describe frequency dependency of the engine mount dynamic stiffness.
- In AVL Excite environment *FTAB joint* coupled with *SLS joint* is sufficient to describe elastomeric mount behavior. *FTAB joint* can describe static stiffness nonlinearity and *SLS joint* can describe dynamic stiffness nonlinearity.

- In AVL Excite environment *FTAB joint* coupled with *triple mass oscillator* is sufficient to describe passive hydraulic mount behavior. *FTAB joint* can describe static stiffness nonlinearity and *triple mass oscillator* can describe dynamic stiffness nonlinearity.

5.2 Recommendations and future work

Some recommendations for future work in this field:

- Main limitation of this thesis was that amplitude dependency of the engine mount dynamic stiffness was neglected. Further step in this field could be to include amplitude dependency. It is possible to implement amplitude and frequency dependency as a table in numerical simulation software and during simulation run solver chooses stiffness value based on load frequency and engine displacement amplitude in current simulation step.
- For further investigation it is recommended to study article [15] where some empirical parameters for amplitude dependency were established.
- In simulation model chassis was considered as a rigid body although engine mount measurements were conducted on vehicle and this includes chassis compliance. To further develop IC engine simulation model that presented in this study the chassis compliance should be considered.
- All considered mathematical models were described with Kelvin - Voigt model which can easily be implemented in the numerical simulation software by using linear spring and damper connection. For some future work *Bouc - Wen model* could be considered. *Bouc - Wen model* is used and explained in [12].
- Elastomeric engine mount can be examined as finite element model and in that form can be implemented in numerical simulation software. For that kind of investigation CAD model of elastomeric engine mount should be available. Elastomeric material can be described by using Mooney-Rivlin material model. This approach is more complicated approach and therefore more computer resources is needed.

6. Literature

- [1] *AVL Excite 2014.1* Documentation, AVL List GmbH, A-8020 Graz, Austria, www.avl.com
- [2] Happian-Smith Julian: “An Introduction in Modern Vehicle Design”, 2002.
- [3] Naganathan G. Nagi, Peelamedu M. Saaravan, Dukkipati V. Rao: “Automotive Vehicle Engine Mounting System: A Survey”, 2001.
- [4] Mahalec I., Lulić Z., Kozarac D. “Konstrukcije motora”, interna skripta, 2014.
- [5] Geck, P. E., and Patton, R. D., 1984, “Front Wheel Drive Engine Mount Optimization”
- [6] Heisler Hanz: *Advanced Vehicle Technology*, Second edition, 2002.
- [7] Miller, L. R., and Ahmadian, M.: “Active Mounts- A Discussion of Future Technological Trends,” Inter-noise Conference, Toronto, Canada, 1992.
- [8] Swanson, D. A. and Miller, L. R.: “Design and Effectiveness Evaluation of and Active Vibration Isolation System for a Commercial Jet Aircraft,”, 1993
- [9] Christopherson J., Mahinfalah M., Jazar N. Reza: “Suspended Decoupler: A New Design of Hydraulic EngineMount”, 2011.
- [10] Reza Madjelsi: “A new Approach in Modeling and Optimization of Engine Mount System”, 2003.
- [11] Singh R., Kim G., Ravindra V.P.: “Linear Analysis of Automotive Hydro-Mechanical Mount With Emphasis on Decoupler Characteristics”, 1992.
- [12] Alkhatib Fadi: “Techniques for Engine Mount Modeling and Optimization”, PhD Thesis, 2013.
- [13] Geisberger A. Aaron: “Hydraulic Engine Mount Modeling, Parameter Identification and Experimental Validation”, Master’s Thesis, University of Waterloo, 2000.
- [14] Heissing B., Ersoy Metin: “Chassis Handbook: Fundamentals, Driving Dynamics, Components, Mechatronics, Perspectives”, ATZ, 2011.
- [15] Singh R., Jeong T.: “Inclusion of measured frequency and amplitude dependent mount properties in vehicle or machinery models”, 2000.

APPENDIX A

MSC Nastran – Triple mass oscillator verification

```
SOL 108
CEND
TITLE = Triple mass oscillator verification
SUBTITLE = Analysis (SOL 108)
$
SPC = 996
$
DLOAD = 999
$
FREQ = 888
$
SUBCASE 1
$
SET 99 = 1
SET 98 = 5
DISPLACEMENT(SORT2,PRINT,PUNCH,REAL)=99
VELOCITY(SORT2,PRINT,PUNCH,REAL)=99
ACCELERATION(SORT2,PRINT,PUNCH,REAL)=99
SPCFORCES(SORT2,PRINT,PUNCH,REAL)=ALL
OUTPUT(XY PLOT)
XYPUNCH,DISP/ 1(T2RM,T2IP)
XYPUNCH,VELO/ 1(T2RM,T2IP)
$
BEGIN BULK
$
RLOAD1,999,997,,901
DAREA,997,1,2,100.0
TABLED1,901,,,,,+TAB901
+TAB901,0.0,1.0,50.0,1.0,ENDT
$
$FREQUENCY RANGE 1-40 Hz
FREQ1,888,1.,0.5,79
$
GRID,1,,0.,200.,0.
GRID,2,,0.,70.,0.
GRID,3,,0.,80.,0.
GRID,4,,0.,60.,0.
GRID,5,,0.,0.,0.
$
GRDSET,,,,,13456
SPC,996,5,2
$
CONM2,1,1,,100e-3
CONM2,2,2,,200e-3
CONM2,3,3,,200e-3
```

CONM2,4,4,,0.01e-3
\$
CBUSH,100,12,1,5,,,0
CBUSH,101,13,1,2,,,0
CBUSH,102,14,2,5,,,0
CBUSH,103,15,1,3,,,0
CBUSH,104,16,3,4,,,0
CBUSH,105,17,4,5,,,0
\$
PBUSH,12,K,,245.00001,,,+1
+1,,B,,0.21
PBUSH,13,K,,0.00001,,,+4
+4,,B,,1.41
PBUSH,14,K,,1281.90001,,,+6
+6,,B,,6.9
PBUSH,15,K,,2172.32001,,,+8
+8,,B,,23.3
PBUSH,16,K,,0.00001,,,+9
+9,,B,,1.63
PBUSH,17,K,,0.00001,,,+10
+10,,B,,41.1
\$
ENDDATA

APPENDIX B

I. CD – R disc